University of Alberta

The Identification of Genes Involved in Mitotic Exit and Nuclear Positioning in the Yeast *Saccharomyces cerevisiae*

by

Darren Allen Bugbee

A thesis submitted to the Faculty of Graduate Studies and Research
in partial fulfillment of the requirements for the degree of

Master of Science
in
Molecular Biology and Genetics

Department of Biological Sciences

Edmonton, Alberta
Spring 2008

Library and
Archives Canada

Published Heritage
Branch

395 Wellington Street
Ottawa ON K1A 0N4
Canada

Bibliothèque et
Archives Canada

Direction du
Patrimoine de l'édition

395, rue Wellington
Ottawa ON K1A 0N4
Canada

Your file Votre référence
ISBN: 978-0-494-45785-6
Our file Notre référence
ISBN: 978-0-494-45785-6

NOTICE:
The author has granted a non-exclusive license allowing Library and Archives Canada to reproduce, publish, archive, preserve, conserve, communicate to the public by telecommunication or on the Internet, loan, distribute and sell theses worldwide, for commercial or non-commercial purposes, in microform, paper, electronic and/or any other formats.

The author retains copyright ownership and moral rights in this thesis. Neither the thesis nor substantial extracts from it may be printed or otherwise reproduced without the author's permission.

AVIS:
L'auteur a accordé une licence non exclusive permettant à la Bibliothèque et Archives Canada de reproduire, publier, archiver, sauvegarder, conserver, transmettre au public par télécommunication ou par l'Internet, prêter, distribuer et vendre des thèses partout dans le monde, à des fins commerciales ou autres, sur support microforme, papier, électronique et/ou autres formats.

L'auteur conserve la propriété du droit d'auteur et des droits moraux qui protège cette thèse. Ni la thèse ni des extraits substantiels de celle-ci ne doivent être imprimés ou autrement reproduits sans son autorisation.

In compliance with the Canadian Privacy Act some supporting forms may have been removed from this thesis.

While these forms may be included in the document page count, their removal does not represent any loss of content from the thesis.

Conformément à la loi canadienne sur la protection de la vie privée, quelques formulaires secondaires ont été enlevés de cette thèse.

Bien que ces formulaires aient inclus dans la pagination, il n'y aura aucun contenu manquant.

Canada

I. Abstract

The cell cycle results in replication of DNA, cell division, and entry into a new cell cycle. A key step in cell division is mitotic exit. Many regulatory mechanisms of mitotic exit remain unknown. I investigated these processes by creating 163 double gene deletion strains with the mitotic exit gene *lte1*Δ. Of these double mutants, 5 were confirmed synthetic sick or lethal, and 16 displayed suppression of *lte1*Δ mitotic exit defects. One gene deletion that was lethal with *lte1*Δ was *bem4*Δ, which, we have found has septin defects and may aid in Cdc42p signaling.

Yeast positions the mitotic spindle between the mother and daughter cells prior to division. The dynein molecular motor is involved in this process. In a second project I took advantage of evolutionary conservation between dynein components to identify a new yeast dynein light chain. This protein is homologous to the Tctex dynein light chain family.

II. Acknowledgements

I would like to thank the department of Biological Sciences for all its help and guidance throughout my degree. I would especially like to thank Dr. Heather McDermid, and Dr. John Locke. As administrators it is very apparent that they care for each and every grad student in the department and RIG.

I would also like to thank Dr. Linda Reha-Krantz for supervising the writing of my thesis, and all the work that this entailed. Her thorough nature and tireless work ethic make her an excellent revisionist as well as scientist. Thank you Linda for all your help.

Finally, I would like to thank Dr. Neil Adames and the Adames lab. Over the past two years the Adames lab has changed my life. Not only has the lab given me a chance to grow scientifically, but it also produced lifelong friendships. Sean, Sabrina, Ranran, Donovan, and Hao have all been wonderful co-workers and terrific friends. It is a treat to work with such kind-hearted people that, like me, have a passion for science. Thank you for all of your help with this work. It was also a pleasure to work with Dr. Neil Adames. His knowledge of the cell cycle and yeast is astounding. I learned so much bouncing ideas off of him over coffee; a process that aided this work more than once. Thank you Neil for all your help in the past and future.

III. Table of contents

CHAPTER 1- INTRODUCTION *1*

1.1 Overview of the *Saccharomyces cerevisiae* cell cycle **2**

1.2 Temporal regulation of the *Saccharomyces cerevisiae* cell cycle **3**

1.3 Mitosis: preparation and exit **5**

1.4 Preparation for mitosis **6**
- 1.4.1 Spindle pole body duplication, microtubule organization, and spindle formation 6
- 1.4.2 Cell/actin polarity 8
- 1.4.3 Nuclear migration/spindle positioning 11
- 1.4.4 The Kar9 pathway 13
- 1.4.5 The dynein pathway 16
- 1.4.6 Septin structure and assembly 24

1.5 Mitotic exit **25**
- 1.5.1 The mitotic exit network (MEN) 27
- 1.5.2 The spindle position checkpoint (SPC) 29
- 1.5.3 The Cdc14 early anaphase release network (FEAR) 32
- 1.5.4 Cdc42 signaling and mitotic exit 34

1.6 The synthetic genetic array (SGA) **35**

1.7 Rationale/objectives: Project #1 .... **38**

1.8 Rationale/objectives: Project #2 .... **41**

CHAPTER 2- MATERIALS & METHODS *42*

2.1 Media **42**

2.2 General methods **44**
- 2.2.1 Mating type testing 44
- 2.2.2 Crossing strains 45
- 2.2.3 Concentration of plasmid DNA or PCR products 45
- 2.2.4 Transformation of *Saccharomyces cerevisiae* 45
- 2.2.5 Confirmation of gene knockouts 46
- 2.2.6 DNA sequencing 49
- 2.2.7 Replica-pinning 49

2.3 Genetic screen for enhancers/inhibitors of mitotic exit (Project #1) **50**
- 2.3.1 Synthetic genetic array 50
- 2.3.2 Phenotypic analysis of deletion strains 55
- 2.3.3 Overexpression of *Saccharomyces cerevisiae* ORFs in the *lte1::KanMX4* mutant 56
- 2.3.4 Characterization of *BEM4* 56

2.4 Identification of *YER071c* as a dynein light chain (Project #2) **58**
- 2.4.1Gene homology/phylogeny 58
- 2.4.2 Nuclear migration assay 59
- 2.4.3 YER071c synthetic interactions 60

CHAPTER 3- GENETIC SCREEN FOR ENHANCERS/INHIBITORS OF MITOTIC EXIT (PROJECT #1) *70*

3.2 Results **70**
- 3.2.1 Genetic screen to identify enhancers/inhibitors of mitotic exit 70

3.2.2 Phenotypes of several candidates 89
3.2.3 Overexpression of candidate ORFs 89
3.2.4 Analysis of *BEM4* 93

3.3 Discussion and conclusions 101
3.3.1 Genetic screen to identify enhancers/inhibitors of mitotic exit 101
3.3.2 New evidence for the activation of mitotic exit by the Cdc42p signaling pathway 102
3.3.3 Proper nuclear migration is necessary in the presence of mitotic exit defects 106
3.3.5 Proper nuclear export is involved in mitotic exit 107
3.3.4 Septin structure and mitotic exit 108
3.3.6 dSLAM vs. SGA 108
3.3.7 Future directions 109

CHAPTER 4- IDENTIFICATION AND CHARACTERIZATION OF YER071c AS A Saccharomyces cerevisiae TCTEX HOMOLOGUE (PROJECT #2) 113

4.2 Results 113
4.2.1 *YER071c* sequence alignment/phylogenetic tree 113
4.2.2 *yer071c*Δ nuclear migration assay 119
4.2.3 Synthetic interactions with *yer071c*Δ 119

4.3 Discussion and conclusions 122
4.3.1 Identification of a new *S. cerevisiae* dynein light chain 122
4.3.2 *YER071c* is the *S. cerevisiae* homologue of the Tctex family of dynein light chains 122
4.3.3 Yer071cp may be redundant with Dyn2p 123
4.3.4 Conclusions 124
4.3.5 Future directions 124

CHAPTER 5- REFERENCES 125

IV. List of tables

Table 2.1. Strains used in this study..61

Table 2.2. Primers used in this study..64

Table 2.3. Plasmids used in this study..69

Table 3.1. Synthetic genetic array of *lte1*Δ and 163 candidate deletion strains....................72

Table 3.2. Descriptions of the gene knockouts that synthetically interact with *lte1*Δ..............79

Table 3.3. Descriptions of gene knockouts that suppress the *lte1*Δ cold lethality phenotype.....83

Table 3.4. Confirmation of synthetic genetic interactions with *lte1*Δ by tetrad analysis.........87

Table 3.5. Confirmation of synthetic genetic interactions with *lte1*Δ by random spore analysis..88

Table 3.6. Synthetic genetic interactions between *bem4*Δ and the CDC42p signaling pathway..96

Table 4.1. Synthetic genetic interactions between *yer071c*Δ and the dynein and Kar9p pathways..121

V. List of figures

Figure 1.1. Regulation of the *S. cerevisiae* cell cycle by Cdc28-Cyclin complexes……………4

Figure 1.2. Preparation for and execution of mitosis………………………………………6

Figure 1.3. SPB duplication and spindle formation in *S. cerevisiae*………………………………7

Figure 1.4. Actin dynamics throughout the cell cycle………………………………………9

Figure 1.5. Summary of nuclear migration steps in *S. cerevisiae*………………………………13

Figure 1.6. Summary of Kar9p and dynein pathways………………………………………23

Figure 1.7. Summary of the pathways leading to mitotic exit………………………………26

Figure 1.8. Spatial isolation model for the spindle position checkpoint…………………………30

Figure 1.9. Examples of outstanding questions in the process of mitotic exit…………………40

Figure 2.1. Schematic of wildtype and knockout PCR tests…………………………………48

Figure 2.2. Tetrad dissection and analysis……………………………………………54

Figure 3.1. Phenotypic analysis of interesting candidates……………………………………91

Figure 3.2. *lte1*Δ dosage suppression assay…………………………………………92

Figure 3.3. Homology of Bem4p protein sequence……………………………………95

Figure 3.4. The effects of *bem4*Δ on septin assembly…………………………………98

Figure 3.5. Quantification of septin morphology defects……………………………………99

Figure 3.6. Effect of *bem3*Δ on *bem4*Δ strain…………………………………………100

Figure 4.1. Homology of Yer071cp protein sequence to dynein light chain TCTEX family homologues……………………………………………………114

Figure 4.2 Homology of *Yer071c* protein sequence to fungal TCTEX family homologues….116

Figure 4.3. Phylogenetic tree predictions for the TCTEX family of dynein light chains……..117

Figure 4.4. Nuclear positioning defects in *dyn2*Δ, *yer071c*Δ, *and dyn2*Δ *yer071c*Δ strains…..120

VI. List of abbreviations

AAA- ATPase associated with various cellular activities

AOTF- acousto-optic tunable filter

APC- adenomatous polyposis coli

APC/C- anaphase promoting complex/cyclosome

Arg- arginine

ATP- adenosine triphosphate

Can- canavanine

CDK- cyclin dependent kinase

cMT- cytoplasmic microtubule

CRIB- Cdc42/Rac interactive binding

CSM- complete supplement mixture

ddH2O- double distilled water

DMSO- dimethyl sulphoxide

dSLAM- diploid synthetic lethality analysis by microarray

EDTA- ethylenediamine tetraacetic acid

F-Actin- filamentous actin

FEAR- CDC fourteen early anaphase release

FRAP- fluorescence recovery after photobleaching

G1- gap phase 1

G2- gap phase 2

G-Actin- globular actin

GAP- GTPase Activating Protein

GDI- guanine nucleotide dissociation inhibitor

GDP- guanine diphosphate

GEF- guanine nucleotide exchange factor

GFP – green fluorescent protein

GTP- guanosine triphosphate

HC- heavy chain

His- histidine

I- interphase

IC- intermediate chain

K/O- knockout

LB- Luria-Bertani media
LC- light chain
LC7(8) - light chain family 7/8
LIC- light intermediate chain
M- mitosis
MAP- microtubule associated protein
MAPKKKK- mitogen activated protein kinase kinase kinase kinase
MEN- mitotic exit network
MTOC- microtubule organizing centre
NaCl- sodium chloride
NaOH- sodium hydroxide
Nat- nourseothricin
nMT- nucleoplasmic microtubule
NPD- non-parental ditype
ORF- open reading frame
PAK- p21 Activated Kinase
PCR- polymerase chain reaction
PD- parental ditype
PEG- polyethylene glycol
pH- power of hydrogen
PP2A- protein phosphatase 2A
RSA- random spore analysis
S- Synthesis phase
SD- synthetic dextrose media
SDS- sodium dodecylsulphate
SGA- synthetic genetic array
SORB- sorbitol
SPB- spindle pole body
SPC- spindle position checkpoint
SRG- synthetic raffinose galactose media
T- tetratype
TA- tetrad analysis
TAE- tris-acetate-EDTA
TCTEX- t complex testis expressed

Tris-HCl- tris-hydroxymethylaminomethane hydrochloric acid

Ura- uracil

WD40- repeat domain of 40 amino acids containing conserved tryptophan and aspartic acid residues

YPAD- yeast extract peptone adenine dextrose media

+TIP- + end tracking protein

CHAPTER 1- INTRODUCTION

My work focuses on further illuminating the process of cell division using *Saccharomyces cerevisiae*. Within this study I have focused on two specific aspects of cell division: the regulation of mitotic exit, and migration of the nucleus via the dynein molecular motor. The fidelity of either of these processes has proved crucial to proper cell division and cell viability [1, 2].

S. cerevisiae (baker's yeast) has been used as a model organism to study cell division since the early 1970s. Since this time yeast has proven to be an essential tool in the investigation of cell division for several reasons. First, *S. cerevisiae* is a eukaryote and, therefore, shares many general characteristics with mammalian cells such as a nucleus and linear chromosomes with centromeres and telomeres. Second, *S. cerevisiae* has a relatively small genome that facilitates genetic manipulation. Third, this species is single-celled and has several characteristics of prokaryotes that facilitate analysis, such as the ability to be cultured and short generation time. Fourth, *S. cerevisiae* can exist in either a haploid or diploid state; thus, mutational studies can be carried out in haploids to easily assess their phenotype. Finally, yeast have a well-defined cell cycle [3-5].

These virtues of the yeast system have now evolved into many powerful and elegant genomic and proteomic techniques. For example, the genetic malleability of *S. cerevisiae* has led to the haploid deletion project, in which the majority of non-essential genes were deleted in the same genetic background. Soon after these deletion strains were available, a genomic technique called the Synthetic Genetic Array (SGA) was developed [6, 7]. The SGA is performed by crossing a known deletion query strain to the haploid deletion set and subsequently scoring the double mutant progeny for a specific phenotype. This screen permits a genome-wide search for genes that genetically interact and has resulted in the identification of many new protein components of relatively uncharacterized cellular processes as well as previously unsuspected interactions between well-known cellular pathways [8].

My primary study uses a smaller version of the SGA method to identify new genes that have the potential to be activators or inhibitors of mitotic exit. Although many studies have described the process of mitotic exit within *S. cerevisiae*, at least several genes in this process have yet to be identified. I will address the nature of these deficiencies within my introduction and describe experiments designed to identify new regulators of mitotic exit. This project will be termed project #1.

Another advantage of *S. cerevisiae* is the significant conservation of its proteins with other eukaryotes, including *Homo sapiens*. One such conserved set of proteins is the dynein molecular motor complex (reviewed in [9]). Although many components within this multiprotein complex have been identified, several of these proteins have no known homologue in *S. cerevisiae*. Thus, we predict that there are dynein components in *S. cerevisiae* that have not yet been identified. Discovery of these components will help in understanding dynein's only known role in yeast - nuclear migration. This understanding of dynein structure and function is important because nuclear migration is a prerequisite to proper cell division [2]. Therefore, I intend to identify homologous dynein subunits in yeast. This experiment will be termed project #2.

1.1 Overview of the *Saccharomyces cerevisiae* cell cycle

Saccharomyces cerevisiae, is a powerful tool for studies of the cell cycle. Although *S. cerevisiae* divides by the process of budding instead of fission (which is most common among eukaryotes), many of the components responsible for the cell cycle and mitosis are conserved [4]. The budding yeast has two cell cycles: meiotic (sexual) division producing gametes (haploid cells), and mitotic (asexual) division producing genetically identical daughter cells. The mitotic cell cycle is broken into two general phases: interphase (I phase) and mitosis (M phase). I phase can be further broken down into three distinct phases: G1 phase, S phase, and G2 phase. G1 phase is a "gap" phase within which the cell produces proteins, acquires nutrients, and prepares for S phase. S phase consists of 'synthesis' (replication) of DNA. The DNA content of the cell is duplicated to prepare for cell division. G2 phase is the second "gap" phase that is responsible for the same growth processes as G1, save that its ultimate goal is to prepare for cell division. M phase follows G2 phase. Like I phase, M phase has many distinct steps. These steps include Prophase (nuclear envelope break down, which does not occur in yeast; spindle assembly; and the condensation of the DNA from chromatin to chromosomes), Metaphase (alignment of chromosomes along the division plane, and chromatin decondensation), Anaphase (chromosome segregation), and Telophase (chromosome decondensation and nuclear envelope reformation). At the very end of M phase, cytokinesis occurs, in which the cleavage furrow pinches in and the mother and daughter (bud) cells separate from each other. As a result, two genetically identical cells are produced, each of which possesses its own haploid or diploid set of chromosomes (reviewed in [10, 11]).

1.2 Temporal regulation of the *Saccharomyces cerevisiae* cell cycle

Cell division refers to the processes of chromosome segregation, spindle disassembly, and cytokinesis. Aberrant cell division can result in chromosome mis-segration or aneuploidy, which usually leads to cell death. However, surviving aberrant cells in metazoans may become cancerous. Consequently, cell division is strictly regulated spatially and temporally by a very elegant system. The budding yeast cell cycle, like other eukaryotic cell cycles, is controlled by cyclin dependent kinases (CDKs) (Figure 1.1). Budding yeast have only one major CDK (Cdc28p) that controls the cell cycle [3, 11]. Cdc28p is a serine/threonine protein kinase that is activated by cyclins - a group of proteins that bind to CDKs and target these kinases to specific substrates appropriate for specific steps in the cell cycle. The cyclins are so named because they undergo oscillations in abundance. Each cyclin is present only during specific phases of the cell cycle. In turn, each cyclin-CDK dimer coordinates the cell cycle by phosphorylating and modulating the activities of specific proteins important for specific phases of the cell cycle (reviewed in [12]).

Within yeast there are 9 major cyclins (Cln1-3p, Clb1-6p). Cln1p, Cln2p and Cln3p are responsible for the initiation of the cell cycle (Start) and progression through G1 phase [13-15]. Prior to entering the mitotic cell cycle, the cell has the potential to mate (if haploid) or sporulate (undergo meiosis, if diploid). Initiation of the mitotic cell cycle occurs when Cln3p binds to Cdc28p [16]. Cln3p-Cdc28p is responsible for activating the transcription of *CLN1* and *CLN2* [17, 18]. Once transcribed/translated, Cln1p and Cln2p allow the accumulation of B-type cyclins, inhibit the response to mating pheromones, and activate spindle pole body duplication (the yeast equivalent to the centrosome) and cell polarization [12, 16, 19-22]. The B-type cyclins, Clb5p/6p, are responsible for DNA replication and progression through S phase [23]. Once S-phase occurs, the remaining B-type cyclins (Clb1-4p) coordinate mitosis by regulating the formation of mitotic spindles and promoting nuclear migration to the mother bud neck [24-26]. Once the nucleus is positioned in the neck and the mitotic spindle is fully formed the cell is ready for division. However, the cyclins must now be removed to allow for cytokinesis, and reset the cell cycle to an early G1 state [1]. This is accomplished by degradation and inhibition of the mitotic B-type cyclins at the end of mitosis.

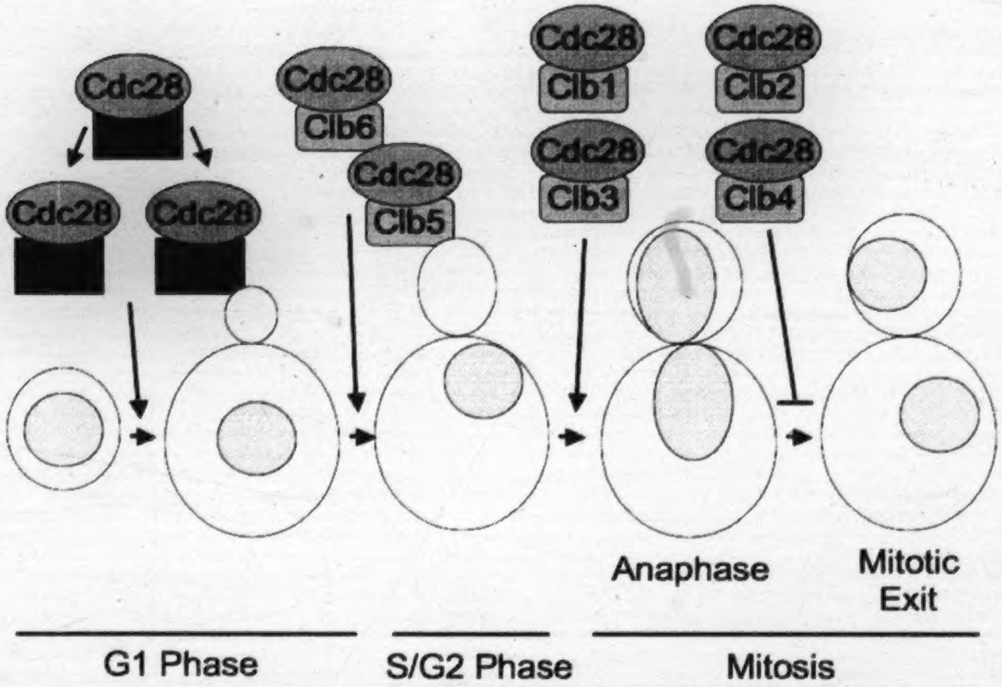
Cdc28
Cdc28
Cdc28
Cdc28
Clb6
Cdc28
Clb5
Cdc28
Clb1
Cdc28
Clb3
Cdc28
Clb2
Cdc28
Clb4
Anaphase
Mitotic Exit
G1 Phase
S/G2 Phase
Mitosis

Figure 1.1. Regulation of the *S. cerevisiae* cell cycle by Cdc28p-Cyclin complexes. The G1-phase cyclins (Cln1p, Cln2p and Cln3p) promote bud emergence, spindle pole body duplication (not shown) and activation of the B-type cyclins. The S-phase cyclins (Clb5p, Clb6p) advance DNA replication (brown nucleus), and the M-phase cyclins (Clb1p, Clb2p, Clb3p and Clb4p) promote spindle formation and the initiation of mitosis. Mitotic cyclins inhibit mitotic exit and cell division. (Modified from [12]).

1.3 Mitosis: preparation and exit

A complex coordination of events has evolved to prepare for and regulate the execution of mitosis in yeast. Preparatory events include: cell growth/bud formation, DNA replication, cell/actin polarization, centrosome duplication, spindle formation, nuclear positioning, and septin assembly (Figure 1.2). Overall, these processes combine to produce within the nucleus a spindle that is positioned parallel to the mother/bud axis. I will address several aspects of this process within the Introduction.

Once preparations are completed the cell can undergo mitosis. Mitosis, is highly regulated within itself. Several signal transduction pathways interact and culminate to perform the various steps of mitosis. One such step is the decision to exit mitosis. Mitotic exit is coordinated by multiple pathways and is an excellent example of the cell cycle's regulatory complexity (Figure 1.2). The central pathway activating mitotic exit is called the Mitotic Exit Network (MEN), which ultimately causes the inactivation of the mitotic cyclin-CDK [1, 27]. The activity of the MEN is controlled by the Cdc14 Early Anaphase Release (FEAR) pathway and the Spindle Position Checkpoint (SPC). The FEAR network is a positive regulator of the MEN and ensures timely and accurate mitotic exit by priming the MEN pathway. In contrast, the SPC inhibits the MEN pathway to prevent exit from mitosis before chromosome segregation between mother and bud has occurred [28-31]. Together these pathways form a highly coordinated set of signals responsible for exit from mitosis (Figure 1.2). Explanation of this intricate process will be a major focus of this introduction.

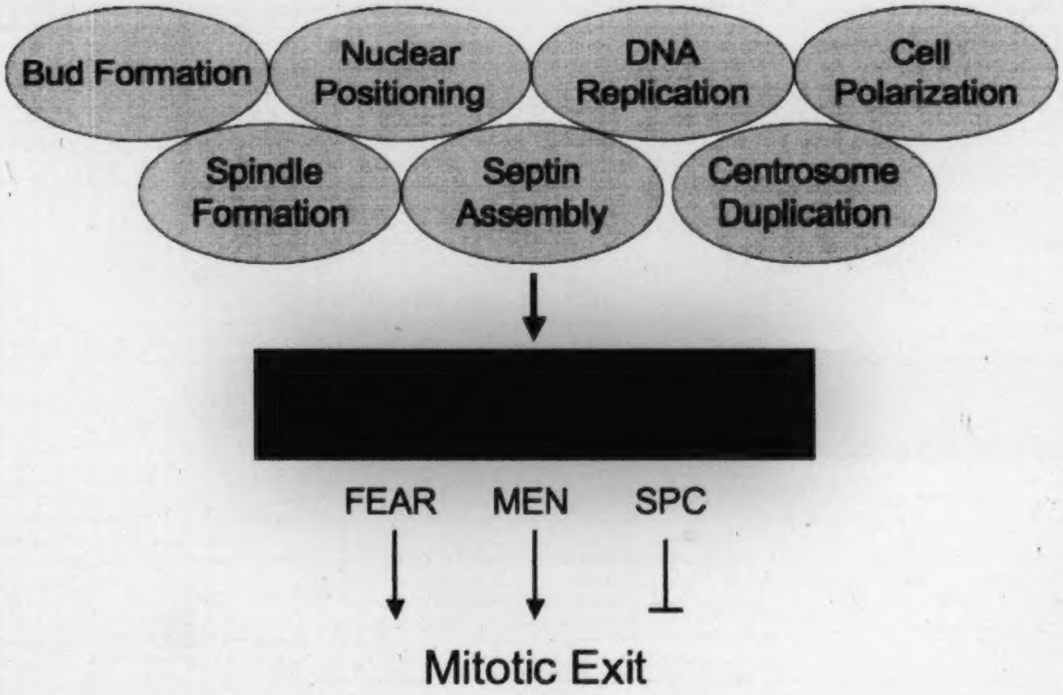
Bud Formation
Nuclear Positioning
DNA Replication
Cell Polarization
Spindle Formation
Septin Assembly
Centrosome Duplication
FEAR
MEN
SPC
Mitotic Exit

Figure 1.2. Preparation for and execution of mitosis. For mitosis to occur, various processes must be successfully completed or setup. Once the cells enter mitosis, and progress to anaphase, three major pathways regulate exit from mitosis. These pathways are the Cdc14 early anaphase release (FEAR), the spindle position checkpoint (SPC), and the mitotic exit network (MEN).

1.4 Preparation for mitosis

1.4.1 Spindle pole body duplication, microtubule organization, and spindle formation

SPB duplication begins in G1 (Figure 1.3). The new SPB is duplicated from the old SPB via a "half bridge" structure and begins to form on the cytoplasmic side of the nuclear membrane. Once a significant portion of the new SPB is formed it inserts into the nuclear membrane where the final components needed for its assembly bind on its nucleoplasmic surface. Succeeding this duplication is the polymerization of microtubules, which leads to spindle formation (for a more detailed description see [32]).

The final components incorporated into the new SPB are involved in tubulin nucleation and binding. γ-tubulin binds these components and subsequently initiates nucleation of microtubules from the SPB [33-35]. Tubulin is made up of α tubulin and β tubulin heterodimers [36, 37]. γ-tubulin nucleates microtubules by binding directly to the α tubulin face of the α/β heterodimer and eventually forming the minus (SPB facing) end of the microtubule [38]. Additional heterodimers then self-assemble onto the γ–bound tubulin heterodimers [39]. These tubulin heterodimers initially bind longitudinally (at their ends) to form protofilaments, which subsequently associate laterally to form a 25 nm tube called a microtubule [38, 39]. Microtubules are the structural girders for the spindle, are tracks for cellular trafficking (in metazoans), and mediate nuclear migration (Figure 1.3).

Upon SPB duplication and microtubule nucleation, the mitotic spindle begins to form between the old SPB and the new SPB (Figure 1.3). This assembly forms a short spindle (~1.5 μm) that, in combination with several kinesin related proteins, pushes the new SPB to the opposite pole of the nucleus [40]. At this point the midzone of the spindle is made up of ~48 antiparallel microtubules from each SPB [41]. These microtubules account for bipolar attachment to each of the 16 chromosomes in *S. cerevisiae* and ~16 antiparallel microtubules that are crosslinked by various kinesins [41, 42]. These antiparallel microtubules create the stabilizing force for proper spindle formation and elongation that culminate in chromosome segregation.

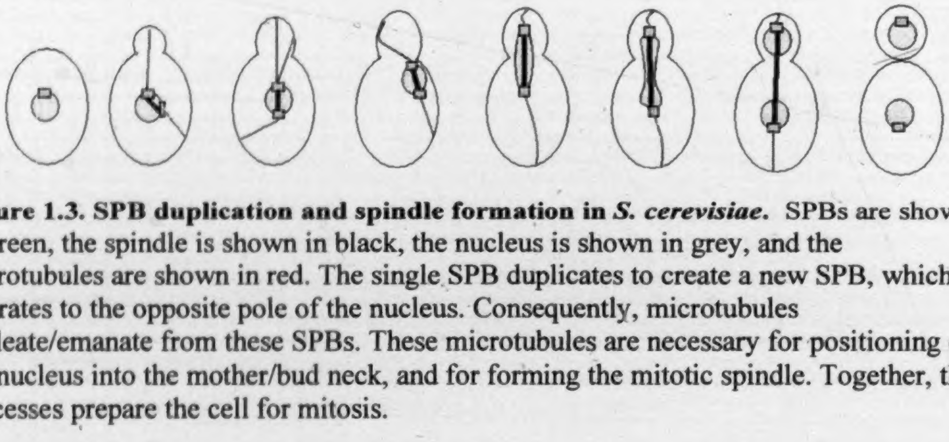

Figure 1.3. SPB duplication and spindle formation in *S. cerevisiae*. SPBs are shown in green, the spindle is shown in black, the nucleus is shown in grey, and the microtubules are shown in red. The single SPB duplicates to create a new SPB, which migrates to the opposite pole of the nucleus. Consequently, microtubules nucleate/emanate from these SPBs. These microtubules are necessary for positioning of the nucleus into the mother/bud neck, and for forming the mitotic spindle. Together, these processes prepare the cell for mitosis.

1.4.2 Cell/actin polarity

Cell/actin polarization is necessary for polarized cell growth, organelle inheritance (including the nucleus), and cytokinesis. Actin is found in two forms: G-actin (globular actin) monomers, and F-actin (filamentous actin) polymers. Using Rhodamine-Phalloidin, researchers have observed three F-actin structures in yeast: cortical actin patches, polarized actin cables/filaments, and a cytokinetic actin ring [43, 44]. The cortical actin patches within the mother and bud cells are vital in the process of endocytosis. Polarized actin cables act as a 'cellular highway' used for trafficking of several vesicles carrying components needed for daughter cell formation/growth. Finally, the cytokinetic ring is the structure responsible for separation of the mother and daughter cells during cytokinesis. Thus, these actin structures have specialized functions that are temporally and spatially regulated throughout the cell cycle (Figure 1.4) (reviewed in [44]).

Adams and Kilmartin characterized the process of actin cable and patch dynamics [45]. According to their study, in G1-phase, actin patches are found at the cell cortex and actin cables are in the cytoplasm. This localization seems to be random. Once the cell is large enough to divide, the cortical actin patches are polarized to the chosen bud site (pre-bud site) [45]. Here cortical actin patches congregate into a ring like structure [45]. Also at this time, actin cables polarize towards the pre-bud site allowing traffic of vesicles containing components necessary for bud growth [45]. This traffic eventually results in the emergence of the bud, in which most of the actin patches remain [45, 46]. During S and G2 phases, trafficking and actin patches are exclusive to the bud. Initially the patches and cables are oriented to the bud tip (apical) but these are redistributed throughout the bud (isotropic) in late S/G2. Finally, at M phase cortical actin patches and actin cables are redistributed throughout the mother and bud cells until late mitosis. During late mitosis actin cables/patches accumulate on both sides of the mother bud neck to facilitate the deposition of the septum during cytokinesis [20, 46]. Also during this time the cytokinetic ring, forms at the neck. This ring consists of actin and myosin (Myo1p) and constricts to separate the mother and bud cytoplasms [47]. After cytokinesis this accumulation of actin at the neck remains until actin patches and cables are randomized throughout the cell to prepare for a new cell division cycle [46].

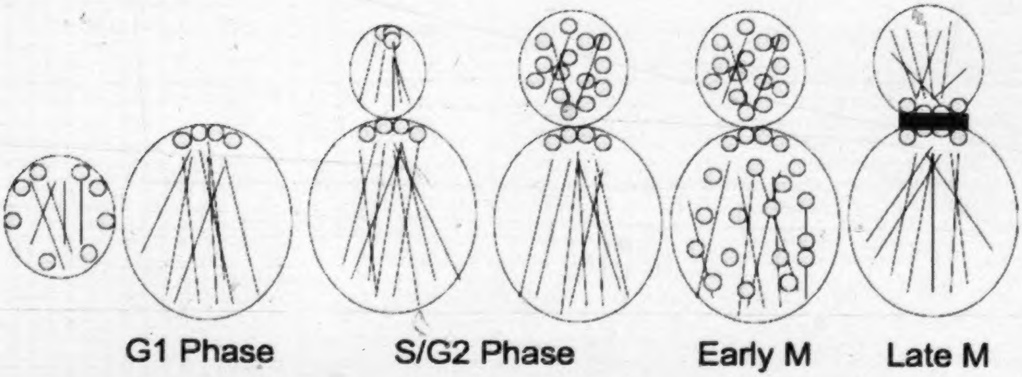

Figure 1.4. Actin dynamics throughout the cell cycle. Pictured here are the three visible F-actin structures: actin patches (shown in light blue), actin cables (black lines), and the actin cytokinetic ring (black bar). The three structures are dynamic throughout the cell cycle. The location of actin patches and cables determine the areas in which growth occurs. The cytokinetic ring forms and contracts at the end of the cell cycle (Modified from [43, 44]).

As these structures/functions of actin are critical for cell growth and division, several regulatory mechanisms have evolved to facilitate actin polarity and function. Actin regulation is dependent on the general cell cycle regulator Cdc28p (Cdk1) and the Rho like GTPase Cdc42p (Reviewed in [20]). The initial signal of polarization is the triggering of degradation of Far1p by Cdc28p-Cln [48]. Far1p is responsible for binding to and sequestering the Cdc42p-guanine nucleotide exchange factor (GEF) Cdc24p within the nucleus [49, 50]. Upon Far1p degradation, Cdc24p exits the nucleus, and is recruited to the site of polarization - the pre-bud site - where it binds the bud site selection protein Bud1p and its membrane adapter protein Bem1p [49, 50]. The next step in this process is the recruitment of Cdc42p to the site of Cdc24p localization [51]. Cdc42p then initiates polarized growth via several signal transduction pathways controlling actin nucleation and organization, membrane trafficking and septin organization.

Several proteins are involved in regulation of the Cdc42p complex. Directly regulating the G-protein is the GEF Cdc24p, which activates the turnover of Cdc42p-GDP (the inactive state) to Cdc42p-GTP (the active state). Conversely, the GTPase activating proteins (GAPs) Rga1p, Rga2p, Bem2p, and Bem3p are thought to promote the conversion of Cdc42p-GTP to Cdc42p-GDP. In addition, the GDP dissociation inhibitor (GDI) Rdi1p prevents exchange of GDP for GTP [52]. However, Rdi1p also plays a role in localization of Cdc42p since Cdc42p is mislocalized when *RDI1* is overexpressed [52]. Overall; these proteins regulate the activation state of Cdc42p, which ultimately coordinates cell polarity through a series of effectors (reviewed in [44]).

Some of the primary effectors of Cdc42p are the formins Bni1p and Bnr1p. Both of these formins are known to physically interact with Cdc42p and become activated upon this interaction [44]. Actin filaments are polar with a barbed end (which is the faster growing end) and a pointed end (which is the slower growing end) [44]. The yeast formins, Bni1p and Bnr1p, aid in the nucleation of actin filaments from the barbed ends [53]. These proteins do this by binding to the barbed ends and stabilizing F-actin intermediates that are usually unstable, as well as recruiting Pfy1p (the yeast profilin) bound to G-Actin which increases the local concentration of actin available for nucleation and polymerization [54, 55]. The result of formin activation is polymerization of actin filaments, which are bundled together and capped by various proteins.

Numerous other effectors of the Cdc42p protein consist of proteins with Cdc42p/Rac interactive binding (CRIB) domains that enable these proteins to physically interact with Cdc42p [56]. Typically this interaction facilitates activation of the downstream effectors of Cdc42p. One of these CRIB domain proteins is one of the p21-activated kinases (PAK) family homologues in yeast, Ste20p [56, 57]. Cdc42p binding of Ste20p's CRIB domain relieves autoinhibition of the CRIB domain on the kinase domain of Ste20p [56, 57]. Once activated, Ste20p acts as a mitogen activated protein kinase kinase kinase kinase (MAPKKKK), which activates several processes involved in cell polarization [58, 59] including control of Bni1p (and thus actin), and myosins [60-62]. Another PAK homologue in yeast, Cla4p, also activates several processes involved in cell polarization, and stimulates distinct processes such as septin organization (which I will address later) [63, 64]. Finally, the structurally related proteins Gic1p and Gic2p were identified in a genome wide screen for CRIB domain-containing proteins [65]. Gic1p and Gic2p were also found to co-localize and interact with Cdc42p. It has been hypothesized that Gic1p and Gic2p act as adapters that link activated Cdc42p to several substrates and stabilize the Cdc42p-GTP bound form [66].

1.4.3 Nuclear migration/spindle positioning

One interesting aspect of the cell division cycle in *S. cerevisiae* is that nuclear envelope breakdown does not occur during mitosis. As a result, the nucleus remains as a discrete structure within the cell and has several distinct functions during mitosis. One such function of the nucleus is migration into the mother/bud neck. The fidelity of this process is essential to the cells survival as cells that cannot position the nucleus to the mother bud neck either arrest or undergo aberrant mitosis which can result in death.

The nucleus moves into the bud via two general movements: movement of the nucleus to a site adjacent to the mother/bud neck, and then movement into the neck [67, 68]. The step of moving the nucleus to the neck has been broken down into several sub-steps (Figure 1.5). A nucleus within an unbudded cell undergoes a period of 'random' movement [69]. The end result of this 'random' movement is a net shift of the nucleus towards the mother/bud neck from its position distal from the neck immediately after the previous cell division [69]. This movement is due to the stochastic growth of astral microtubules emanating from a single SPB pushing against the cell cortex [69]. Next, microtubules growing from the daughter-bound SPB are captured by the incipient bud site or the bud tip cortex depending on the stage of bud development [68, 69]. The captured microtubules now shorten pulling the nucleus towards the neck [68]. This behavior is termed Capture/Shrinkage. Later on during G2/M phase, the microtubules closest to the bud move laterally along the bud cortex, pivoting at the daughter bound SPB [68, 70]. This behavior helps align the short spindle along the mother-bud axis [68].

Once the nucleus is positioned adjacent to the mother/bud neck, passage into the neck takes place concomitant with chromosome segregation. Microtubule "plastering" and consequent sliding of the microtubules along the bud cortex pulls the nucleus and spindle into the mother/bud neck [68, 70]. Sliding in the mother also occurs in order to keep the nucleus in the neck and prevent it from moving completely into the bud [68]. Now that the nucleus is in the neck the cells can undergo cytokinesis and divide into two distinct cells.

Many mutants have been identified and characterized that are lacking one or several of these nuclear migration processes. Mutants in *KAR9, BIM1, BNI1, BUD6* and *KIP3* have all been shown to have a deficiency in positioning the nucleus next to the neck

[68, 71-76]. Conversely, the yeast cytoplasmic dynein heavy chain, Dyn1p, and dynactin (the dynein regulatory complex) components-Arp1p, Nip100p and Jnm1p, have been implicated in transferring the nucleus into the neck [2, 70, 77, 78]. Thus, two sequential pathways control this process: one to position the nucleus next to the neck, and another to transfer the nucleus into the neck. Furthermore, although these pathways are distinct, they are partially redundant as synthetic defects (lethality or impaired growth) are seen in mutants between the two pathways [8, 73, 79, 80]. As a result, the two generalized steps of nuclear migration are named the "Kar9" and "Dynein" pathways, respectively (Figure 1.5).

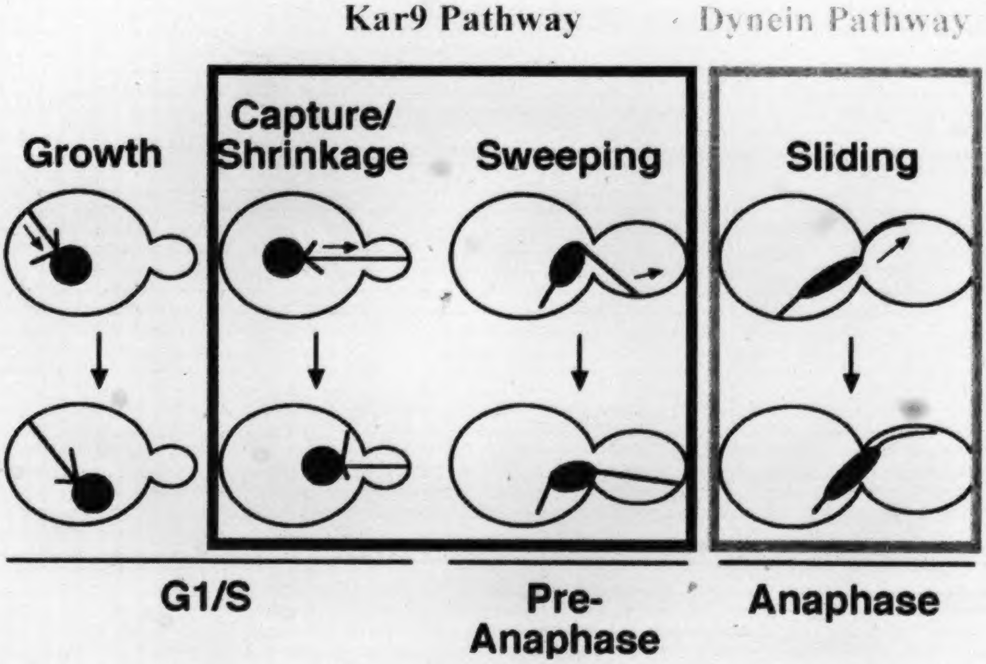

Figure 1.5. Summary of nuclear migration steps in *S. cerevisiae*. Here the microtubules move the nucleus adjacent to the mother/bud neck with the help of a set of proteins collectively called the Kar9 pathway (denoted in red). The nucleus then moves into the neck via microtubule sliding facilitated by another set of proteins called the Dynein pathway (denoted in green) (Modified from [68] with permission from author).

1.4.4 The Kar9 pathway

The Kar9p protein was first identified by a genetic screen that identified bilateral karyogamy mutants, which are unable to undergo nuclear fusion upon mating [81]. However, upon further analysis of this mutant it was clear that the karyogamy phenotype originally identified was due to a general defect in nuclear positioning and microtubule orientation rather than a defect in nuclear fusion [72]. Currently, it has been deduced that these defects are due to a lack of the Capture/Shrinkage and Sweeping mechanisms of nuclear migration (Figure 1.6) [68].

Both spatial and temporal fidelity is essential for proper nuclear migration. The most important step in positioning the nucleus adjacent to the neck is the temporally regulated dynamic localization of Kar9p. GFP fusion studies of Kar9-GFP (Kar9p fused with the green fluorescent protein) show that Kar9p localizes to the SPB, astral microtubules, and the bud tip cortex [72, 82, 83]. These localization studies have now illuminated the mechanism of Kar9p. In G1 Kar9p binds to the daughter-bound SPB [82]. Upon progression to G1/S, Cdc28p phosphorylates Kar9p which initiates transport of Kar9p to microtubule plus ends by the kinesin-related microtubule motor Kip2p [83]. The association of Kar9p with the microtubule plus end is then stabilized via phosphorylation by Cdc28p-Clb5p, which is hypothesized to facilitate an interaction between Kar9p and the microtubule binding protein Bim1p [83].

Bim1p is the yeast homologue of mammalian EB1 [84-86]. EB1 is a known microtubule plus end tracking protein (+TIP) [87]. +TIPs are defined as proteins that facilitate microtubule interactions by accumulating at and tracking/surfing on the plus end of microtubules and interacting with other proteins [88]. In addition to facilitating microtubule plus-end interactions, both EB1 and Bim1p stabilize microtubules [89, 90]. Interestingly, Kar9p, like many other nuclear positioning proteins shows some sequence homology to the human proteins [88]. In this case Kar9p displays homology to the known tumor suppressor adenomatous polyposis coli (APC) protein. The APC is known to bind EB1 and facilitate microtubule interactions with the cell cortex and chromosomes [91]. This homology is found within the Kar9p-Bim1p interaction domain and is homologous to the region with which APC interacts with the EB1 protein [91, 92]. As discussed below, the interaction of Bim1p with Kar9p is necessary for Capture/Shrinkage and Sweeping mechanisms of nuclear migration (Figures 1.5 and 1.6).

1.4.4.1 Microtubule capture/shrinkage

When Kar9p and Bim1p are present at the plus end of a microtubule, capture of the microtubule at the bud tip can occur. Previously, Kar9p was thought to be the cortical capture site of microtubules for this step. However, it was recently demonstrated by Huisman *et al.* that a *kar9*Δ strains maintained cMT capture, and this capture was dependent on the presence of the protein Bud6p [93]. As a result, Kar9p is now thought to provide proper microtubule delivery into the bud, but is not necessary for the subsequent capture and shrinkage [92, 93]. Once captured by the Bud6p cortical protein, shrinkage is able to occur.

Gupta *et al.* found that Kip3p (which has long been implicated in the Kar9 pathway by genetic interactions) is the microtubule depolymerization factor involved in microtubule capture-shrinkage [94, 95]. Kip3p is a plus-end directed kinesin that has a unique ATPase domain capable of causing microtubule catastrophe [95]. Not surprisingly, Kip3p migrates to microtubule plus ends where it accumulates. Thus, upon capture of a microtubule carrying accumulated Kip3p by a Bud6p cortical site, Kip3p-dependent microtubule catastrophe occurs, which pulls the nucleus towards the bud neck and produces the capture/shrinkage behavior observed in nuclear migration. However, it should be noted that Kip3p is not the only microtubule depolymerization factor as capture-shrinkage still occurs in kip3Δ cells.

1.4.4.2 Microtubule sweeping

Given that Kar9p-GFP is found at the bud cortex, which is known to be an area of actin polarization, Miller *et al.* [79] examined whether Kar9p was affected by actin stability. Upon treatment of cells with Latrunculin A, an actin depolymerizing drug, Kar9p was lost from the cortex [74, 79]. Moreover, this sensitivity was mimicked by the inactivation of the actin regulating formin, Bni1p, and the actin interacting protein Bud6p [73, 79]. Thus, it was hypothesized that Kar9p was a link between cMTs and cortical actin.

Concrete data for the interaction between actin and cMTs via Kar9p came upon the discovery that Kar9p interacted with the cargo-binding domain of the yeast type V myosin protein, Myo2p [74, 96]. Myo2p is responsible for transporting elements of the cell such as vesicles into the bud [96]. When switched to a non-permissive temperature, a *myo2-66* temperature sensitive strain was not able to localize Kar9p-GFP to the actin cortex of the bud [74]. In turn, this finding lead to the idea that Kar9p, which is attached to microtubule plus ends by Bim1p, associates with Myo2p found at the bud cortex. This hypothesis was addressed by an elegant experiment using a Myo2p-Bim1p fusion protein. This fusion protein bypassed the requirement for Kar9p and suppressed the nuclear migration defects seen in *kar9* mutants [97].

So how exactly does this interaction aid in nuclear migration? As described previously, cMTs (presented by the daughter bound SPB) are decorated by Kar9p-Bim1p complexes at their plus end. These plus ends then bind to the actin motor Myo2p at the mother-bud neck. The Myo2p protein then transports the Kar9p-Bim1p-cMT complex towards the bud tip [74, 96], exerting a pulling force on the nucleus and positioning of the nucleus adjacent to the bud neck [96].

The coordinated action of the capture/shrinkage and sweeping behaviors of cMTs provide the pulling forces necessary to prepare the nucleus for entry into the mother-bud neck (Figure 1.5). Once adjacent to the neck the Dynein pathway can complete proper nuclear migration by pulling the nucleus into the neck.

1.4.5 The dynein pathway

The movement of the nucleus into the mother/bud neck is also dependent on cytoplasmic dynein [68, 78]. Sliding of cytoplasmic microtubules along the bud cortex drives this movement (Figure 1.6) [68]. Experiments with GFP fused to the dynein heavy chain Dyn1p, have shown that dynein localizes dynamically to microtubule plus ends and statically at the bud cortex [98, 99]. As a result of localization studies, a dynein offloading model was proposed [98, 99]. According to this model, dynein is transported to the cMT plus ends where it is offloaded to the bud cell cortex, anchored, and finally activated [99]. At this point the dynein motor domain attaches to the cMTs emanating from the daughter bound SPB and pulls them towards the bud tip. This action is responsible for the sliding behavior of cMTs during spindle movement into the neck.

Dynein is originally known as an ATPase that was necessary for movement in cilia and flagella. However, a cytoplasmic role was also identified for dynein in which it was found to be necessary for retrograde axonal transport in neurons [100]. The two types of dyneins (flagellar and cytoplasmic) are different, but homologous proteins. Currently, more is actually known about the vertebrate cytoplasmic dynein components than their respective homologues in *S. cerevisiae*. To date *S. cerevisiae* has only been shown to have one heavy chain (HC), one intermediate chain (IC), one light intermediate chain (LIC), and one light chain (LC).

1.4.5.1 Composition of the dynein molecular motor

Each subunit of cytoplasmic dynein has distinct roles. The best understood role of the dynein components is that of the HC, which is conserved among the majority of eukaryotes. Dynein contains multiple AAA ATPase domains, several P-loop nucleotide triphosphate hydrolase domains, and a microtubule-binding domain [101]. One of the AAA ATPase domains is responsible for hydrolyzing ATP and, thus, provides the energy for translocation of dynein along microtubules [102, 103]. These elements thus make up the motor domain of dynein. The yeast homologue of the dynein HC was discovered through its homology to a known homologue in *Dictyostelium* [2, 78]. Upon further characterization of dynein in *S. cerevisiae*, researchers demonstrated that *dyn1*Δ cells grown at ~14°C have aberrant localization of nuclei [2, 78]. Instead of one nucleus in the mother and one in the daughter, a large proportion of cells contain two nuclei in the mother (binucleate) and none within the bud (anucleate) [2, 78]. This phenotype reflects defects in nuclear migration. However, these defects are not accompanied by defects in spindle assembly, spindle elongation, or chromosome segregation [2, 78]. Together these characteristics are known as the dynein phenotype and are common to mutants in most dynein components.

Of the dynein accessory components, the most well known are the ICs which fall in the size range of 60-75 kDa [101]. The ICs contain a conserved N-terminal domain that interacts with the dynein regulatory component dynactin [101, 104, 105]. Furthermore, the C-terminal domain contains a WD40 repeat domain that is conserved in all dynein ICs [101, 105, 106]. This WD40 repeat domain mediates interactions with other dynein components including the HC [105, 106]. Thus, HC and IC components act as scaffolds for the whole dynein complex. The only known *S. cerevisiae* IC homologue is Pac11p [98]. Pac11p is linked to the dynein pathway because, like *dyn1*Δ cells, binucleate mother cells are observed in *pac11*Δ mutants. Cells lacking Pac11p also show synthetic growth defects with Kar9 pathway components *KAR9, KIP3, BNI1, BIM1*, and *MYO2* [8, 98]. Moreover, Pac11p has also been shown to physically interact with Dyn1p *in vivo* [107]. Dyn1p-3GFP (Dyn1p fused to a triple copy GFP tag) is not able to accumulate on the microtubule plus ends in *pac11*Δ cells [98]. In addition there are decreased levels of Dyn1p in *pac11*Δ cells [98]. These data suggest that Pac11p is necessary for Dyn1p stability and is consistent with a scaffold function for Pac11p.

Other dynein subunits have not been characterized to the same extent as the HC and ICs. Studies in other eukaryotes have produced the hypothesis that LICs and LCs interact with different cargoes that dynein transports [98, 101]. Recently, the *S. cerevisiae* LIC was discovered by a genome wide screen of the dynein phenotype and also by a screen for synthetic lethality with *kar9*Δ [8, 98]. Upon the observation that this protein co-localized and co-immunoprecipitated with Dyn1p, this protein was named Dyn3p [98]. As in the case of the IC Pac11p, functional analysis was carried out on Dyn3p by observing Dyn1-3GFP localization. Interestingly, Dyn1p-3GFP accumulates normally on microtubule plus ends in *dyn3*Δ cells [98]. However, Dyn1p-3GFP was not able to offload onto the cell cortex [98]. The conclusion for these observations was that Dyn3p is necessary for the offloading process (possibly by enabling attachment to the cortex) but is not required to target dynein to plus ends or for stability of the dynein complex [98].

Although the dynein LCs are arguably the least understood of the dynein subunits, the importance of these proteins is clear by the finding that multiple families of these proteins are found in both flagellar and cytoplasmic dyneins [9]. There are three major classes of dynein light chains associated with cytoplasmic dynein - Tctex, LC8, and LC7/roadblock [108-111]. All of these LCs interact with the dynein IC [112-114]. This specific binding of LCs to the ICs cause the ICs to form a more ordered structure [112-114]. This conformational change is speculated to aid in the dimerization of the ICs [115].

The second and probably most important function of the LCs is to facilitate binding of cargo. Several studies show that LCs bind multiple proteins and that this binding is necessary for their transport and subsequent localization [9].

The Tctex family is one major family of light chains (As reviewed in [9]). The Tctex family consists of two major subgroups - Tctex-1, and Tctex-2. The first Tctex proteins (Tctex-1, and Tctex-2) were found within mice. These genes were found within the *t* complex region of chromosome 17 within mice. This *t* complex is known to be an area that is inherited in a non-mendilian ratio through a process called transmission ratio distortion [9]. Although the process of this distortion is still not fully elucidated it has been noted that *t* complex mice have immobile sperm [9]. This finding has now been explained by the Tctex light chains in flagellar dynein [9]. Since this discovery the role of the Tctex proteins in dynein function has been investigated further. Native gel analysis and yeast two-hybrid analysis demonstrated that the Tctex-1 family forms a dimer *in vivo* while the Tctex-2 family members are found as monomers [116]. The Tctex-2 family monomers have been shown to stabilize dynein ICs and aid motor function [117]. Tctex-1 family on the other hand is involved in dynein-cargo interactions and as such transports several molecules throughout the cell. For example, Tctex-1 mutations cannot effectively traffic rhodopsin [118]. Thus, literature shows that Tctex members are capable of both light chain functions and have shown crucial to several processes.

Out of the diverse group of LC proteins only one homologue has been found in *S. cerevisiae*. This protein was identified by its homology to LC8 family of light chains in human, *Drosophila*, and *C. elegans* and was consequently named Dyn2p [119]. Up to now, the identity of Dyn2p as a LC has only been confirmed by the synthetic genetic interactions of *dyn2*Δ mutants with the mutants in the Kar9 pathway [8]. This work presented will demonstrate that a new yeast Tctex homologue may be a dynein LCs.

1.4.5.2 Composition of the dynactin regulatory complex

Although not a component of the cytoplasmic dynein complex, a 1200 kDa regulatory complex named dynactin (*dyn*ein *act*ivator) has been described as an intimate partner to dynein as it is utilized in every dynein-dependent process known to date, with the exception of intraflagellar transport [120, 121]. The function of dynactin is best described from a structural standpoint. The structure of dynactin has been examined by Rotary shadow EM [122]. This study demonstrated that dynactin is composed of two distinct domains: a 10 x 40 nm rod and a 50 nm arm [122]. These two structures provide the ability of dynactin to interact with various components within the cell such as different cargo and dynein (reviewed by [121]).

The dynactin rod is thought to bind to cargo for dynein, including organelles via their membranes [121]. The rod is composed of an actin related protein filament called Arp1p [123]. Arp1p forms into a short octamer [123]. Also like conventional actin, the Arp1p filament is capped on the minus and plus (barbed) ends [122]. The barbed end is capped by the common actin plus end capping protein CapZp, and the minus end is capped Arp11p, which is specific to Arp1p filaments [122, 124]. Finally, the last components of the rod complex found in vertebrate cells are: p25, p27, and p62 [121]. Although, some characterization has been accomplished for these components they will not be addressed further as they have not been identified in budding yeast *S. cerevisiae*.

In contrast to the rod structure, the arm of dynactin contains only three subunits: p150$^{\text{Glued}}$, p50$^{\text{dynamitin}}$, and p24/22 [121]. Each arm contains dimmers of *p150*^{Glued}, and *p24/22*, as well as a tetramer of dynamitin. The main function of the oligomer comes from the *p150*^{Glued} subunit which physically interacts with dynein and increases dynein's processivity [104, 125, 126]. This may be achieved by the globular head, which is capable of microtubule binding [127]. This microtubule binding capability is necessary to increase dynein's processivity [126]. The middle portion of the p150$^{\text{Glued}}$ protein provides dynein intermediate chain binding [104, 122, 124, 125]. Dynamitin and p22/24 fill the essential role of connecting the *p150*^{Glued} arm with the *Arp1* rod as they bind to both p150$^{\text{Glued}}$ and Arp1p [122, 124]. In summary, the dynactin arm connects to the dynein molecular motor complex providing attachment of dynein to cargo and cellular components that are attached to the rod. Further, the microtubule binding capability of the arm increases the processivity of the motor action of dynein.

Several homologues of the vertebrate dynactin complex have been found within *S. cerevisiae*. The dynactin arm is composed of Nip100p, Jnm1p, and Ldb18p, which are homologues of p150$^{\text{Glued}}$, dynamitin, and p24/22, respectively [128] (Ranran Zhang/Neil Adames, unpublished data). Further, the rod component Arp1p is homologous to the yeast protein of the identical name [77]. The dynactin barbed-end capping protein is also represented in yeast by the conventional capping heterodimer of Cap1p and Cap2p [128]. What is more interesting is the finding that loss of function mutations in almost any of these yeast dynactin homologues leads to nuclear migration defects as severe as that in a *dyn1*Δ strain [77, 107, 128, 129]. This suggests that the dynein pathway is completely knocked out when dynactin is inactivated. The finding that the yeast dynactin genes are synthetically lethal with the Kar9 pathway supports this statement [8]. Thus it can be concluded that the dynactin complex is imperative to the process of nuclear migration.

Dynactin might increase the processivity of dynein and help attach dynein to the bud cortex, allowing movement of the nucleus into the bud.

In addition to the dynein molecular motor and the dynactin regulatory complex, there are several accessory proteins required for proper localization and functioning of dynein. As I have referred to earlier, dynein localizes to microtubule plus ends. Presumably, this localization facilitates the offloading process. This offloading model incorporates two cooperative pathways. The first pathway is composed of Bik1p (the yeast homologue of the human +TIP *CLIP-170*), and the kinesin Kip2p, while the second pathway is composed of Pac1p (the yeast Lissencephaly protein homologue) and Ndl1p [130-132]. The yeast *CLIP-170* homologue, Bik1p is necessary for accumulation of dynein to MT plus ends [132]. However, unlike its human homologue, Bik1p requires the kinesin Kip2p for this function [132]. Here it is predicted that Kip2p transports Bik1p to the plus end since they co-migrate to microtubule plus ends *in vivo* [132]. Interestingly, Kip2p is also necessary for dynein transport to the plus ends [132].

The second pathway for localizing dynein to the microtubule plus ends is facilitated by the lissencephaly protein (*LIS1*) homologue [99]. Also involved in this pathway is Ndl1p, whose loss causes a ~ 10-fold decrease in Dyn1p-3GFP targeting to the microtubule plus ends [133]. Ndl1p loss also causes mislocalization of Pac1p-3GFP but not Bik1p-GFP. Thus, Ndl1p seems to localize dynein to the microtubule plus ends via Pac1p but not Bik1p [133]. Consistently, loss of Pac1p causes the loss of Ndl1p from microtubule plus ends [133]. The Bik1p-Kip2p and Pac1p-Ndl1p pathways have little or no effect on the localization of the other [133]. Interestingly, deletion of either pathway results in a significant decrease of dynein at the microtubule plus ends and correlative nuclear migration defect [133]. Therefore, these pathways are independent of each other, but localize dynein in a cooperative manner.

Once dynein is transported to the plus ends it is offloaded to the cell cortex. This process requires a cortical anchor. This leads us to one of the final accessory components - the cortical attachment protein Num1p. Num1p was originally linked to the dynein pathway because *num1Δ* mutants have the dynein mutant phenotype [134] – they have many binucleate cells, microtubule sliding during anaphase is abrogated, and the mutant shows synthetic genetic interactions with mutants in the Kar9p pathway [135]. Num1p is localized to cortical patches and not microtubules suggesting that it may be cortical anchor for dynein-dynactin [134]. This model is supported by the observation that Num1p co-immunoprecipitates with Pac11p [135].

In summary, yeast cytoplasmic dynein is assembled into a large multi-subunit complex composed of homodimers of Dyn1p, Dyn2p, Pac11p, and Dyn3p. This complex is transported from the SPB and minus ends of microtubules to the plus ends via Kip2p/Bik1p and Pac1p/Ndl1p. This plus end-associated dynein is then offloaded from the plus end onto the cortical anchor protein Num1p [98]. Dyn3p dissociation from dynein is required at this step as *dyn3*Δ strains cannot undergo offloading and Dyn3p is not present in cortically associated dynein from microtubule plus ends [98]. Furthermore, dynactin is known to be necessary for the attachment of dynein to the cell cortex as dynactin mutants are also unable to offload dynein [98]. However, the temporal regulation of dynactin attachment to dynein is unknown, as no one has been able to assess dynactin localization. Once cortically attached, the motor domain of the dynein-dynactin complex attaches to cMTs and moves in a minus end directed manor. Subsequently, cortically-anchored dynein pulls on the cMTs producing the dynein-dependent sliding motion and pulling the nucleus into the mother/bud neck [68].

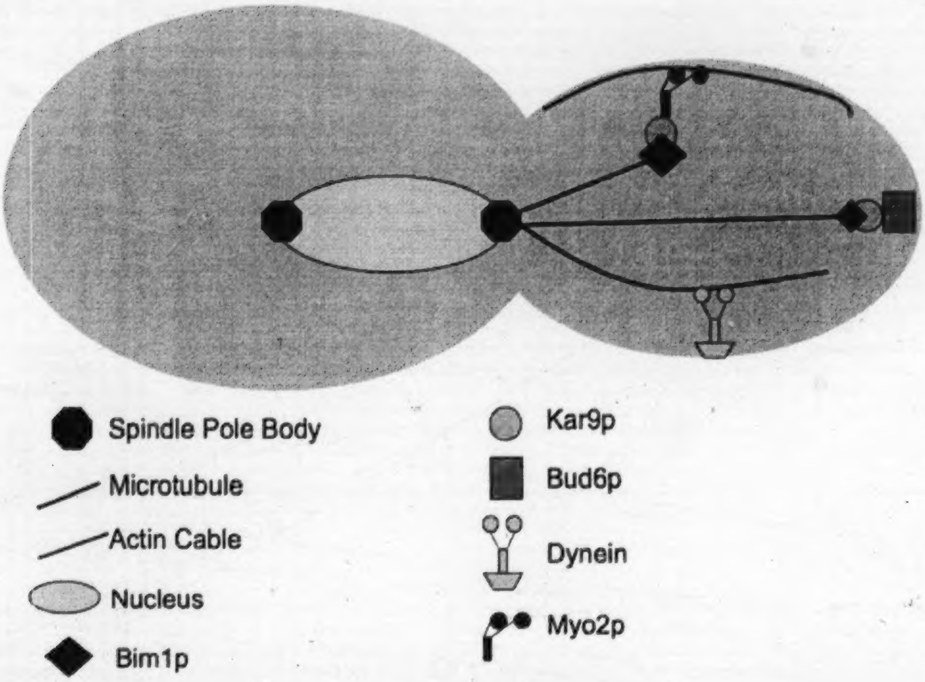
Spindle Pole Body
Microtubule
Actin Cable
Nucleus
Bim1p
Kar9p
Bud6p
Dynein
Myo2p

Figure 1.6. Summary of Kar9 and dynein pathways. Microtubules emanate from the daughter bound SPB and with the help of Bim1p/Kar9p bind the cortical attachment site (Bud6p) and the molecular motor Myo2p. This binding enables movement of the nucleus to a site adjacent to the neck via shrinkage and sweeping of microtubules. Microtubules also bind the cortically bound dynein molecular motor and slide the nucleus towards the daughter cell (Modified from [136]).

1.4.6 Septin structure and assembly

Septins are a highly conserved group of proteins that form a hetero-oligomeric structure (reviewed in [137, 138]). In *S. cerevisiae*, they form a ring that is found at the mother-bud neck. *S. cerevisiae* encodes seven septins, most of which were identified as temperature sensitive mutations that were defective in cytokinesis [139]. Septins act as a membrane associated scaffold and as a mother/daughter cell diffusion barrier [137]. Moreover, these functions are essential to proper mitotic exit [137]. The mitotic septins include: Cdc3p, Cdc10p, Cdc11p, Cdc12p, and Shs1p/Sep7p. The septin structure assembles in a temporally and spatially regulated manor that is explained by a three-step model proposed by Longtine and Bi [138]. In the first step of this model, the septins start assembling in G1 where they are seen as a small ring or 'cap' like structure that contains highly mobile components found at the incipient bud site. This localization of the septins to the incipient bud site is regulated by the Cdc42p cell polarity GTPase (as discussed earlier). The second step in this process is the formation of a cortical septin ring at the incipient bud site. This step has been observed to take place at S phase [137]. The trigger for this step seems to be GTP hydrolysis by Cdc42p as deletions in the Cdc42p GAPs (*bem3*Δ, *rga1*Δ, and *rga2*Δ) cause a delay in septin ring formation [140, 141]. The third step in this process is the transformation of the septin ring on the mother side of the neck to a stable septin hourglass-shaped structure spanning the mother-bud neck during G2 [138]. The hourglass shape is caused by the expansion of the cortical ring through the neck into the bud. The Cdc42p effectors Cla4p and Gin4p trigger the assembly of this hourglass structure. Here Cla4p phosphorylates the septins Cdc3p, Cdc10p, and Cdc11p, while Gin4p phosphorylates Shs1p exclusively [64, 142-144]. During mitotic exit, the septin collar splits into two distinct rings – one inherited by the mother, the other by the bud. This splitting process is thought to be controlled by the PP2A complex associated with the B-type regulator Rts1p [145].

1.5 Mitotic exit.

Once the genetic content has been equally distributed to both mother and daughter cells, exit from mitosis can occur. Ultimately, mitotic exit is the preparation and completion of cytokinesis. Accordingly, for exit from mitosis to occur, both activation and inhibitory events must occur. For example, activation of karyokinesis, relocalization of components (such as actin) to the primary septum, and cytokinesis occur during mitotic exit. Conversely, several processes initiated and necessary for proper mitosis are inactivated. These processes include spindle disassembly, and chromosomal decondensation. Additionally, mitotic exit requires the inactivation of the mitotic Cdc28p-Clbp complex. This inactivation is carried out by the orchestrated interaction of several pathways called the mitotic exit network (MEN), spindle position checkpoint (SPC), and the Cdc fourteen early anaphase release (FEAR). Recently, the addition of the Cdc42p cell polarity pathway has been implicated in the general regulation of this process. Thus, the overall regulation of mitotic exit is complex yet effective (Figure 1.7).

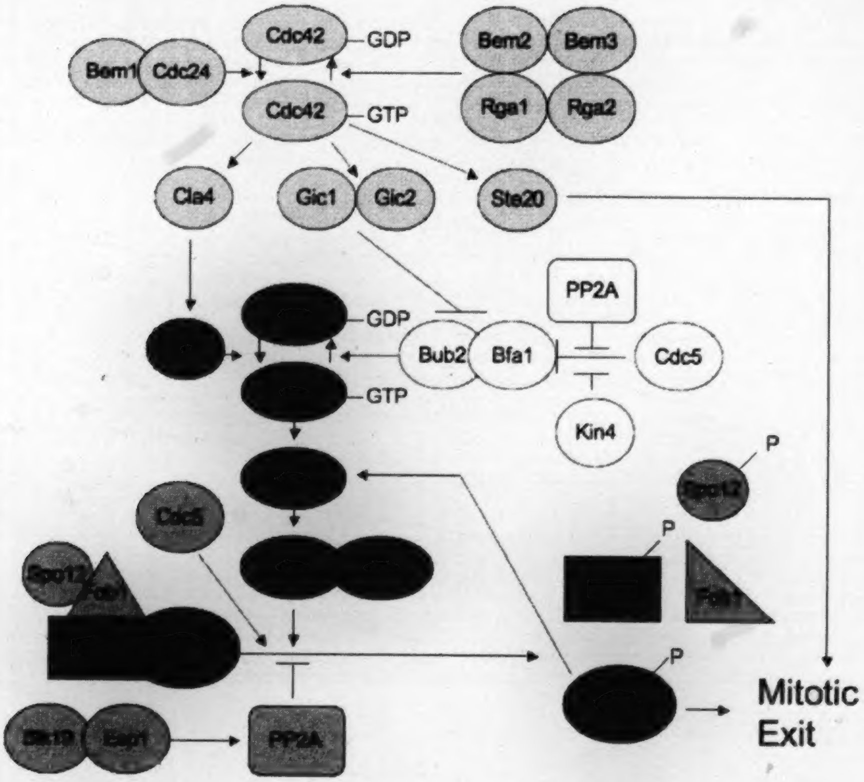
Cdc42
GDP
Bem2
Bem3
Bem1
Cdc24
Cdc42
GTP
Rga1
Rga2
Cla4
Gic1
Gic2
Ste20
PP2A
GDP
Bub2
Bfa1
Cdc5
GTP
Kin4
P
Spo12
Cdc5
P
Spo12
Fob1
Fob1
P
Slk19
Esp1
PP2A
Mitotic
Exit

Figure 1.7. Summary of the pathways leading to mitotic exit. The mitotic exit network (MEN) is shown in red, the spindle position checkpoint (SPC) is shown in yellow, and the Cdc14 early anaphase release (FEAR) pathway is shown in blue, and the Cdc42p signaling pathway is shown in green.

1.5.1 The mitotic exit network (MEN)

A groundbreaking study by Jaspersen *et al.* [1] used several temperature sensitive alleles of essential genes that result in large budded cells arrested in late mitosis. These strains were used to produce an epistatic pathway of genes required for mitotic exit. These alleles include: *cdc15-2, cdc5-1, cdc14-1, dbf2-2,* and *tem1-3.* Jaspersen *et al.* [1] demonstrated that overexpression of the mitotic cyclin Clb2p exacerbated the mitotic exit defect of these conditional alleles suggesting that these genes are required for Clb2p degradation during mitotic exit. These this subsequent ordered pathway was termed the mitotic exit network or MEN (Figure 1.7) [1].

The MEN pathway hinges on one essential Ser/Thr phosphatase called Cdc14p [146, 147]. This protein phosphatase is the major cause of inactivation of the mitotic CDKs in yeast. Inactivation of mitotic CDKs occurs by three pathways. First, dephosphorylation of Sic1p by Cdc14p allows this protein to bind and inhibit mitotic CDKs [147-149]. Secondly, mitotic CDK's are inhibited through specific targeting and degradation of their mitotic cyclins [147]. This process is accomplished through the Cdc14p dependent activation of APC^{Cdh1}, an E3 ubiquitin ligase, that targets the mitotic cyclins for degradation [147, 150]. Once the mitotic CDKs are properly inactivated mitotic exit occurs. Finally, Cdc14p directly dephosphorylates CDK substrates thus antagonizing the mitotic CDKs [147].

So how is the protein phosphatase Cdc14p regulated? The activity of Cdc14p is tightly regulated by its inhibitor Net1p (Figure 1.7) [151-153]. Net1p is thought to be a direct inhibitor of Cdc14p's function by binding to Cdc14p and blocking its active site [154]. Moreover, Cdc14p is also sequestered by Net1p within the nucleolus [151]. Upon progression to anaphase, Cdc14p is released from the nucleolus into the cell to begin dephosphorylation steps that result in mitotic exit [151].

Previous genetic analyses have placed *TEM1, CDC5, CDC15,* and *DBF2* upstream of the *CDC14-NET1* complex [155-157]. This was concluded by studies showing that loss of *NET1* or overexpression of *CDC14* can suppress the mitotic arrest caused by temperature sensitive alleles of the other MEN components. Thus, the MEN was hypothesized to converge on the Cdc14p-Net1p complex and thus regulate the release of Cdc14p from the nucleolus (Figure 1.7). In fact, release of Cdc14p from the nucleolus seems to be triggered by phosphorylation of Cdc14p and Net1p in concert [153, 158, 159]. Phosphorylation of Net1p depends upon a kinase cascade from Tem1p to Cdc15p to Dbf2p [160], while Cdc14p is phosphorylated by Cdc5p [159].

Genetic and functional analyses have shown that the Ras-like GTPase Tem1p activates the MEN pathway (Figure 1.7) [155]. Here Tem1p acts as a switch which can activate the MEN when Tem1p is in its GTP-bound form but not when in its GDP-bound form [1, 151, 153]. This GDP to GTP state conversion is initiated by the presumed guanine nucleotide exchange factor Lte1p [161, 162]. The temporal and spatial regulation of this exchange elegant and essential. As shown by fluorescence microscopy, Tem1p is found at the daughter-bound SPC while Lte1p is found exclusively on the cell cortex of the bud [163]. The two proteins are spatially isolated from each other until the daughter bound SPB enters the bud during anaphase. Penetration of the daughter-bound SPB into the daughter allows Tem1p to come into contact with Lte1p and causes a GDP to GTP switch [161]. This conversion to Tem1p-GTP activates Cdc15p, most likely through a direct interaction as the two proteins co-immunoprecipitate [155, 164].

Once Cdc15p is activated it then can activate the next protein in the pathway Dbf2p by phosphorylation. Dbf2p phosphorylation by Cdc15p depends upon the interaction of Dbf2p with its essential binding partner Mob1p [160, 165]. After phosphorylation of Dbf2p-Mob1p by Cdc15p, the Dbf2p-Mob1p complex is thought to migrate to the nucleolus from the SPB as Mob1p has been shown to co-localize with Cdc14p in anaphase cells [166]. Dbf2p-Mob1p has been suggested to be the kinase that directly phosphorylates Net1p as predicted by proteome kinase chip analysis [167]. However, this finding has never been directly confirmed by kinase assays or co-immunoprecipitation.

The second step in Cdc14p release is the phosphorylation of Cdc14p itself (Figure 1.7). This step seems to occur prior to MEN activation and requires the Polo kinase Cdc5p. This phosphorylation results in the early release of Cdc14p. Cdc14p early release is also dependent upon several other proteins, which, together with Cdc5p, called the FEAR pathway. As FEAR signaling is complex and separate from the MEN it will be addressed below. Upon phosphorylation of Cdc14p and Net1p by the FEAR and MEN, total Cdc14p release can occur. The final step of the pathway facilitated by a positive feedback loop. Release of Cdc14p acts in a positive feedback mechanism by dephosphorylating Cdc15p which increases its MEN enhancing activity [27]. In turn, this step ensures an efficient release of Cdc14p leading to a timely exit from mitosis.

Obviously this process must be highly regulated. Premature release of Cdc14p can be detrimental to the cell by causing early mitosis or antagonism to the mitotic CDKs. Thus, a relatively complex system has evolved to regulate this process by both direct inhibition and timely activation.

1.5.2 The spindle position checkpoint (SPC)

The first indication of direct inhibition of the MEN pathway actually came from examining dynein mutants, which are defective in the transport of the daughter-bound SPB into the bud. Interestingly, these cells do not progress through mitosis until the spindle is properly aligned and inserted in the mother-bud neck [168]. It seemed as though the cells could 'sense' the mispositioning of the spindle and mitosis was arrested until proper orientation could occur. This arrest was termed the SPC (Figure 1.7, Figure 1.8). Researchers then determined that *bub2*Δ mutants lacked the anaphase arrest observed in dynein mutants [30]. Further, it was soon observed that Bub2p formed a heterodimeric GTPase activating complex with Bfa1p that serves to inhibit Tem1p [169].

Bub2p and Bfa1p are found at the cytoplasmic face of the daughter-bound SPB during early mitosis and physically interact with Tem1p [170, 171]. This direct interaction activates the GAP activity of Tem1p which keeps the protein in its GDP bound form [169]. As Lte1p is found at the bud cortex an attractive spatial isolation model has been proposed (Figure 1.8). This Model proposes that the SPC is the result of spatial isolation of Lte1p and Tem1p-GDP/Bub2p/Bfa1p until the spindle spans the neck. At this time Lte1p is able to activate the turnover of Tem1p-GDP to Tem1p-GTP thus initiating Cdc14p release (Figure 1.8).

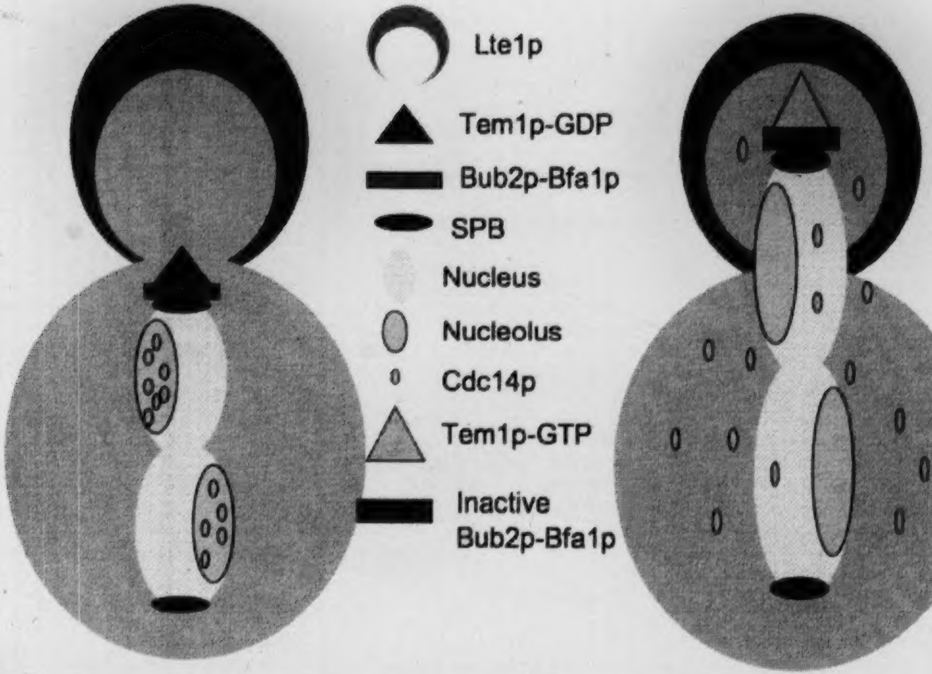

Figure 1.8. Spatial isolation model for the SPC. The GAP complex Bub2p/Bfa1p on the daughter bound spindle pole body keeps the G-protein Tem1p in its inactive GDP bound form. When the spindle spans through the mother-bud neck, Lte1p in the bud activates Tem1p and overcomes the Bub2p/Bfa1p GAP activity. Active Tem1p-GTP signals the release of Cdc14p from the nucleolus leading to down-regulation of the mitotic CDKs and thus exit from mitosis (Modified from [172]).

Although this model does not explain how an *lte1*Δ strain undergoes mitotic exit with normal kinetics when grown at 30° C or 37°C [31]. Furthermore, this hypothesis is supported by observations that *lte1*Δ dynein double mutants delay their cell cycle upon spindle mispositioning. However once the spindle enters the neck the cells exit mitosis with proper kinetics [31]. Additionally, proper mitotic exit in these mutants is dependent upon the presence of the SPC genes *BUB2* and *BFA1* [31]. These observations point to an alternate activator of mitotic exit independent of Lte1p. So what is this alternate activator? Interestingly, several mutants that are defective in cytoplasmic microtubules (cMTs) are also defective for the SPC in a dynein mutant background [31]. Moreover, in cells with mispositioned spindles, there is a correlation between the absence of cMTs protruding through the neck and the loss of the SPC. This apparent involvement of the neck-cMT interactions in the regulation of mitotic exit is supported by observation that the same improper mitotic exit occurs in an *lte1*Δ septin mutant (*cdc10*Δ) [173]. Thus, it has been hypothesized that is a spindle/microtubule sensor at the mother/bud neck that is capable of inactivating Bub2p/Bfa1p in the absence of cMT-neck interactions or that is necessary to maintain Bub2p/Bfa1p activity in the presence of cMT-neck interactions [31].

Support for this hypothesis comes from data showing that Bub2p and Bfa1p are both inhibited by hyperphosphorylation [28, 29, 170, 171]. Bub2p and Bfa1p are phosphorylated in part by Cdc5p [28, 29]. Moreover, the mitotic exit defect of a *cdc5-2* conditional allele is partially suppressed by deletions of *BUB2* or *BFA1* [28, 29]. Thus, a cytoplasmic microtubule sensor residing at the mother-bud neck could inhibit or activate Cdc5p. Consequently; this inhibition would lead to hypophosphorylation of Bub2p and Bfa1p, subsequently maintaining activation of the SPC. However, to date this sensor has not been identified.

In addition to Bub2p and Bfa1p, the Kin4p kinase is also necessary for the SPC [174, 175]. Kin4p was identified as a SPC protein by two distinct methods. First the *kin4*Δ mutation was shown in a genomic screen to be synthetically lethal with *kar9*Δ [8, 175]. This synthetic lethality was shown to be caused by a combination of mispositioned spindles and premature mitotic exit. Thus, the double mutants accumulated binucleate mother cells and anucleate bud cells. Secondly, Kin4p mutations were also shown by Angelika Amon's group to rescue mitotic exit deficient cells [174]. Kin4p, was also shown to be necessary for the SPC as overexpression of Kin4p in normal cells caused a block of mitotic exit [174, 175]. However, most interestingly was their finding that Kin4p localization was limited to the *mother*-bound SPB and the *mother* cell cortex [174, 175]. This is in contrast to the other SPC components which are found on the cytoplasmic side of the *daughter*-bound SPB [176]. However, in the presence of spindle mispositioning, Kin4p is re-localized to both SPBs [175]. Furthermore, in cells that overexpress Kin4p, Bfa1p phosphorylation levels drop, but loss of Kin4p increases phosphorylation of Bfa1p which is dependent on the presence of Cdc5p [174]. This suggests that Kin4p has an unknown inhibitory role upon the polo kinase Cdc5p [174, 175].

Previous genetic screens have identified Cdc55p as a mitotic checkpoint protein by showing that *ctf13-30* (a temperature sensitive allele that is known to be synthetic lethal with mitotic checkpoint mutants) was synthetically lethal with a *cdc55*Δ mutation [177]. The role of Cdc55p in the spindle position checkpoint remained elusive until the protein phosphatase machinery PP2A was shown to be involved in the SPC [176, 178, 179]. PP2A is a protein phosphatase that is involved in several essential processes within the cell [180]. The PP2A complex is composed of the scaffold protein Tpd3p, one of two catalytic components (Pph21p or Pph22p), and one of the B-type regulatory subunits (Rts1p or Cdc55p) [179-181]. As PP2A is a known phosphatase, it is hypothesized that its inhibitory role on the MEN is by dephosphorylation of the SPC components Bub2p and Bfa1p. The finding that *cdc55*Δ strains show an increase in Bfa1p phosphorylation supports this hypothesis [179]. However, a separate study demonstrated the converse of this finding [176]. Therefore, the exact mechanism by which the PP2A affects the SPC remains unclear.

1.5.3 The Cdc14 early anaphase release network (FEAR)

The second mechanism by which Cdc14 release is regulated is coordinated by the Cdc14p early anaphase release or FEAR, which I referred to earlier (Figure 1.7). The FEAR pathway is semi-parallel to the MEN. Intriguingly, the FEAR pathway is not essential for mitotic exit unless the MEN is compromised. The first indication of the FEAR pathway was that MEN deficient cells still display a small/temporary release of Cdc14p-GFP from the nucleolus during early anaphase [182, 183]. Various methods have now been used to identify the components for this early release of Cdc14p and are collectively called the FEAR network. The proteins Spo12p, Spo12p's homologue Bns1p, Slk19p, Esp1p, Cdc5p, Fob1p, and PP2A have been identified as FEAR components [179, 182, 184]. Overall this pathway effects Cdc14p release via two mechanisms: inhibition of Net1p, or phosphorylation of Cdc14p. Prior to anaphase the release of Cdc14p from Net1p is monitored by PP2A and Fob1p. Here PP2A prevents phosphorylation of Net1p by the MEN thus leaving Cdc14p sequestered in the nucleolus

[179]. Fob1p was also identified as a negative regulator of Cdc14p release [184]. Fob1p is thought to bind Net1p directly and inhibit the release of Cdc14p as shown by immunoprecipitation and gene knockout studies [184]. This inhibition remains throughout the cell cycle until the FEAR protein Spo12p is activated. Spo12p and Fob1p are binding partners. Spo12p is phosphorylated during anaphase, which abolishes its interaction with Fob1p [184]. This loss of interaction is thought to cause an allosteric change in the Fob1p protein that abrogates its inhibitory action upon Net1p phosphorylation.

In contrast to Spo12p, Fob1p and PP2A, which are negative regulators of Cdc14p release, Slk19p, and Esp1p are activators of the FEAR. Consistent with this role, these genes are both synthetically lethal with MEN mutants [182]. These activators of FEAR work by inhibiting PP2A [179]. This inactivation starts with the bi-orientation of kinetochores with nuclear microtubules. Upon this bi-orientation and proper tension on the kinetochores the cells progress into anaphase. Progression into anaphase is triggered by the degradation of the protein securin (Pds1p) resulting in the release and activation of the separase Esp1p that is involved in cleaving proteins that prevent progression into anaphase [185]. One such protein that Esp1p cleaves is another FEAR component - Slk19p [182, 186, 187]. However, this cleavage activity seems to be unnecessary for the FEAR network as a Slk19p mutant engineered to be resistant to cleavage by separase is still capable of releasing Cdc14p in early anaphase [187]. Slk19p is hypothesized to target Esp1p to the kinetochore [187]. Esp1p activation by Pds1p degradation, and targeting via Slk19p, facilitates a direct interaction between Cdc55p and Esp1p which downregulates PP2A activity [179]. In turn, this decrease in PP2A activity is hypothesized to allow the accumulation of Net1p phosphorylation, aiding Cdc14p release [179].

Overall the FEAR network allows transient amounts of Cdc14p to be released upon progression into early anaphase. Although the FEAR pathway is not essential for mitotic exit, FEAR mutations do show a delay of mitotic exit onset [182]. Accordingly, it is thought that the FEAR may trigger the MEN in a timely manner by causing a positive feedback loop through dephosphorylation and activation of Cdc15p by the early-released Cdc14p. Consistently, Cdc15p is not properly dephosphorylated during anaphase in

FEAR mutants [182]. These observations support the hypothesis that the FEAR pathway releases transient amounts of Cdc14p, which causes a positive feedback loop via dephosphorylation of the MEN component Cdc15p. In turn, this action facilitates several functions required prior to mitotic exit and ultimately timely and efficient execution of mitotic exit by the MEN.

1.5.4 Cdc42 signaling and mitotic exit

In addition to regulating cell polarity and growth, several studies have now linked Cdc42p and several of its effectors to mitotic exit (Figure 1.7) [188-191]. For example, the Cdc42p effector Ste20p was found to be a multi-copy suppressor of *lte1*Δ cells [188]. Additionally, conditional alleles of Cdc42p and Cdc24p as well as *ste20*Δ were all found to be synthetically lethal with *lte1*Δ cells [188]. In contrast, *cla4*Δ cells do not show synthetic interactions with *lte1*Δ but do so with *ste20*Δ [188]. Thus, these data have shown that Ste20p activates mitotic exit via a pathway distinct from Lte1p. Further, this pathway could be activated by Cdc42p and Cdc24p as they are synthetically lethal with *lte1*Δ. To date the mechanism by which Ste20p activates mitotic exit is unknown.

Several studies have shown that Cdc42p, Cdc24p, and one of their effectors help localize Lte1p to the bud. Lte1p-GFP has been shown to mislocalize within *cla4*Δ cells [188]. Furthermore, Cla4p has been shown to phosphorylate Lte1p [188, 190]. This phosphorylation allows Lte1p's association with Ras2p, which in turn targets the protein to the bud cortex [190, 192]. Thus Cla4p is involved in the same mitotic exit activating pathway as Lte1p, a conclusion supported by the lack of synthetic lethality between *cla4*Δ and *lte1*Δ. However, it should be noted that this localization is necessary for timely mitotic exit but does not hinder the process significantly as Clb2p levels are only slightly raised in *cla4*Δ cells.

The final set of Cdc42p effectors that have been found to have a role in mitotic exit activation are the structurally related proteins Gic1p and Gic2p as well as the scaffold protein Bem1p. Bem1p is a multi-copy suppressor of *lte1*Δ *ste20*Δ cells [189]. However, Bem1p is only known as a scaffold protein for the Cdc42p machinery; thus its mechanism of suppression remains a mystery. The mechanism of suppression by Gic1p /Gic2p has been elucidated and hinges on the SPC. The protein Gic1p physically interacts with Bub2p, Bfa1p, and Tem1p [189]. Moreover, the interactions between Tem1p and Bub2p-Bfa1p are inhibited by Gic1p *in vitro*, but deletion of the CRIB domains in the Gics prevents inhibition of Tem1p-Bub2p/Bfa1p interaction by the Gics [189]. Finally, Gic1p-GFP localizes to the bud cell cortex until its activation by Cdc42p. At this time it accumulates in the cytoplasm. Thus, Gic1p and Gic2p are thought to be activated by Cdc42p, which results in Gic relocalization to the cytoplasm where they can disrupt the interaction between Bub2p-Bfa1p and Tem1p and permit the activation of mitotic exit.

Overall, it seems that the regulators of cell polarity play a large role in mitotic exit enhancement. However, several steps and components are still missing in our understanding of mitotic exit regulation. These missing pieces include: regulation of Cdc42 activation of mitotic exit, the mechanism by which Ste20 activates mitotic exit, and the role of Bem1p within mitotic exit (Figure 1.9).

1.6 The synthetic genetic array (SGA)

Within *S. cerevisiae* there are about 4800 non-essential genes (not necessary for viability) [193]. Although removal of these genes is not lethal, the phenotypic consequences of some deletions can be quite severe. Conversely, many gene deletions predicted to have severe defects have little or no phenotype. As I have mentioned before, this is the case for *lte1*Δ in the MEN. These perplexing observations may indicate the presence of redundant/partially overlapping pathways. Pathway redundancy seems to have evolved to create an elaborate system of checks and balances for backup mechanisms or for better efficiency. Solving these redundancies have produced models of the vast network of protein and genetic interactions within the cell. An analysis of interacting networks is daunting, but the use of haploid deletion mutant yeast strains and the ability to construct multiply mutant strains provides the means to probe these complex interaction networks.

The synthetic genetic array (SGA) is the process of crossing a known deletion mutant to the haploid deletion set and then selecting for haploid double knockouts. Once the double knockouts are obtained they can be screened for a variety of phenotypes. Synthetic lethality is one such phenotype. Synthetic lethality occurs when two non-essential gene deletions are lethal when combined in a haploid strain [193]. As a result, this interaction can unearth complex interactions between genes in redundant pathways if one gene compensates for the loss of the other [193]. For example, the combination of *dyn1*Δ and *kar9*Δ are synthetically lethal and are major components of the semi-redundant nuclear migration pathways [8]. Another phenotype is slow growth (rather than lethality) of double mutants, termed synthetic sick/slow-growth [193]. Thus, in both these cases the combination of the two deletions reveals a phenotype not present in either of the single knockouts, or enhances defects present in either of the single knockouts. Conversely, SGA can also be used to construct double mutant strains for the identification of phenotypic suppressors of a gene deletion. Thus, inhibitors of a specific process may be identified in this manner.

There have been many success stories since the development of the SGA in 2001 [193]. Probably the most notable is the Tong *et. al.* publication in 2004 [8]. Amy Tong in Charlie Boone's lab (the developer of the technique) used 132 query strains to identify ~4000 interactions within ~1000 genes [8]. This huge set of data produced an elaborate interaction map, identified several new linkages between cellular processes, and identified several new components to specific pathways [8]. Interestingly, one of these new components was the dynein light intermediate chain *DYN3* [8]. Another exciting study was the SGA carried out using the *cla4*Δ strain [61]. The *cla4*Δ mutation was shown to be synthetically lethal in combination with a relatively unknown p21 activated kinase *STE20* [61]. This study linked Ste20p to the process of actin polarity [61]. Ste20p is now known to be a major player in the majority of actin regulatory processes. Overall, previous literature attests to the power and usefulness of the SGA procedure.

Although the SGA is a powerful genetic tool, there are deficiencies. The SGA is known to detect false positives and a false negative rate of 17-41% [8, 193]. Subsequently, false positives have to be addressed by performing the screen in triplicate and confirming interactions by Tetrad Analysis (TA) or Random Spore Analysis (RSA) [8, 193]. Both of these processes re-cross the strains and observe the dissected tetrads or colonies of etherized spores to confirm that double mutants have the expected phenotype.

On the other hand, the high false negative rate is much harder to address. This high error rate seems to be due to second site modifier mutations that have accumulated within the haploid deletion set due to selective pressure placed on the strains by their gene deletions [194, 195].

Improvements have been made to avoid some problems encountered with the SGA and to save time during the confirmation steps. One such improvement is the production of a sister technique called heterozygote diploid-based synthetic lethality analysis by microarray dSLAM [194, 195]. This technique uses a pool of heterozygote diploid knockouts that have been knocked out and include molecular barcodes of 20bp that are unique to each ORF. These heterozygous diploids are presumably under no selective pressure to retain modifier mutations. Additionally, each barcode is flanked by known sequence and thus can be used to create ORF specific barcode amplification. The pool is then transformed with a query gene knockout cassette and haploid double mutants or haploid single mutants are then selected for. Thus the whole pool of double deletion haploids is grown up together in a single culture. Presumably the synthetic lethal strains will not grow and the synthetic sick strains will be out competed by the healthy double mutant strains. The culture is then used for genomic isolation and subsequent amplification of each molecular barcode. The barcodes are amplified using opposing fluorescently tagged primers; Cy3 for the double knockouts and Cy5 for the single knockouts. The amplified DNA is then pooled and used to probe a yeast barcode microarray. The ratio of Cy3 and Cy5 is then used to determine the growth of each of the double knockouts and a threshold (low ratio) is chosen to define synthetic lethality and synthetic sickness [194, 195].

While dSLAM does avoid the genetic complications of SGA, it still produces errors [194, 195]. The error rate changes depending on the Cy3/Cy5 ratio used as a threshold. Furthermore, some true synthetic interactions that were identified by the SGA have been missed by the process of dSLAM [194, 195]. Therefore, neither of these processes has proven to be 100% accurate. Furthermore, the competition of the strains when grown up together may exacerbate a synthetic sick phenotype to look lethal because they are out-competed for nutrients by healthy strains. Therefore, I have chosen the SGA method to probe the regulation of mitotic exit because of the proven successes of this method.

1.7 Rationale/objectives: Project #1

Although the cell cycle has been intensively studied, especially using *S. cerevisiae* as a model organism, there remain many inconsistencies and gaps in our knowledge of mitotic exit (Figure 1.9). This is particularly the case for the spindle position checkpoint. For example, the microtubule sensor hypothesized to regulate the checkpoint has never been identified. Second, the mechanism of Kin4p inhibition of Cdc5p has yet to be determined. It is feasible that this mechanism includes other proteins, as Kin4p is transported to the daughter bound SPB upon checkpoint activation. Furthermore, it is unknown how an *lte1Δ* strain can exit mitosis at a near wild-type rate at 30° C [31]. This could be explained by Ste20p activation of mitotic exit as a redundant pathway. However, this explanation is not conclusive as the mechanism of Ste20p on mitotic exit is unknown. Finally, it is unknown how Cdc42p is regulated during mitotic exit. It is possible that the regulation of Cdc42p differs from its regulation of cell polarity. Overall, these are just a few of the outstanding questions concerning how mitotic exit is regulated (Figure 1.9). Therefore, I intend to screen and select for further components involved in regulating mitotic exit by looking for genes that interact genetically with a MEN mutant, *lte1Δ*.

Using the SGA method I intend to address this goal. Lte1p is the presumed GEF for Tem1p found at the top of the MEN (Figure 1.9). This gene is perfect for this type of analysis for several reasons. First, *LTE1* is a non-essential gene and can be deleted. Most of the components of the MEN are essential and, therefore, do not easily lend themselves to SGA unless conditional alleles are used. Conditional alleles for SGA have two drawbacks. One is the allele must be linked with a selectable or autotrophic marker –an extra step I chose to avoid. The second is that there are no conditional alleles for MEN components that are viable under restrictive conditions. Therefore, synthetic lethality can only be assessed at permissive or semi-permissive temperatures in the hopes that there is a partial loss of function of the conditional allele. Another reason why I chose *lte1Δ* is that although Lte1p is not essential at optimal temperatures, it is essential at low temperatures, thus its name 'low temperature essential' [196, 197]. As I stated before this implies the existence of redundant mechanisms that would be prime targets for a synthetic lethal screen. Further, the location of Lte1p in the MEN pathway was also a factor in our choice of mutant. Lte1p is at the top of the MEN pathway and thus generally interacts with the preparatory processes for mitotic exit. For example, the nuclear positioning pathways are known to genetically interact with *LTE1*. This is unlike the components farther downstream that have more specific roles in mitotic exit and thus show some allelic specificity in their genetic interactions. Finally, because Lte1p is essential for mitotic exit at low temperatures, I can test viable *lte1*Δ *xxx*Δ knockouts for suppression of the low temperature lethality phenotype. Mutant suppressors of *lte1*Δ likely have an inhibitory role on mitotic exit. In contrast, mutants that are synthetically lethal/sick with *lte1*Δ are redundant to the action of Lte1p thus could be activators of mitotic exit. I predict that the SGA approach using the *lte1*Δ query strain will enable us to find new regulators of mitotic exit.

During the process of this analysis a similar study looking for functional interactions on a global scale analyzed the *lte1*Δ strain using the dSLAM technique [198]. Nevertheless, I continued to carry out our analysis for two major reasons. Primarily, our study was completed using a different method and previous studies have shown that neither of these techniques are 100% effective in identifying genetic interactions. Thus, these two studies are complimentary [8, 193, 198]. Second, our study also selected for suppressors of the *lte1*Δ defects, which is a novel approach.

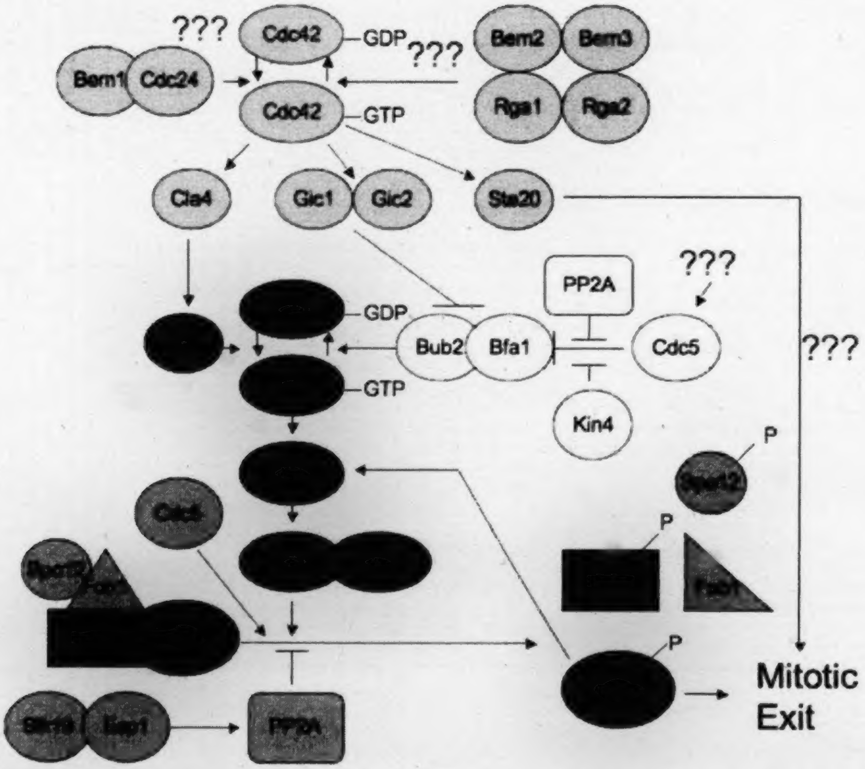
???
Cdc42
GDP
???
Bem2
Bem3
Bem1
Cdc24
Cdc42
GTP
Rga1
Rga2
Cla4
Gic1
Gic2
Ste20
???
PP2A
GDP
Bub2
Bfa1
Cdc5
???
GTP
Kin4
P
Spo12
Cdc5
P
Spo12
Fob1
Fob1
P
Mitotic
Exit
Slk19
Esp1
PP2A

Figure 1.9. Examples of several outstanding questions in the process of mitotic exit. The MEN is shown in red, SPC is shown in yellow, FEAR pathway is shown in blue, and the Cdc42p signaling pathway is shown in green. The unknown mechanisms of Cdc42p regulation, SPC regulation, and mitotic exit activation via Ste20p are denoted by the red question marks.

1.8 Rationale/objectives: Project #2

A large cohort of proteins and processes are conserved among all eukaryotes- including many cell cycle processes from cyclin/CDK activity to chromosome segregation [4]. Therefore, we can use simple organisms such as *S. cerevisiae* to study these processes and apply what we learn to other eukaryotes, including humans.

One such well-conserved protein complex is cytoplasmic dynein. In metazoans, cytoplasmic dynein components are encoded by multiple genes giving rise to various isoforms. In addition, cytoplasmic dynein is essential and mutations in dynein components are associated with several diseases, particularity neurological diseases. For example, mutations in the human gene *LIS1* has been linked to lissencephaly of the brain. Lissencephaly or literally 'smooth brain' is a disorder characterized by a lack of convolutions in the brain that is caused by defective neuronal migration [199]. This gene has a conserved homologue in *S. cerevisiae* (Pac1p) which has since been characterized in some detail [98, 135]. Pac1p is now known to target yeast dynein to the microtubule plus ends which is crucial for proper nuclear migration [99]. In another example, a recent study has shown that up-regulation of the human dynein light chain 1 (*DLC1*) promotes tumorigenesis [200].

In contrast to metazoan dynein subunits, cytoplasmic dynein in yeast is not essential and all of the dynein subunits have only one gene/isoform. These features of *S. cerevisiae* dynein facilitate a detailed observation of dynein function. To date only one functional homologue of the LCs has been identified within *S. cerevisiae.* This homologue is *DYN2*, which is a LC8 family homologue [119]. However, two remaining families (Tctex, and roadblock/LC7) of LCs have no identified *S. cerevisiae* homologue. My aim in this project was to identify new LC proteins in yeast.

Unlike the amino acid sequences, the proposed secondary structure of the *S. cerevisiae* dynein/dynactin homologues is well conserved. Fortunately, this structural conservation can allow us to identify new homologues within *S. cerevisiae* of the dynein/dynactin components. The identification of all cytoplasmic dynein subunits will allow us to characterize their specific functions within the dynein complex and provide a greater understanding of dynein function and associated neurological pathologies.

CHAPTER 2- MATERIALS & METHODS

* All chemicals were purchased from Sigma, St. Louis, MO unless otherwise stated.

2.1 Media

2.1.1 Bacterial growth media

LB

-1% tryptone (Becton-Dickinson & Co., Sparks , MD), 0.5% yeast extract (Becton, Dickinson & Co., Sparks , MD), 0.5% NaCl (EMD, Gibbstown, NJ), 2% dextrose (A.E. Staley MFG. Co., Decatur, IL), and 2% agar (plates only) (Invitrogen, Carlsbad, CA)

LB+(ampicillin, carbenicillin)

-Add ampicillin or carbenicillin to a final concentration of 20 μg/ml for stringent plasmids (low copy) or a concentration of 50 μg/ml for relaxed plasmids (high copy).

2.1.2 Yeast growth media

YPAD

-2% peptone (Merck, Darmstadt, Germany), 1% yeast extract (Becton, Dickinson & Co., Sparks , MD), 0.004% adenine (Q-Biogene, Carlsbad, CA), 2% dextrose (A.E. Staley MFG. Co., Decatur, IL), and 2% agar (plates only) (Invitrogen, Carlsbad, CA)

YPAD+ drugs (G418 [Geneticin] Nat [Nourseothricin])

- To YPAD add G418 (Q-Biogene, Carlsbad, CA) to a final concentration of 200 μg/ml (for maintainance, 400 μg/ml for selection) or add Nat (Q-Biogene, Carlsbad, CA) to a final concentration of 100 μg/ml.

SD drop out media

-0.67% yeast nitrogen base w/o amino acids (Becton, Dickinson & Co., Sparks , MD), 2% dextrose (A.E. Staley MFG. Co., Decatur, IL), 0.054% CSM-ade-his-leu-lys-trp-ura (Q-Biogene, Carlsbad, CA), leave out any of the following to test for appropriate auxotrophic markers: 0.004% adenine (Q-Biogene, Carlsbad, CA), 0.002% histidine (Q-Biogene, Carlsbad, CA), 0.01% leucine (Q-Biogene, Carlsbad, CA), 0.005% lysine (Q-Biogene, Carlsbad, CA), 0.005% tryptophan (Q-Biogene, Carlsbad, CA), 0.002% uracil (Q-Biogene, Carlsbad, CA), and 2% bacto agar (plates only) (Becton, Dickinson & Co., Sparks , MD)

SD drop out media + drugs (G418 [Geneticin] Nat [Nourseothricin])

-0.17% yeast nitrogen base w/o amino acids and ammonium sulphate (Q-Biogene, Carlsbad, CA), 0.1% monosodium glutamate, 0.054% CSM-ade-his-leu-lys-trp-ura (Q-Biogene, Carlsbad, CA), leave out any of the following to test for appropriate auxotrophic markers: 0.004% adenine (Q-Biogene, Carlsbad, CA), 0.002% histidine (Q-Biogene, Carlsbad, CA), 0.01% leucine (Q-Biogene, Carlsbad, CA), 0.005% lysine (Q-Biogene, Carlsbad, CA), 0.005% tryptophan (Q-Biogene, Carlsbad, CA), 0.002% uracil (Q-Biogene, Carlsbad, CA), add G418 (Q-Biogene, Carlsbad, CA) to a final concentration of 200 μg/ml (for maintainance 400 μg/ml for selection) and/or add Nat (Q-Biogene, Carlsbad, CA) to a final concentration of 100 μg/ml.

SRG -ura

-0.67% yeast nitrogen base w/o amino acids (Becton, Dickinson & Co., Sparks , MD), 2% raffinose (Q-Biogene, Carlsbad, CA), and/or 2% galactose (Q-Biogene, Carlsbad, CA), 0.054% CSM-ade-his-leu-lys-trp-ura (Q-Biogene, Carlsbad, CA), leave out any of the following to test for appropriate auxotrophic markers: 0.004% adenine (Q-Biogene, Carlsbad, CA), 0.002% histidine (Q-Biogene, Carlsbad, CA), 0.01% leucine (Q-Biogene, Carlsbad, CA), 0.005% lysine (Q-Biogene, Carlsbad, CA), 0.005% tryptophan (Q-Biogene, Carlsbad, CA), and 2% bacto agar (plates only) (Becton, Dickinson & Co., Sparks , MD)

SD-arg-his+can

-0.17% yeast nitrogen base w/o amino acids and ammonium sulphate (Q-Biogene, Carlsbad, CA), 0.1% monosodium glutamate, 0.07% CSM-arg-his (Q-Biogene, Carlsbad, CA), 2% bacto agar (plates only) (Becton, Dickinson & Co., Sparks , MD),and canavanine (Q-Biogene, Carlsbad, CA) to a final concentration of 100 μg/ml.

SD-arg-ura+can

-0.17% yeast nitrogen base w/o amino acids and ammonium sulphate (Q-Biogene, Carlsbad, CA), 0.1% monosodium glutamate, 0.07% CSM-arg-ura (Q-Biogene, Carlsbad, CA), 2% bacto agar (plates only) (Becton, Dickinson & Co., Sparks , MD), and canavanine (Q-Biogene, Carlsbad, CA) to a final concentration of 100 μg/ml.

SD-arg-his-ura+can+G418

-0.17% yeast nitrogen base w/o amino acids and ammonium sulphate (Q-Biogene, Carlsbad, CA), 0.1% monosodium glutamate, 0.07% CSM-arg-ura (Q-Biogene, Carlsbad, CA), 2% bacto agar (plates only) (Becton, Dickinson & Co., Sparks , MD), Add canavanine (Q-Biogene, Carlsbad, CA) to a final concentration of 100 μg/ml and G418 (Q-Biogene, Carlsbad, CA) to a final concentration of 200 μg/ml (for maintainance 400 μg/ml for selection).

Minimal Sporulation Media

-1% potassium acetate, and 2% bacto agar (plates only) (Fisher Scientific, Pittsburgh, PA)

2.2 General methods

2.2.1 Mating type testing

The ploidy and mating types of strains were determined by testing for the secretion of mating pheromone. The strains were patched out on YPAD plates and grown overnight at 30° C. The next day a loop full of the *MAT***a** (Y2081) (Table 2.1) mating type tester strain was suspended in 1 ml of ddH20. Of this 1 ml yeast suspension, 200 μl was spread on a new YPAD plate and left to dry. This step was then repeated with the *MAT*α mating type tester strain (Y2082) (Table 2.1). The candidate strains were then replica-plated onto the plates containing lawns of the mating test strains. The plates were then incubated at 30° C overnight to test for a lack of growth of the mating type tester strain surrounding the candidate strain. The lack of growth or 'halo' indicates the candidate strain is the opposite mating type to the tester strain. The halo is a product of a G1 phase arrest induced by mating pheromone. This G1 phase arrest facilitates shmooing (the production of the mating projection) and mating. Thus the candidate should produce no halo on the tester lawn of the same mating type. If no halo is produced on either tester strain the candidate strain is likely diploid.

2.2.2 Crossing strains

Several strains were crossed to observe double mutants for synthetic interactions between deletions. The strains to be crossed were PCR tested to ensure purity and identity of strain. Confirmed strains were then crossed to each other by patching them together on YPAD solid media and incubating at 30° C for 1 day. Diploids were then grown on the appropriate selection media at 30° C over 2 days. Diploids were confirmed by mating type test. Confirmed Diploids were then sporulated for 5 days on minimal sporulation media at 30° C. Progeny were then selected for accordingly.

2.2.3 Concentration of plasmid DNA or PCR products

To concentrate isolated plasmids or amplified PCR products 2 volumes of 100% ethanol and 0.1 volumes of 5 M sodium acetate was added to the DNA sample. The DNA was then precipitated by incubating the mixture at 4° C for 20 min and then pelleted by centrifugation (Eppendorf 5415 D/R) at 16,110 x g for 5 min. The supernatant was then decanted and washed with 500 μl of 70 % ethanol was added and the ethanol and DNA was mixed gently. The DNA was then again pelleted by centrifugation at 16,110 x g for 1 min. The supernatant was then decanted again and the pellet was dried at 37° C for 30 min then resuspended in the desired amount of ddH20 or appropriate buffer.

2.2.4 Transformation of *Saccharomyces cerevisiae*

The process of transformation was performed as described by Knop *et al*, 1999 [201]. Yeast cells were made competent to take up DNA by the following procedure. A fresh culture was grown by diluting a 5 ml YPAD overnight to an OD_{600} of 0.1. Cells were then grown to an OD_{600} of 1.0 and isolated by centrifugation (Eppendorf 5415 D/R) at 500 x g for 5 min. Cells were washed with sterile water followed by sterile SORB solution (100 mM Lithium acetate, 10 mM Tris-HCl pH 8.0, 1 mM EDTA/NaOH pH 8, 1 M sorbitol pH 8.0) The cells were then resuspended in 360 µl SORB solution and 40 µl of boiled and sheared salmon DNA for every 50 ml of original culture. The competent cell solution was divided into 50 µl aliquots and frozen at -80° C [201].

Transformation was performed by adding 10 µl (~1µg) of DNA to 50 µl of competent cells. A six times volume of poly ethylene glycol (PEG) solution (100mM Lithium acetate, 10 mM Tris-HCl pH 8.0, 1 mM EDTA/NaOH pH 8.0, 40 % PEG 3350) was added to the cell-DNA mix and incubated for 30 min. Then a 1/19th volume of DMSO was added to solution, which was then heat shocked at 42° C for 15 min. Finally, cells were spun down at 4880 x g for 2 min, resuspended in 200 µl ddH_2O and plated on selective media [201].

2.2.5 Confirmation of gene knockouts

Candidate strains were grown overnight in 5 ml media of which 1.5 ml was spun down at 16,110 x g for 5 min in a 1.5 ml centrifuge tube. The supernatant was removed and cells were resuspended in 300 µl lysis buffer (2% Triton X-100, 1% SDS, 0.1 M NaCl, 0.01 M Tris/HCl pH 8.0, 0.01 M EDTA/NaOH pH 8.0). Alternatively, this step can be replaced by suspending a single colony isolate in 300 µl lysis buffer. Glass beads (200 µl) and (25:24:1) Phenol:Chloroform:Isoamyl Alcohol (EMD, Gibbstown, NJ) (200 µl) were then added to the lysis solution and vortexed at 4° C for 6 min. The lysis slurry was then centrifuged at 16,110 x g for 5 min. The aqueous layer was removed and DNA was precipitated by adding 450 µl of 95 % ethanol and incubating at 4° C for 20 min. The solution was then centrifuged at 16,110 x g for 5 min and supernatant was aspirated. DNA was then washed with 70 % ethanol and centrifuged at 16,110 x g for 1 min. Again supernatant was aspirated and the DNA pellet was dried at 37° C for 20 min. DNA was finally resuspended in 50 µl of ddH20.

In order to confirm the identities of knockout strains, PCR tests were performed on single colony isolates. These single colony isolates were used to perform the genomic isolation procedure. Primers were chosen in order to detect either the knockout cassette or the wildtype gene. To test the knockout gene a forward primer upstream of the gene of interest was combined with a reverse primer internal to the knockout cassette. To test for a wildtype gene the same forward primer used in the knockout test was combined with a reverse primer internal to the wild type gene. Which primer pair produces a product of the correct size will show the presence of a gene knockout, a wildtype gene, or both in each clonal colony (Figure 2.1). The PCR reactions were set up as follows:

K/O PCR

-0.5 µl Genomic DNA
-1 µl Forward primer (25 µM)
-1 µl Reverse primer (25 µM)
-0.5 µl dNTPs (Invitrogen, Carlsbad, CA)
-0.75 µl $MgCl_2$ (Invitrogen, Carlsbad, CA)
-2.5 µl 10x buffer (Invitrogen, Carlsbad, CA)
-1 µl Taq (5U/µl) (Invitrogen, Carlsbad, CA or MBSU)
-17.75 ddH_2O
25 µl Total Reaction Volume

This mixture was mixed well and amplified (Eppendorf Mastercycler) via the following protocol:

1. 94° C for 3 min
2. 94° C for 45s
3. 55-60° C for 30s
4. 72° C for 2 min
5. repeat steps 2-4 35 times
6. 72° C for 10 min
7. Hold at 4° C

The resulting products were then separated on a 1-2% agarose (EMD, Gibbstown, NJ) TAE (0.4M Tris, 0.01M EDTA, 0.2M sodium acetate) gel at 90 V for 25-50 min. The gel was then stained with 10 µg/ml ethidium bromide for 10 min and observed using a Bioimager gel dock system (Syngene Gene Genius).

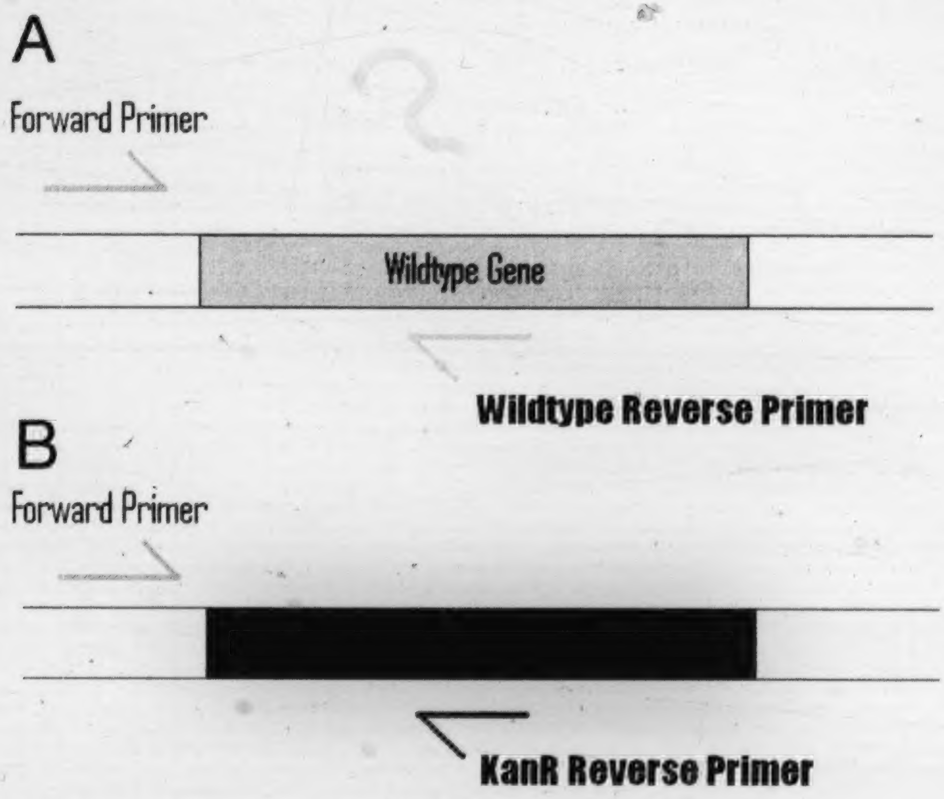
A
Forward Primer
Wildtype Gene
Wildtype Reverse Primer
B
Forward Primer
KanR Reverse Primer

Figure 2.1. Schematic of wildtype and knockout PCR tests. A) Wildtype test where a forward primer is used in combination with a reverse primer internal to the gene to test whether the wildtype copy is present. If the gene is present then amplification should occur. If the wildtype gene is present and the knockout cassette reverse primer is used in stead of the wildtype reverse primer then again no product will be observed. B) Knockout test where a forward primer is used in combination with a reverse primer internal to the knockout cassette to test whether the knockout has occurred and is present. If the gene is knocked out properly then amplification should occur. Again a wildtype test should not amplify a product in this situation.

2.2.6 DNA sequencing

All sequencing reactions of DNA were performed using a modified BigDye Terminator v3.1 Cycle Sequencing Kit (Applied Biosystems) as follows:

Sequencing Reaction

-2 μl Big Dye (Applied Biosystems)

-6 μl Buffer (200 mM Tris, pH 9.0, 5mM $MgCl_2$)

-100 ng template

-5 pMol primer

-ddH_2O up to a volume of 20 μl

This mixture was mixed well and amplified (Eppendorf Mastercycler) via the following protocol:

1. 96° C for 30sec
2. 50° C for 15sec
3. 60° C for 2 min
4. repeat steps 1-3 for 25 cycles

The product was then prepared for analysis by ethanol precipitation (Section 2.2.3). The DNA pellet was then resuspended in ddH_2O and sequenced on an ABI 3730 DNA Analyzer (MBSU, University of Alberta).

2.2.7 Replica-pinning

2.2.7.1 12x8 method

Manual pinning was performed by washing the manual 96 pin comb in: ddH20 for 2 min, 10% bleach for 30 sec, ddH20 for 30 sec, and 95% ethanol for 30 sec. The comb was then flamed three times to ensure it was dry and sterile. Once sterile, the comb was placed into a 96 well plate to collect cells which were pinned onto the solid media with the aid of the pinning guide apparatus to ensure reproducible and accurate distribution of cells. This transfer procedure was conducted three times for each plate. Alternativly, cells were pinned from solid media to solid media in the same fashion however, transfer was only performed once. Plates were then grown at 30° C for 2 days [193].

2.2.7.2 5x5 method

Strains to be replica-pinned were grown at 30° C in 5 ml liquid selection media for overnight. The overnight cultures were then diluted to an OD_{600} of 0.1 and placed back at 30° C until all strains had grown to an OD_{600} of 0.5 +/- ~0.05 (an OD_{600} of 1.0 was used for strains that grew poorly or when assaying cold temperatures). Each strain was then diluted serially 1 in 10 four times from the original culture in a sterile microfuge rack. The volumes used for dilutions were greater than 400 µl to ensure sufficient depth to cover comb. All five cultures (original and 4 dilutions) were then transferred to a plate using a 5x5 replica pinning comb. The comb was sterilized by sitting in 95% ethanol for 2 min and then flamed 3 times prior to pinning. Up to 5 strains and their dilutions can be placed on one plate. The plates either contained a compound, which was being assayed, or were placed at various temperatures to judge their effects on the different strains.

2.3 Genetic screen for enhancers/inhibitors of mitotic exit (Project #1)

2.3.1 Synthetic genetic array

This procedure was adapted from Tong et al. 2004 [193].

2.3.1.1 Creation of query strain

The *MATα his3Δ1 leu2Δ0 lys2Δ0 ura3Δ0 lte1Δ::KanR* (Table 2.1) query strain was obtained from the α haploid deletion set and made competent. Plasmid p4348 (pCRII-TOPO::*MX4-URA3*) (Table 2.1) was used to amplify the *URA3MX4* cassette via the following procedure:

Amplification PCR

-0.5 µl template (~0.1 µg p4348 DNA)

-2 µl forward primer (25 µM) (MX4.F)

-2 µl reverse primer (25 µM) (MX4.R)

-1 µl dNTPs (2.5 µM; Promega, Madison, WI.)

-5 µl 10X Buffer (Roche, Indianapolis, IN)

-38.75 µl ddH$_2$0

-0.75 Expand Long Template Mix (5U/µl) (Roche, Indianapolis, IN)

7

50 µl Total Reaction Volume

This mixture was created 4 times, mixed well, and amplified (Eppendorf Mastercycler) via the following protocol:

1. 95° C for 2 min
2. 95° C for 30 sec
3. 55° C for 30 sec
4. 72° C for 1.5 min
5. repeat steps 2-4 24 times
6. 72° C for 7 min
7. Hold at 4° C

5 µl of the amplified insert was run on a 1% agarose gel to ensure proper amplification occurred. The four reactions were then concentrated into 50 µl. 10 µl of concentrated insert was then used to transform the competent query strain cells. Transformants were selected on SD-ura plates. Within these cells the *URA3-MX4* cassette will recombine via the flanking *MX4* homologous regions into *KanRMX4* knockout cassette previously used to knock out the wildtype gene. Thus, these transformants were able to grow on the SD-ura media and will no longer be able to grow on media containing G418.

The loss of the *KanRMX4* cassette was confirmed by lack of growth on YPAD + G418 solid media (400 µg/ml). Replacement of the Kan knockout cassette with the URA3 cassette was confirmed by PCR. Genomic isolations were performed on query strains and were assayed for the presence of the lte1Δ query gene knocked out with the *URA3* cassette. This was achieved by using a primer upstream of the *lte1*Δ and a reverse primer within the KO URA cassette (Table 2.2).

The *MATα lte1Δ::URA3* strain was then crossed to the mating type switcher strain (Y3598 *MAT***a** *can1Δ::MFA1pr-HIS3-MFα1pr-LEU2 ura3Δ leu2Δ his3Δ lys2Δ*) on YPAD and grown overnight at 30° C (Table 2.1). Diploids were then streaked for single colony isolates and confirmed by lack of pheromone production in halo tests. Diploids were transferred to sporulation media and grown at 30° C for 5 days. Spores produced were resuspended in Water:Ether (1:1) and were vortexed for 3 min to kill off remaining diploids (See Random Spore Analysis). The haploids were then plated on SD-arg-ura+canavanine and grown for 3 days at 30° C. Canavanine (an arginine analogue) is taken up by yeast via the arginine permease gene *CAN1* where it is then incorporated into proteins making them non-functional. This is used as a selective tool for deletions in the *CAN1* gene. The resulting colonies were tested for production of pheromone indicating a *MAT***a** or α colony. Again genomic isolations were performed on the candidate query strains and the presence of the knockout cassette and absence of the wild type gene was confirmed by PCR. These strains were then grown in SD-arg-his+can to an OD_{600} of 0.5, and frozen down in 20% glycerol at -80° C. Therefore, query strains were *MAT***a** *lte1Δ::URA3 can1Δ::MFA1pr-HIS3-MFα1pr-LEU2 ura3Δ leu2Δ his3Δ lys2Δ* (Table 2.1).

2.3.1.2 Cross of query strain to possible MEN enhancer/suppressors

163 knockout strains were chosen to cross to the *lte1Δ* strain based on their possible enhancing or inhibitory effects upon the MEN. We chose the *slk19Δ*, *spo12Δ*, *dyn1Δ*, *arp1Δ*, *kar9Δ*, *dcc1Δ*, *ctf4Δ*, *ctf8Δ*, *ctf18Δ*, and *ste20Δ* strains to serve as the synthetic interaction positive controls. Also we chose the *bub2Δ*, *bfa1Δ*, and *kin4Δ* strains to serve as the positive controls for the suppression selection. Each strain was isolated from the α haploid deletion set by wooden applicator and transferred to a 0.5 ml 96 well pate (Corning Inc., Corning, NY) containing 200 μl YPAD in each well. In total two plates were created. Plates were placed at a 45° angle and shaken at 30° C for 2 days. Cells from each well were then transferred to YPAD solid media plates (Corning Inc., Corning, NY) via manual pinning.

The *lte1Δ* query strain was grown in 50 ml SD-ura liquid media to an OD_{600} of 1.0 and transferred to a 96 well plate (200 μl/well). The query strain was then manually pinned using the 12x8 pinning method onto SD-ura solid media and grown at 30° C for 2 days.

Once both the deletion plates and query strain plate were grown, both were pinned sequentially onto the same fresh YPAD solid media such that each deletion strain could mate with the query strain. The strains were mated at 30° C for 1 day. Once mating had occurred, the respective diploids were selected by manually pinning to SD-ura+G418 plates which were grown at 30° C for 2 days. The diploids were then manually pinned (three times) to sporulation media and grown at 30° C for 5 days. Asci from each cross were then transferred to 0.5 ml tubes containing 100 µl SD-arg-his+can each. 100 µl of ether was then added to each tube to kill off remaining diploids and 3 of 4 spores in each tetrad. Tubes were vortexed for 1 min then centrifuged (Eppendorf 5415 D/R) at 4880 x g for 2 min. Supernatant was decanted and cells were resuspended in 200 µl SD-arg-his+can and transferred to a 96 well plate. The plate was then placed at a 45° angle and shaken at 30° C for 2 days. Media lacking histidine is used here to select for the *MAT***a** cells. The *HIS3* gene in these strains is driven by the *MFA1* promoter meaning that only *MAT***a** cells have the *MAT***a** specific transcription factors necessary for the induction of the *HIS3* gene. As a result, only haploid *MAT***a** cells can grow on this media. Next, the cells grown within the 96 well plate were transferred to SD-arg-his+can solid media by manual pinning (three times). These plates were incubated at 30° C for 2 days. Finally, cells were transferred to SD-arg-his-ura+G418+can plates by manual pinning (one time). The final selection plates were placed at 30° C for 2 days, and a second batch at 10° C for 3 weeks. The 30° C were scored by eye for lethality (complete lack of growth) or synthetic sickness or growth defects. We defined a synthetic sickness as anything that could indicate a lack of growth of the colony Although this definition may produce false positives it helps prevent missing double mutants with weak growth defects. Growth phenotypes of double mutants were later confirmed in plate assays of double mutant progeny after re-crossing the single mutants.

After these crosses were finished two sequential crosses were undertaken in parallel. Subsequent crosses were carried out in the same manner except etherization was performed in a 96 well plate for convenience.

2.3.1.3 Confirmation of results

The processes of tetrad analysis or random spore analysis were used to confirm genetic interactions. To facilitate both these processes the *lte1Δ::URA3* knockout strain was crossed again to all *xxxΔ::KanR* knockouts, which were hits in the screen. These diploids were then sporulated on minimal sporulation media for a minimum of 5 days [5, 8, 193].

Tetrad analysis was only performed on candidates we hoped to pursue. A loop-full of one of the sporulated diploids was taken and suspended in 100 μl of ddH20. 10 μl of β-Glucuronidase was then added to the cell suspension and left to digest the spore coat for 5-10 min. The digested spores were then spread across the upper half of the plate via a sterile loop to create 2 full lines across the plate. Tetrad spores were picked on a TDM400 tetrad dissection microscope (Nikon) and separated on the plate in sequential columns. The resulting dissected spores were then incubated for 2 days at 30° C (Figure 2.2).

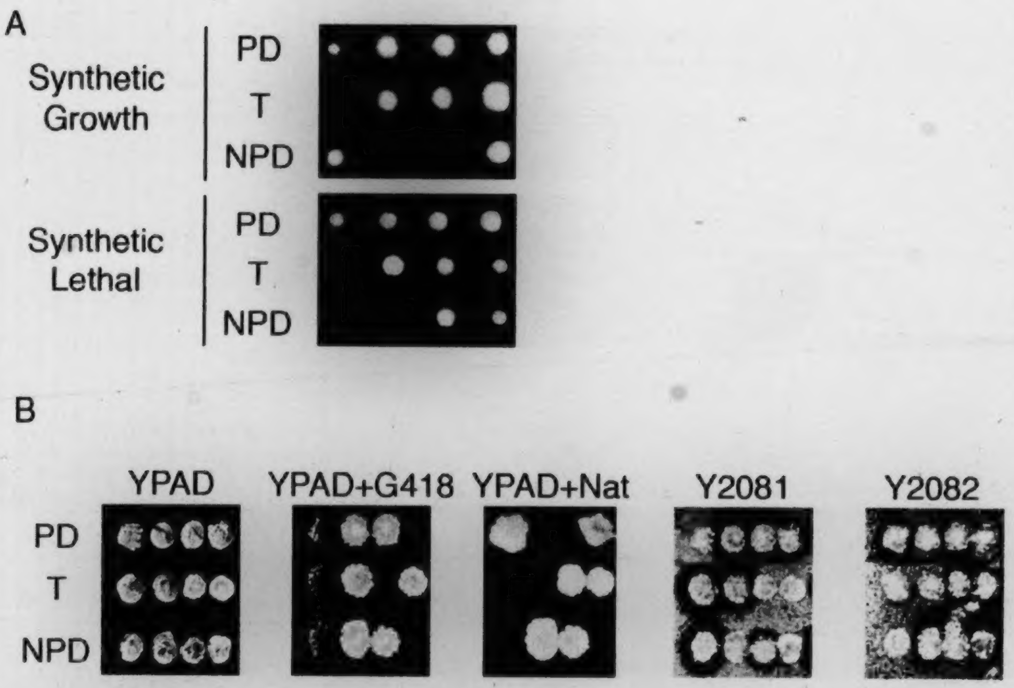

Figure 2.2. Tetrad dissection and analysis. A) Dissected tetrads showing either Synthetic Growth defects or Synthetic Lethality. B) Tetrads which have been spotted out then Replica-Plated to test for segregation of knockouts (and subsequently their markers) and mating type. PD= parental ditype, T= tetratype, and NPD= non-parental ditype. Resutls of *bem4Δ::NatR* x *rga1Δ::KanR* shown.

The resulting tetrad spores were then spotted out onto a YPAD plate and grown overnight at 30° C to facilitate replica plating. Next, the spotted spores were replica-plated onto mating tester plates to ensure they are haploid and that there is a 2:2 segregation of the **a** and α mating types within tetrads. Further, the spores were replica-plated onto media selecting for each of the two knockouts to show a 2:2 segregation of the knockout genes to their wildtype copy. The replica-plated plates were then incubated for 1 day at 30° C. The resulting plates were then scored for parental ditype, non-parental ditype, and tetratype segregation as well as synthetic lethality or synthetic growth defects in the double knockouts (Figure 2.2) [5].

Synthetic interactions of remaining candidates were confirmed by Random Spore Analysis (RSA) [8]. A large loopful of cells was collected from solid sporulation media and a dense suspension of sporulating yeast cells was made in 0.5 ml of liquid media. 0.5 ml of ether (EMD, Gibbstown, NJ) was then added to the cell suspension. The ether-media mixture is then vortexed on high speed for 4 min to ensure sporulation mixture had sufficient contact with the ether to kill remaining diploids and 3 of 4 spores in asci. Once vortexed, 30 μl of the lower aqueous layer (media) was spread on plates selecting for each of the original knockouts and plates selecting for the double knockouts. The plates were then incubated at 30° C for 2 days and scored for synthetic lethality or a synthetic growth defect as shown by lack of growth, or slow growth, on double selection media [5, 8].

2.3.2 Phenotypic analysis of deletion strains

The single knockouts of the confirmed candidates (*bem1Δ, bem4Δ, ldb18Δ,* and *sac3Δ)* were then isolated from tetrads of crosses to lte1Δ, and were PCR tested to ensure their identity (Table 2.1, Table 2.2). Once tested and confirmed, the strains and a wildtype control were replica-pinned using the 5x5 method onto YPAD. Once dry, the plates were placed at 15° C, 30° C, and 37° C to test the temperature dependence of the knockout strains. These different temperatures displayed the growth phenotypes of the different knockouts.

2.3.3 Overexpression of *Saccharomyces cerevisiae* ORFs in the *lte1::KanMX4* mutant

Single colony isolates of *lte1*Δ*::KanMX4* were PCR tested to ensure a lack of the *LTE1* gene and presence of the knockout cassette (Table 2.2). The cells were made competent and transformed with each of: p*GAL*-Empty (BG1805), p*GAL-BEM1*, p*GAL-BEM4*, p*GAL-LDB18*, and p*GAL-SAC3* (Table 2.3) (Open Biosystems) [202]. All plasmids were sequenced using a T7 primer to ensure the identity of the plasmid (T7.TEST). Further, BY4742 (WT) was also made competent and transformed with p*GAL*-Empty for a positive control.

The transformed strains were then grown overnight at 30° C in SD-ura media. The resulting overnights were then diluted to an OD_{600} of 0.1 and grown to an OD_{600} of 0.5 at 30° C. The strains were then replica-pinned using the 5x5 method onto SD-ura media and SRG-ura media. Each of the two media was then placed at 30° C for 4.5 h to ensure overexpression had commenced prior to transferring to 15° C or leaving at 30° C. Plates at 30° C were grown for 2 days to observe the growth phenotype of overexpression at optimal growing temperatures. Plates at 15° C were grown for 5 days to observe the phenotype of overexpression at semi-lethal temperatures for *lte1*Δ.

2.3.4 Characterization of *BEM4*

2.3.4.1 Creation of the *bem4*Δ query strain

*MAT***a** *bem4*Δ cells were taken from the sporulated heterozygote and made competent.

1 mg of Plasmid p4339 (pCRII-TOPO::*MX4-NatR*) was cut with *Enco*re in a 100 μl total volume. 10 μl of the cut plasmid was run on a 1% agarose gel with the uncut plasmid to ensure full digestion occurred. Cut plasmid was concentrated into 10 μl and then used to transform *MAT***a** *bem4*Δ competent cells and selected on YPAD + Nat plates. Cells in which the *NatMX4* cassette had recombined to replace *KanMX4* knockout cassette are be able to grow on this media.

Loss of the KanMX4 cassette was confirmed by lack of growth on YPAD + G418 solid media (200 μg/ml). Further, replacement of the knockout cassette was confirmed by PCR using a primer upstream of the *bem4*Δ query gene and a reverse primer within the KO cassette (Table 2.2) [8, 193].

2.3.4.2 Cross of query strain to *CDC42* pathway

The *bem4::NatMX4* query strain was crossed to deletion strains lacking components of the cell polarity pathway implicated in mitotic exit control (Table 2.1). The non-essential *CDC42* pathway components (*BEM1, BEM3, RGA1, RGA2, CLA4, GIC1, GIC2, STE20,* and *RDI1)* were isolated from the *MAT*α haploid deletion set and PCR tested for the proper deletion (Section 2.2.5) (Table 2.1, Table 2.2). These strains were then crossed to the *MAT***a** *bem4*Δ query strain. The subsequent diploids were selected on YPAD+G418+Nat plates. The diploids were then sporulated for 5 days and subjected to tetrad analysis to test for synthetic interactions with any of these components.

2.3.4.3 Observation of septin assembly via GFP fluorescence microscopy

Cells transformed with plasmid p1316, which expresses Cdc3p-GFP, have fluorescently labeled septin collars, which can be observed for defects. To observe septin defects in a *bem4*Δ strain, competent *MAT***a** *BEM4* cells and *MAT***a** *bem4*Δ cells were obtained from a *BEM4/bem4*Δ diploid. These haploids were transformed with p1316 and selected on SD-leu plates. The plasmid p1316 is a *LEU2* centromeric plasmid containing *CDC3*-GFP. The cells that grew expressed the septin *CDC3* fused to a GFP tag.

A minimum of one single colony isolate from each transformation was PCR tested to confirm the deletion status of *BEM4* (Table 2.2). The confirmed transformants were then used to inoculate 5 ml of YPAD and incubated overnight at 30° C. Overnight cultures were then used to inoculate a 5 ml culture of SD-leu media to an OD_{600} of 0.05. The culture was then incubated for 6-8 hours until mid log phase (OD_{600} 0.5). From this culture 100 μl was transferred to a 4 well chamber slide (Nalge Nunc, Rochester NY) and allowed to attach to the adhesive material at the bottom of the slide for 15 min. The cells were then observed using a microscope with the Ultraview spinning disc confocal system under the 100x objective (Zeiss Axioscope II). GFP signal was observed using a Acousto-Optic Tunable Filter (AOTF) set to a band pass (for observation of a GFP signal) of 530 nm with a 488 nm laser (for excitation of a GFP signal) (Perkin Elmer). Images were acquired using a 0.1 s exposure time on a Hamamatsu EMCCD camera with a gain setting of 80-100. Image acquisition and analysis was performed using UltraVIEW LSI version 2.7 (Perkin Elmer).

3D image stacks of cells were obtained by acquiring multiple images of each field of view in a series of focal planes with 0.5 μm intervals. Using 3D images ensured that all of the cellular structures could be observed. 2D projections were created from the 3D stacks by combining them and using the maximum algorithm, which, for each pixel, takes the brightest value from any of the 3D stack images and uses that value in a single image 2D projection, ensuring that each pixel is shown as its brightest value throughout the entire 3D stack . Quantification of aberrant septin morphology was accomplished by counting normal and abnormal septin morphologies found within 3 2D projections of the wildtype and *bem4*Δ strains. Aberrant morphology was defined as a septin collar that is either thickened, fragmented, incomplete in separation, or of the presence of multiple rings in one cell.

2.3.4.4 *bem4*Δ *bem3*Δ phenotyping

From the synthetic interaction crosses, *bem4*Δ, *bem3*Δ, and *bem4*Δ *bem3*Δ strains were isolated from a single tetratype tetrad. The strains were then replica pinned via the 5x5 method onto YPAD. The resulting plates were then placed at 15° C, 30° C, and 37° C to test for suppression of the original *bem4*Δ phenotype.

2.4 Identification of *YER071c* as a dynein light chain (Project #2)

2.4.1Gene homology/phylogeny

The protein sequence of *YER071c* was obtained from the *Saccharomyces* Genome Database and NCBI Position-Specific Iterated (PSI) BLAST was performed with this sequence [203]. Related proteins detected by PSI BLAST were then used for the BCM search launcher to produce a ClustalW alignment (http://searchlauncher.bcm.tmc.edu/). The resulting alignment was then imported into Jalview version 2.2.1 to manually edit the alignment [204]. Shading to display similarity and identity was accomplished by import into BoxShade version 3.2.1 (http://www.ch.embnet.org/software/BOX_form.html). A functional final version of the alignment was then created by adding the BoxShade alignment to the Jalview predicted secondary structure in Photoshop version 8.0.

The Jalview output was imported into TreeTop Phylogenetic Tree Predictor to produce a phylogenetic distance matrix (http://www.genebee.msu.su/services/phtree_reduced.html). The matrix was then imported into TreeView version 0.5.1 to produce a graphic representation of the phylogenetic tree (http://taxonomy.zoology.gla.ac.uk/rod/treeview.html). Bootstrap values produced by TreeTop were then added to the phylogenetic tree produced by TreeView in Photoshop version 8.0.

2.4.2 Nuclear migration assay

*yer071c*Δ single colonies were isolated from the haploid deletion set by streaking. Deletion status was confirmed by PCR. 5 ml cultures were grown overnight for each isolate. The overnight cultures were diluted 100 fold to an OD_{600} of 0.05 and grown at 15° C. Once the cells reached an OD_{600} of 0.7 +/- 0.1 each culture was fixed with 10 ml of 95% ethanol. This procedure was repeated in triplicate.

In order to observe nuclear position, the DNA was stained with 4'-6'-Diamidino-2-phenylindole (DAPI). 1.5 ml of each culture was centrifuged at 4880 x g for 2 min and the supernatant was decanted. The cell pellet was then resuspended in 1.5 ml potassium phosphate buffer (0.615M K_2HPO_4, 0.385M KH_2PO_4, pH 7.0) Buffer. Cells were again pelleted then resuspended in 100 μl of 1X DAPI solution in phosphate buffer and incubated at room temperature for 10 min. Cells were then pelleted again and washed twice in 1.5 ml of phosphate buffer. The cells were finally resuspended in 50 μl of phosphate buffer and scored under a microscope using a DAPI filter (exciter: D360/40, emitter: D460/50, Olympus). Each of the strains were scored for cells which were:

a) unbudded; single nucleus
b) budded; single nucleus (mother cell)
c) budded; binucleate (one nucleus in mother, one in bud)
d) unbudded; binucleate
e) budded; binucleate (both in mother)
f) multinucleate (multiple nuclei in mother and/or bud)

The categories a-c were grouped together as normal cells and categories d-f were grouped together as abnormal multinucleate cells.

2.4.3 YER071c synthetic interactions

The *yer071c*Δ was isolated from the *MAT*-α haploid deletion set and PCR tested to ensure purity (Table 2.2). This deletion was then subjected to the same protocol as the *lte1*Δ strain to create a query strain. The resulting strain was *MAT***a** *yer071cΔ::URA3 can1Δ::MFA1pr-HIS3-MFα1pr-LEU2 ura3Δ leu2Δ his3Δ lys2Δ* [8, 193].

Components of the dynein and Kar9 pathway (*dyn1*Δ, *dyn3*Δ, *pac1*Δ, *pac11*Δ, *nip100*Δ, *jnm1*Δ, *arp1*Δ, *bik1*Δ, *bim1*Δ, *kar9*Δ, *bni1*Δ) were then isolated from the *MAT*α haploid deletion set and PCR tested to ensure purity (Table 2.2). The dynein and Kar9 pathway components were then crossed to the *yer071c*Δ*::URA3* query strain and selected on SD-ura+G418 media. The diploids were then sporulated for 5 days and subjected to tetrad analysis to test for synthetic genetic interactions.

Table 2.1. Strains used in this study

Strain Name	Genotype	Origin or Source
BY4742 (WT)	*MATα his3Δ1 leu2Δ0 lys2Δ0 ura3Δ0*	Open Biosystems, Huntsville, AL
BY4741 (WT)	*MAT**a** his3Δ1 leu2Δ0 met15Δ0 ura3Δ0*	Open Biosystems
Y2081	*MATα sst2Δ ste3Δ*	Charlie Boone
Y2082	*MAT**a** bar1Δ*	Charlie Boone
lte1Δ::KanMX4	Same as BY4742 except *LTE1* deletion	Open Biosystems
lte1Δ::URA3MX4	Same as BY4742 except *LTE1* deletion	This Study
lte1Δ query strain	*MAT**a** can1Δ::MFA1pr-HIS3-MFα1pr-LEU2 ura3Δ leu2Δ his3Δ met15Δ lys2Δ lte1Δ::URA3*	This Study
yer071cΔ::KanMX4	Same as BY4742 except *YER071c* deletion	Open Biosystems
yer071cΔ::URA3MX4	Same as BY4742 except *YER071c* deletion	This Study
yer071cΔ query strain	*MAT**a** can1Δ::MFA1pr-HIS3-MFα1pr-LEU2 ura3Δ leu2Δ his3Δ met15Δ lys2Δ yer071c::URA3*	This Study
Y3598	*MAT**a** can1Δ::MFA1pr-HIS3-MFα1pr-LEU2 ura3Δ leu2Δ his3Δ met15Δ lys2Δ*	Charlie Boone
yer071cΔ::URA3MX4 dyn2Δ::KanMX4	Same as BY4742 except *YER071c* deletion and *DYN2* deletion	This Study
bem1Δ::KanMX4	Same as BY4742 except *BEM1* deletion	Open Biosystems
bem4Δ::KanMX4	Same as BY4742 except *BEM4* deletion	Open Biosystems
sac3Δ::KanMX4	Same as BY4742 except *SAC3* deletion	Open Biosystems
ldb18Δ::KanMX4	Same as BY4742 except *LDB18* deletion	Open Biosystems
Y8028	*MAT**a** bem4Δ::KanMX4* strain created from BY4742 *BEM4* deletion heterozygote	This Study
Y8029	*MATα bem4Δ::KanMX4* strain created from BY4742 *BEM4* deletion heterzygote	This Study
bem4Δ::NatMX4	Y8028 transformed with *EcoR* I cut p4339	This Study

bem4Δ::KanMX4 *CDC3*-GFP	Same as BY4742 except *BEM4* deletion and transformation with p1316	This Study
CDC3-GFP	Same as BY4742 except transformation with p1316	This Study
arp1Δ::KanMX4	Same as BY4742 except *ARP1* deletion	Open Biosystems
bik1Δ::KanMX4	Same as BY4742 except *BIK1* deletion	Open Biosystems
bim1Δ::KanMX4	Same as BY4742 except *BIM1* deletion	Open Biosystems
bni1Δ::KanMX4	Same as BY4742 except *BNI1* deletion	Open Biosystems
dyn1Δ::KanMX4	Same as BY4742 except *DYN1* deletion	Open Biosystems
dyn2Δ::KanMX4	Same as BY4742 except *DYN2* deletion	Open Biosystems
dyn3Δ::KanMX4	Same as BY4742 except *DYN3* deletion	Open Biosystems
jnm1Δ::KanMX4	Same as BY4742 except *JNM1* deletion	Open Biosystems
kar9Δ::KanMX4	Same as BY4742 except *KAR9* deletion	Open Biosystems
nip100Δ::KanMX4	Same as BY4742 except *NIP100* deletion	Open Biosystems
num1Δ::KanMX4	Same as BY4742 except *NUM1* deletion	Open Biosystems
pac1Δ::KanMX4	Same as BY4742 except *PAC1* deletion	Open Biosystems
pac11Δ::KanMX4	Same as BY4742 except *PAC11* deletion	Open Biosystems
bem2Δ::KanMX4	Same as BY4742 except *BEM2* deletion	Open Biosystems
bem3Δ::KanMX4	Same as BY4742 except *BEM3* deletion	Open Biosystems
cla4Δ::KanMX4	Same as BY4742 except *CLA4* deletion	Open Biosystems
gic1Δ::KanMX4	Same as BY4742 except *GIC1* deletion	Open Biosystems
gic2Δ::KanMX4	Same as BY4742 except *GIC2* deletion	Open Biosystems
rdi1Δ::KanMX4	Same as BY4742 except *RDI1* deletion	Open Biosystems
rga1Δ::KanMX4	Same as BY4742 except *RGA1* deletion	Open Biosystems
rga2Δ::KanMX4	Same as BY4742 except *RGA2*	Open Biosystems

	deletion	
ste20Δ::KanMX4	Same as BY4742 except *STE20* deletion	Open Biosystems

Table 2.2. Primers used in this study (IDT Coralville, IA)

Primer Name	Sequence	Comments
KAN.RTEST	CGATTGTATGGGAAGCCCG	Reverse primer for testing *KanMX* module (600bps after start codon)
URA3.RTEST	CGCAATGTCAACAGTACCCTT	Reverse primer for testing *URA3* module (495bps after start codon)
NAT.RTEST	TCCGATTCGTCGTCCGATTC	Reverse primer for testing NatMX module (660bps after start codon)
YER071C.FTEST	TGAAGTACCTGCCCCAACTAA	Forward primer for testing *YER071c* deletion
YER071C.RTEST	CATATTGTGGAAATCTGGCG	Reverse primer for testing *YER071c* deletion
LTE1.FTEST	GGCTGTTCTCCTTACTCATC	Forward primer for testing *LTE1* deletion
LTE1.RTEST	TGCTCAGTCGGCTTCCTCTT	Reverse primer for testing *LTE1* deletion
ARP1.FTEST	CATCAGGAATTAGCAAGGGC	Forward primer for testing *ARP1* deletion
ARP1.RTEST	CTGCTCTGTGATATCTGCTC	Reverse primer for testing *ARP1* deletion
BIK1.FTEST	GCAGTAAAAGAACCTTGACC	Forward primer for testing *BIK1* deletion
BIK1.RTEST	TCATTCATGTGGCCATTGTC	Reverse primer for testing *BIK1* deletion
BIM1.FTEST	TACCGGTCAATCTGCTGATG	Forward primer for testing *BIM1* deletion
BIM1.RTEST	GCTTGTATCGCTACCAACTG	Reverse primer for testing *BIM1* deletion
BNI1.FTEST	ACTCCATACCACACACACAC	Forward primer for testing *BNI1* deletion
BNI1.RTEST	GAGGCAGTGGAAGAAGATGT	Reverse primer for testing *BNI1* deletion
DYN1.FTEST	GCGAATGGAGTAGGCAATCT	Forward primer for testing *DYN1* deletion

DYN1.RTEST	GACGATACGCCATGTGTGAT	Reverse primer for testing *DYN1* deletion
DYN2.FTEST	GAGAAGAGAATGCTTGGATGG	Forward primer for testing *DYN2* deletion
DYN2.RTEST	ATCCTCTTTCAGCTTGTCGGTC	Reverse primer for testing *DYN2* deletion
DYN3.FTEST	CCAGCCATTCGTTACAACCAT	Forward primer for testing *DYN3* deletion
DYN3.RTEST	ACTGCCATACTGTAGTGTGTC	Reverse primer for testing *DYN3* deletion
JNM1.FTEST	ATCTTGACAACCGTCCATAGG	Forward primer for testing *JNM1* deletion
JNM1.RTEST	GTTTCGAGAAGCTTCTTCCTC	Reverse primer for testing *JNM1* deletion
KAR9.FTEST	GTAAGGAGCATGATGACCAG	Forward primer for testing *KAR9* deletion
KAR9.RTEST	CAGTTGTCTCCGTATGCGTT	Reverse primer for testing *KAR9* deletion
NIP100.FTEST	CATTACTACTACTCTGTCGCC	Forward primer for testing *NIP100* deletion
NIP100.RTEST	TGTTTCTTGCGCTGCATTACC	Reverse primer for testing *NIP100* deletion
NUM1.FTEST	TAAGGATTTGGCAGCTGCAGT	Forward primer for testing *NUM1* deletion
NUM1.RTEST	AGTGAGCTCCTCAATCTTGTC	Reverse primer for testing *NUM1* deletion
PAC1.FTEST	AAACCATTCAGGTCTTGCGTG	Forward primer for testing *PAC1* deletion
PAC1.RTEST	GTAGTTTGACGGAAGTGACAG	Reverse primer for testing *PAC1* deletion
PAC11.FTEST	GCATATCGAGGAATCCCATTG	Forward primer for testing *PAC11* deletion
PAC11.RTEST	ATCCTGTTGCATGTTCGATGG	Reverse primer for testing *PAC11* deletion
BEM1.FTEST	GGCAACCTGGATAAGACACT	Forward primer for testing *BEM1* deletion
BEM1.RTEST	CTCCACAGAACCAAGGCTAA	Reverse primer for testing *BEM1* deletion
BEM4.FTEST	TGCCGTGTTTCTAAGACCA	Forward primer for testing *BEM4* deletion

BEM4.RTEST	TCTTCCATTGCCTGCAATTC	Reverse primer for testing *BEM4* deletion
SAC3.FTEST	ATGGAATGGGAGACCAAGAA	Forward primer for testing *SAC3* deletion
SAC3.RTEST	GCATAAGCTCGAAATTCAGCC	Reverse primer for testing *SAC3* deletion
LDB18.FTEST	TGTCTGGAGACCAAGTGAAG	Forward primer for testing *LDB18* deletion
LDB18.RTEST	TCTGGAACTGGAAGAATCCG	Reverse primer for testing *LDB18* deletion
BEM2.FTEST	AACTGGAACGAAGACACTTCC	Forward primer for testing *BEM2* deletion
BEM2.RTEST	TAAATCTGGGTGCGGGTAAA	Reverse primer for testing *BEM2* deletion
BEM3.FTEST	AAAGTTATATGGCGGCGGT	Forward primer for testing *BEM3* deletion
BEM3.RTEST	TTTTGGCTGCTGAAGTAGGA	Reverse primer for testing *BEM3* deletion
RGA1.FTEST	TCCGTGCTAAACTCGCAAAT	Forward primer for testing *RGA1* deletion
RGA1.RTEST	TGGGTGTGTTGACGATGATT	Reverse primer for testing *RGA1* deletion
RGA2.FTEST	AACTGGAACGAAGACACTTCC	Forward primer for testing *RGA2* deletion
RGA2.RTEST	TAAATCTGGGTGCGGGTAAA	Reverse primer for testing *RGA2* deletion
STE20.FTEST	ATTGCGATTCTGGGACCATA	Forward primer for testing *STE20* deletion
STE20.RTEST	TGAAGCGGACGCAGAAGAT	Reverse primer for testing *STE20* deletion
CLA4.FTEST	ATGATATCAAACGCGTGGGT	Forward primer for testing *CLA4* deletion
CLA4.RTEST	TTTAATGGAGACGGAGATGGG	Reverse primer for testing *CLA4* deletion
GIC1.FTEST	AACGATGTTCAAGGCATCGA	Forward primer for testing *GIC1* deletion
GIC1.RTEST	TACCATCGTGGTGAGAATCCA	Reverse primer for testing *GIC1* deletion
GIC2.FTEST	TTCCTTCTTTGGGTGTTGTG	Forward primer for testing *GIC2* deletion
GIC2.RTEST	TGTTTTGGAGATGCGTTTGG	Reverse primer for testing *GIC2* deletion

STE50.FTEST	TCAAACACATGTCCCAAGTGT	Forward primer for testing *STE50* deletion
STE50.RTEST	ATGCACGCAACTGTTTTAACG	Reverse primer for testing *STE50* deletion
RDI1.FTEST	AAGTGCCTCATGAAGGTCCTA	Forward primer for testing *RDI1* deletion
RDI1.RTEST	ATCTTGTCAACGGCAATACCC	Reverse primer for testing *RDI1* deletion
TUF1.FTEST	GCAATTATCGCTTTCCGACA	Forward primer for testing *TUF1* deletion
TUF1.RTEST	TTTAACGGTACCTGGCTTAGC	Reverse primer for testing *TUF1* deletion
RBG1.FTEST	TTTTCACGCTTTGCCTTCTC	Forward primer for testing *RBG1* deletion
RBG1.RTEST	TCTTGACGAAGCTTCCAAAAC	Reverse primer for testing *RBG1* deletion
RAS1.FTEST	ACTGACACGATGACGTTTGTG	Forward primer for testing *RAS1* deletion
RAS1.RTEST	TTTCTCTATCCGCTGTTGCA	Reverse primer for testing *RAS1* deletion
RHO5.FTEST	AAAAATGTCAAACAAGCGTCC	Forward primer for testing *RHO5* deletion
RHO5.RTEST	TTGTCAAGCTCTAGGGGGCTA	Reverse primer for testing *RHO5* deletion
VPS8.FTEST	GCCGATGAATTCGACTCTTTC	Forward primer for testing *VPS8* deletion
VPS8.RTEST	TCAACAAGTTTGCCAGTGGA	Reverse primer for testing *VPS8* deletion
BMH1.FTEST	AGAGCCAAGCACGGACTAAT	Forward primer for testing *BMH1* deletion
BMH1.RTEST	GGTAACTCTGTGGTGGCAAT	Reverse primer for testing *BMH1* deletion
RTS1.FTEST	TGGATGGTGAAATTGCTGAG	Forward primer for testing *RTS1* deletion
RTS1.RTEST	CTGGTCAACTTTGGCAATGA	Reverse primer for testing *RTS1* deletion
RTS3.FTEST	TCCGAGTTGTAGGGCAAAAT	Forward primer for testing *RTS3* deletion
RTS3.RTEST	CGTCTTGCTCCTTTTCCATT	Reverse primer for testing *RTS3* deletion
TPD3.FTEST	ACGACCAGGGTATTGTTCACA	Forward primer for testing *TPD3* deletion

TPD3.RTEST	CATCGATATATGCTTGGTTGG	Reverse primer for testing *TPD3* deletion
AMN1.FTEST	ATAGGCACTCATAGGCCACAA	Forward primer for testing *AMN1* deletion
AMN1.RTEST	AGCAATGCAAACAACACCTG	Reverse primer for testing *AMN1* deletion
ATS1.FTEST	AAGACTTGCCAATTGGATGC	Forward primer for testing *ATS1* deletion
ATS1.RTEST	GGATTTGGGCTCTTGCAATT	Reverse primer for testing *ATS1* deletion
AXL1.FTEST	CTTTTGCATTTCTGCTTCCAC	Forward primer for testing *AXL1* deletion
AXL1.RTEST	AAAGGCAAAACAGCCTGTGA	Reverse primer for testing *AXL1* deletion
AXL2.FTEST	TTAGTGGTTGCAAAGCTGGT	Forward primer for testing *AXL2* deletion
AXL2.RTEST	TCAACGGCAGAAAATCCTTC	Reverse primer for testing *AXL2* deletion
BUD4.FTEST	AAGACCATATTCCGCTCGAA	Forward primer for testing *BUD4* deletion
BUD4.RTEST	TGAAGCTTTTTGGTATCCCAG	Reverse primer for testing *BUD4* deletion
BFA1.FTEST	TTAAAAGAGCTAACTAAGGAGGC	Forward primer for testing *BFA1* deletion
BFA1.RTEST	CTCCATGTCCTGATCATCGTC	Reverse primer for testing *BFA1* deletion
BUB2.FTEST	TGCTTCCACTGCGTCGTATC	Forward primer for testing *BUB2* deletion
BUB2.RTEST	ACGCCATAGGTTCAGAAGGA	Reverse primer for testing *BUB2* deletion
KIN4.FTEST	CTTTGGTCATGCTTTGAATGC	Forward primer for testing *KIN4* deletion
KIN4.RTEST	TGGAGACATTCGATGTTGCT	Reverse primer for testing *KIN4* deletion
MX4.F	ACATGGAGGCCCAGAATACCC	Forward primer of MX4 deletion cassettes
MX4.R	CAGTATAGCGACCAGCATTCAC	Forward primer of MX4 deletion cassettes
T3	GCGCAATTAACCCTCACTAAAG	Sequencing primer
T7	TAATACGACTCACTATAGGGG	Sequencing primer

Table 2.3. Plasmids used in this study

Plasmid Name	Description
p1316	*PRS315 CDC3*-GFP
p4339	pCRII-TOPO::*MX4-NatR*
p4348	pCRII-TOPO::*MX4-URA3*
pGal-Empty	BG1805 pGal vector (Open Biosystems)
pGal-*BEM1*	BG1805 pGal vector containing *BEM1* (Open Biosystems)
pGal-*BEM4*	BG1805 pGal vector containing *BEM4* (Open Biosystems)
pGal-*LDB18*	BG1805 pGal vector containing *LDB18* (Open Biosystems)
pGal-*SAC3*	BG1805 pGal vector containing *SAC3* (Open Biosystems)

CHAPTER 3- GENETIC SCREEN FOR ENHANCERS/INHIBITORS OF MITOTIC EXIT (PROJECT #1)

3.2 Results

3.2.1 Genetic screen to identify enhancers/inhibitors of mitotic exit

3.2.1.1 Synthetic genetic array

The synthetic genetic array (SGA) is performed by crossing a haploid yeast mutant to a series of haploid deletion strains. The resulting diploids are sporulated and haploid double knockouts selected. The resulting double mutants are tested for growth defects or viability, which predicts the two genes are involved in related/redundant processes. For example, mutants involved in nuclear migration are frequently lethal when combined [8]. On the other hand, there is the possibility that the defects seen in the original single mutant could be suppressed by the deletion of another gene. For example, many mitotic exit mutants can be suppressed by deletion of spindle position checkpoint components [175, 205].

There are ~4800 non-essential ORFs in *S.cerevisiae*. Rather than using all 4800 possible mutants I chose 163 strains that I thought were likely candidates to act as suppressors or show synthetic lethality with *lte1*Δ. The 163 strains were chosen based on several criteria. One group of strains added was ones carrying deletions of G-protein related genes. Here I included deletions of known GEFs, GAPs and GTPases as the MEN is ultimately controlled by a small Ras like GTPase which may have other GAPs or GEFs controlling its activity. Furthermore, other GTPases may have a role in mitotic exit, much like Cdc42p, which has recently been implicated in this process [188, 189]. These three sets of strains are grouped into deletions of GEFs, GTPases, and GAPs (Table 3.1). I also included several Cdc42p regulatory or interacting proteins as the role of Cdc42p activating mitotic exit is still not fully understood. These strains are combined in the miscellaneous section with several other strains I have chosen based on: general mitotic defects such as arrest, potential to localize MEN components, protein interactions with MEN components with no known mitotic exit role, and involvement in processes suspected but not linked to mitotic exit prior (Table 3.1).

Additionally, a large proportion of the strains chosen contained deletions in genes that are components of specific processes that have been implicated in mitotic exit. However, these genes themselves have not been tested for their effects on mitotic exit. These classes include: the septin collar components, the protein phosphatase PP2A, sumoylation, and nuclear migration. The septins and related proteins have been shown to be necessary for proper mitotic exit as some of them have been shown to localize Lte1p to the bud [173]. Thus, several other components of the septin ring may also have roles in mitotic exit [173]. The protein phosphatase PP2A has been shown to have a role in the FEAR as well as the SPC (Figure 1.8). However, only the role of the regulatory component Cdc55p (the PP2A regulatory component) has been examined, thus we included the other components in our screen [145, 176, 179, 181]. Nuclear migration components were included as some of them are known to interact genetically with *LTE1* [8]. Sumoylation is the process of small ubiquitylation like post-translational modification of proteins. Sumoylation has been shown to have a role in rDNA segregation via sumoylating a component of the condensin complex [206]. Interestingly, this sumoylation is dependent on proper functioning of the FEAR. Thus, sumoylation may play a role in mitotic exit [206]. Finally, we included a series of sister chromatid cohesion gene deletions as several have been shown to interact with *lte1*Δ, thus serving as positive controls and expanding on this area (Table 3.1) [207].

3.2.1.2 Results of the screen

Once the 163 strains were chosen and the *MAT**a** lte1Δ::URA3* query strain was created, the crosses were carried out. The crosses were placed at either 30°C to test for synthetic lethality (SL)/slow growth (SG) phenotypes, or 10°C to identify suppression (Sup) of the *lte1*Δ low temperature mitotic arrest. I performed the crosses three times and included the positive controls *slk19*Δ, *spo12*Δ, *dyn1*Δ, *arp1*Δ, *kar9*Δ, *dcc1*Δ, *ctf4*Δ, *ctf8*Δ, *ctf18*Δ and *ste20*Δ [8, 193]. The screen produced 43 candidates that displayed synthetic growth interactions with *lte1*Δ at 30° C. 19 of these 43 candidates was identified in all three trials. Also, 20 candidates suppressed *lte1*Δ cold sensitivity and 12 of these suppressed in all three trials (Table 3.1). These hits included the chosen positive controls of *bub2*Δ, *bfa1*Δ, and *kin4*Δ.

Table 3.1. Synthetic genetic array of *lte1*Δ and 163 candidate deletion strains. The haploid *lte1*Δ (*MAT**a** lte1*Δ*::URA3*) query strain was crossed to 163 candidate deletions strains (*MAT*α *xxx*Δ*::KanR*). Candidate deletions were chosen based on their involvement in: G-protein signaling (GEFs, GAPs, G-proteins), protein dephosphorylation (PP2A), MEN relation, nuclear migration, septin function/assembly, sumoylation, and sister chromatid cohesion. The haploid knockout stains were crossed and the resulting diploids were sporulated. The resulting spores were then subjected to selection for progeny containing both knockouts. The haploid double knockouts were tested for synthetic interactions with *lte1*Δ at 30°C. and at 10°C for suppression of the *lte1*Δ. This screen was performed in triplicate. Synthetic interactions were scored as synthetic growth defect (SG), synthetic lethal (SL), or suppression (Sup). Yellow rows represent positive controls for the 30°C tests and green rows represent positive controls for the 10°C tests. Black boxes represent loss of the strain during the construction of the SGA. Results of the screen to date are given in the final result column for correspondence with raw data. N/A= not applicable, FP= false positive, FN= false negative, Confirmed (TA)= tetrad analysis, Confirmed(RSA)= random spore analysis.

Deletion Strains	30 Deg.			10 Deg.			Final Result
	#1	#2	#3	#1	#2	#3	
GEFS							
Δgea1		■			■		N/A
Δmid2							N/A
Δsdc25							N/A
Δsec7							N/A
Δsyt1							N/A
Δtuf1		■		Sup	■		Unconfirmed
Δtus1							N/A
Δvps9							N/A
Δyll017w							N/A
GTPases							
Δarf3							N/A
Δarl1							N/A
Δarl3							N/A
Δbts1							N/A
Δcin4			SL				FP
Δdnm1							N/A
Δfzo1		■	■		■	■	N/A
Δguf1							N/A
Δmgm1	SG	SG	SG				Confirmed (RSA)
Δmog1	SG	SG	SG				Confirmed (RSA)
Δras1				Sup			Unconfirmed
Δras2							N/A

Deletion Strains	30° C			10° C			Final Result
	#1	#2	#3	#1	#2	#3	
Δrbg1				Sup	Sup	Sup	Unconfirmed
Δrbg2							N/A
Δrhb1			SL				FP
Δrho2							N/A
Δrho4							N/A
Δrho5				Sup			Unconfirmed
Δrsr1							N/A
Δsey1							N/A
Δsst2			■			■	N/A
Δvps1							N/A
Δvps21							N/A
Δylf2							N/A
Δypt11			■			■	N/A
Δypt31							N/A
Δypt32							N/A
Δypt52							N/A
Δypt53			■			■	N/A
Δypt7							N/A
GAPS							
Δbag7							N/A
Δbem2				Sup	Sup	Sup	Unconfirmed
Δbem3							N/A
[redacted]	[redacted]	[redacted]	[redacted]	[redacted]	[redacted]	[redacted]	[redacted]
Δbud2							N/A
Δgyl1							N/A
Δgyp1							N/A
Δgyp5							N/A
Δgyp6							N/A
Δgyp7							N/A
Δgyp8							N/A
Δira2		SL					FP
Δlrg1							N/A
Δmdr1							N/A
Δmsb3							N/A
Δmsb4							N/A
Δrdg1							N/A
Δrga1		■			■		N/A
Δrga2				Sup	Sup	Sup	Unconfirmed
Δrgd2							N/A

Deletion Strains	30° C			10° C			Final Result
	#1	#2	#3	#1	#2	#3	
Misc. Interactions							
Δaxl1				Sup	Sup	Sup	Unconfirmed
Δaxl2				Sup	Sup	Sup	Unconfirmed
Δbem1		SL	SL	Sup			Confirmed (TA)
Δbem4	SL	SL	SL				Confirmed (TA)
Δbmh1		■		Sup	■	Sup	Unconfirmed
Δdcs2							N/A
Δerf2		SG	■			■	Unconfirmed
Δfar1			SL				FP
Δfus3	■			■			N/A
Δgic1							N/A
Δgic2							N/A
Δgis1							N/A
Δgis4							N/A
Δgtr1							N/A
Δgtr2							N/A
Δmdg1							N/A
Δmdv1			SL				FP
Δmog1	SG	SG	SG				Confirmed (RSA)
Δmsi1							N/A
Δmsl1							N/A
Δpex25							N/A
Δplp1							N/A
Δpxl1	SG						FP
Δrdi1		■			■		N/A
Δrgs2							N/A
Δrpi1							N/A
Δsac3	SL	SG	SL				Confirmed (TA)
Δsed4							N/A
Δshr5	■	SG	SG	■			Unconfirmed
Δsic1		SL	SL				Unconfirmed
Δskm1							N/A
Δstb4							N/A
Δste14							N/A
Δste20							**FN**
Δste4							N/A
Δsys1							N/A
Δtaz1							N/A
Δugo1	SG	■	SG		■		Confirmed (RSA)
Δvps8				Sup	Sup	Sup	Unconfirmed
Δyip3							N/A
Δyip4							N/A

Deletion Strains	30° C			10° C			Final Result
	#1	#2	#3	#1	#2	#3	
Δyip5							N/A
Δzeo1							N/A
PP2A							
Δpph21							N/A
Δpph22							N/A
Δppm1							N/A
Δppm2							N/A
Δrts1		SG		Sup		Sup	FP/Unconfirmed
Δrts3				Sup	Sup	Sup	Unconfirmed
Δtpd3	SL	[redacted]			[redacted]	Sup	FP
Men Related							
Δamn1				Sup	Sup	Sup	Unconfirmed
[redacted]	[redacted]	[redacted]	[redacted]	[redacted]	[redacted]	[redacted]	[redacted]
Δbub1	SG	SG	SG				Unconfirmed
[redacted]	[redacted]	[redacted]	[redacted]	[redacted]	[redacted]	[redacted]	[redacted]
Δbub3	SG	SG	SG				Unconfirmed
Δdbf2	SL	SL	SL				Unconfirmed
Δdbf20	[redacted]			[redacted]			N/A
Δfob1	[redacted]		[redacted]	[redacted]		[redacted]	N/A
[redacted]	[redacted]	[redacted]	[redacted]	[redacted]	[redacted]	[redacted]	[redacted]
Δmad1							N/A
Δmad2							N/A
Δmad3							N/A
Δshe1	[redacted]			[redacted]			N/A
Δshe10							N/A
Δslk19	**SL**		**SL**				**Syn + control**
Δspo12		**SG**	**SG**				**Syn + control**
Δyjl213w	[redacted]			[redacted]			N/A
Nuclear Migration							
Δarp1	**SG**		**SG**				**Syn + control**
Δats1				Sup	Sup	Sup	Unconfirmed
Δbik1	SG	SG	SG				FP
Δbim1	SG	SG	SG				Unconfirmed
Δbni1		SG	SG				Unconfirmed
Δdyn1	**SG**	**SG**	**SG**				**Syn + control**
Δdyn2	SG	SG	SG				FP
Δdyn3		SG	SG				FP
Δjnm1		SG	SG				Unconfirmed
Δkar9							**FN**
Δldb18	SG	SL	SG				Confirmed (TA)
Δnip100	SG	SG	SG				Confirmed (RSA)

Deletion Strains	30° C #1	30° C #2	30° C #3	10° C #1	10° C #2	10° C #3	Final Result
Δnum1	SG		SG				Unconfirmed
Δpac1	SG	SG	SG				FP
Δpac11	SL	SG	SG				Confirmed (RSA)
Δpac2							N/A
Δpat1							N/A
Δtub3	SG	■	■		■	■	FP
Septin Related							
Δbud3							N/A
Δbud4	■			■	Sup	Sup	Unconfirmed
Δcdc10							N/A
Δnis1	■			■			N/A
Δshs1		SG	SG				Confirmed (TA)
Sumo Related							
Δnfi1							N/A
Δsiz1							N/A
Δwss1							N/A
Δyjr024c							N/A
Sister Chromatid Cohesion							
Δcik1	SL	■	SL		■		Unconfirmed
Δctf18							FN
Δctf4	SL	SG	SG				Syn + control
Δctf8	SL	SG	SG				Syn + control
Δdcc1	SG	SG	SG				Syn + control
Δndj1							N/A
Δrec8	SL						Unconfirmed
Δspo13							N/A
Δvik1							N/A

The synthetic lethal/sick candidates consisted of groups of genes involved in the following processes: G-protein signaling, mitochondrial fission/fusion, protein palmitoylation, cell polarization, the MEN, nuclear migration, sister chromatid cohesion, and nuclear export (Table 3.2).

Unfortunately, the screen did not identify three known SL/SG interactions between *lte1*Δ and *ste20*Δ, *ctf18*Δ, and *kar9*Δ. I also did not identify three other hits that the dSLAM analysis discovered (*she1*Δ, *she10*Δ, and *fus3*Δ) [198]. These inconsistencies are either due to problems with the query strain (*lte1*Δ), the candidate strains, or the resulting double mutant strains from the SGA. Considering that a series of positive controls were identified with the query strain, the query strain appears to be of good quality. Thus, the inability to detect the synthetic interactions with *ste20*Δ, *ctf18*Δ, *kar9*Δ, *she1*Δ, *she10*Δ, and *fus3*Δ must be due to the candidate strains. These strains may have been contaminated or have accumulated second site mutations that improve growth. However, in another SGA screen performed in our lab (H. Wang and N. Adames, unpublished results), the *dyn1*Δ query strain and the *kar9*Δ strain from the deletion set were PCR tested and found to carry only the appropriate deletion alleles. Nevertheless, the *dyn1*Δ *kar9*Δ strain, which should be lethal, was instead disomic (i.e., it carried both the wt and deletion alleles of *KAR9*), suggesting that strong selection for growth during SGA selects for disomic double mutants. This selection could be evident in mutants involved in chromosome segregation, such as *kar9*Δ and *ctf18*Δ - two of the problematic strains in my screen.

The suppressor candidates fell into only a few groups. Suppressors were identified in the following groups: protein dephosphorylation (PP2A components), Rho GAPs, and axial budding pattern proteins. Several candidates were also identified as miscellaneous suppressors (due to no other related suppressors identified in the screen). Although, a large group of unrelated suppressors were identified this should not cast doubt on their validity given that I only examined 163 of 4800 viable deletion strains. Moreover, the screen also identified several known deletion suppressors of *lte1*Δ such as spindle position checkpoint proteins *bub2*Δ, *bfa1*Δ, and *kin4*Δ (Table 3.3) [29, 169, 174, 175, 208]. The screen also identified the 'antagonist of mitotic exit network' *amn1*Δ, which is a characterized inhibitor of the Tem1p Cdc15p interaction [208]. Thus this interaction, although new, is an expected result.

Interestingly, the *lte1*Δ linked gene deletion *ats1*Δ suppresses in our selection. This result is curious as the two genes, being linked, would only create a double mutant when a crossover occurred between the two genes. As this is a rare event one would expect that a small proportion of double mutants would be produced thus possibly creating a false positive. However, in our case we obtained viable doubles that suppressed the *lte1*Δ. This observation can be explained by one of two possibilities. First, the *ats1*Δ could suppress the *lte1*Δ as it has been shown prior to be an inhibitor of the cell cycle [209]. On the other hand, this suppression could simply be due to another case of disomy. Being that the two genes are linked this may create selective pressure upon creating disomics that have both of the *LTE1* and *ATS1* containing chromosomes. As a result, these cells will not only be viable but will suppress the *lte1*Δ defect. Thus, this candidate will need to be confirmed accordingly in the future.

Tables of synthetic and suppressor candidates are given with their characterization summary from the Saccharomyces Genome Database (www.yeastgenome.org) for interest and comparison among groups.

Table 3.2. Descriptions of the gene knockouts that synthetically interact with *lte1*Δ. All candidates that interacted with *lte1*Δ are provided here along with their description as presented in the Saccharomyces Genome Database (http://www.yeastgenome.org/). Although the *erf2*Δ candidate only interacted once with *lte1*Δ it was included as its functional partner *shr5*Δ was observed to interact twice. Candidates were then grouped according to their description into the following categories: G-protein signaling, mitochondrial fission/fusion, protein palmitoylation, cell polarization, the MEN, nuclear migration, sister chromatid cohesion, and nuclear export.

Synthetic Candidates	Description
G-Protein Signaling	
mog1Δ	Conserved nuclear protein that interacts with GTP-Gsp1p, which is a Ran homolog of the Ras GTPase family, and stimulates nucleotide release, involved in nuclear protein import, nucleotide release is inhibited by Yrb1p
Mitochondrial fission/fusion	
ugo1Δ	Protein of unknown function; outer membrane component of the mitochondrial fusion machinery; Ugo1p bind directly to Fzo1p and Mgm1p and thereby link these two GTPases during mitochondrial fusion
mgm1Δ	Mitochondrial GTPase related to dynamin, present in a complex containing Ugo1p and Fzo1p; required for normal morphology of cristae and for stability of Tim11p; homolog of human OPA1 involved in autosomal dominant optic atrophy
Protein Palmitoylation	
shr5Δ	Subunit of a palmitoyltransferase, composed of Shr5p and Erf2p, that adds a palmitoyl lipid moiety to heterolipidated substrates such as Ras1p and Ras2p through a thioester linkage; palmitoylation is required for Ras2p membrane localization
erf2Δ	Subunit of a palmitoyltransferase, composed of Erf2p and Shr5p, that adds a palmitoyl lipid moiety to heterolipidated substrates such as Ras1p and Ras2p through a thioester linkage; mutants partially mislocalize Ras2p to the vacuole

Nuclear Export

sac3Δ	Nuclear pore-associated protein, forms a complex with Thp1p that is involved in transcription and in mRNA export from the nucleus

Cell Polarization

bem1Δ	Protein containing SH3-domains, involved in establishing cell polarity and morphogenesis; functions as a scaffold protein for complexes that include Cdc24p, Ste5p, Ste20p, and Rsr1p
bem4Δ	Protein involved in establishment of cell polarity and bud emergence; interacts with the Rho1p small GTP-binding protein and with the Rho-type GTPase Cdc42p; involved in maintenance of proper telomere length

MEN Related

bub3Δ	Kinetochore checkpoint WD40 repeat protein that localizes to kinetochores during prophase and metaphase, delays anaphase in the presence of unattached kinetochores; forms complexes with Mad1p-Bub1p and with Cdc20p, binds Mad2p and Mad3p
bub1Δ	Protein kinase that forms a complex with Mad1p and Bub3p that is crucial in the checkpoint mechanism required to prevent cell cycle progression into anaphase in the presence of spindle damage, associates with centromere DNA via Skp1p
dbf2Δ	Ser/Thr kinase involved in transcription and stress response; functions as part of a network of genes in exit from mitosis; localization is cell cycle regulated; activated by Cdc15p during the exit from mitosis
spo12Δ	Nucleolar protein of unknown function, positive regulator of exit from mitosis; involved in regulating the release of Cdc14p from the nucleolus in early anaphase; proposed to play similar role in meiosis
slk19Δ	Kinetochore-associated protein required for normal segregation of chromosomes in meiosis and mitosis; component of the FEAR regulatory network, which promotes Cdc14p release from the nucleolus during anaphase; potential Cdc28p substrate

sic1Δ	Inhibitor of Cdc28-Clb kinase complexes that controls G1/S phase transition, preventing premature S phase and ensuring genomic integrity; phosphorylation targets Sic1p for SCF(*CDC4*)-dependent turnover; functional homolog of mammalian Kip1p
shs1Δ	One of five related septins (Cdc3p, Cdc10p, Cdc11p, Cdc12p, Shs1p) that form a cortical filamentous collar at the mother-bud neck which is necessary for normal morphogenesis and cytokinesis

Nuclear Migration

dyn1Δ	Cytoplasmic heavy chain dynein, microtubule motor protein, required for anaphase spindle elongation; involved in spindle assembly, chromosome movement, and spindle orientation during cell division, targeted to microtubule tips by Pac1p
dyn2Δ	Cytoplasmic light chain of dynein microtubule motor protein
dyn3Δ	Dynein light intermediate chain (LIC); localizes with dynein, null mutant is defective in nuclear migration
pac1Δ	Protein involved in nuclear migration, part of the dynein/dynactin pathway; targets dynein to microtubule tips, which is necessary for sliding of microtubules along bud cortex; synthetic lethal with *bni1*Δ; homolog of human LIS1
pac11Δ	Dynein intermediate chain, acts in the cytoplasmic dynein pathway, forms cortical cytoplasmic microtubule capture site with Num1p; null mutant is defective in nuclear migration, essential in the absence of *CIN8*
ldb18Δ	Protein of unknown function; null mutant shows a reduced affinity for the alcian blue dye suggesting a decreased net negative charge of the cell surface
arp1Δ	Actin-related protein of the dynactin complex; required for spindle orientation and nuclear migration; putative ortholog of mammalian centractin
nip100Δ	Large subunit of the dynactin complex, which is involved in partitioning the mitotic spindle between mother and daughter cells; putative ortholog of mammalian p150(glued)
jnm1Δ	Component of the yeast dynactin complex, consisting of Nip100p, Jnm1p, and Arp1p; required for proper nuclear migration and spindle partitioning during mitotic anaphase B

num1Δ	Protein required for nuclear migration, localizes to the mother cell cortex and the bud tip; may mediate interactions of dynein and cytoplasmic microtubules with the cell cortex
bni1Δ	Formin, nucleates the formation of linear actin filaments, involved in cell processes such as budding and mitotic spindle orientation which require the formation of polarized actin cables, functionally redundant with *BNR1*
bim1Δ	Microtubule-binding protein that together with Kar9p makes up the cortical microtubule capture site and delays the exit from mitosis when the spindle is oriented abnormally
bik1Δ	Microtubule-associated protein, component of the interface between microtubules and kinetochore, involved in sister chromatid separation; essential in polyploid cells but not in haploid or diploid cells; ortholog of mammalian CLIP-170

Sister Chromatid Cohesion

dcc1Δ	Subunit of a complex with Ctf8p and Ctf18p that shares some components with Replication Factor C, required for sister chromatid cohesion and telomere length maintenance
ctf4Δ	Chromatin-associated protein, required for sister chromatid cohesion; interacts with DNA polymerase alpha (Pol1p) and may link DNA synthesis to sister chromatid cohesion
ctf8Δ	Subunit of a complex with Ctf18p that shares some subunits with Replication Factor C and is required for sister chromatid cohesion
cik1Δ	Kinesin-associated protein required for both karyogamy and mitotic spindle organization, interacts stably and specifically with Kar3p and may function to target this kinesin to a specific cellular role; has similarity to Vik1p

Table 3.3. Descriptions of gene knockouts that suppress the *lte1*Δ cold lethality phenotype. Candidates that suppressed the *lte1*Δ cold sensitivity are described as presented in the Saccharomyces Genome Database (http://www.yeastgenome.org/). The candidates were then grouped into the following categories: the spindle position checkpoint (positive controls), protein dephosphorylation (PP2A components), Rho activity, axial budding patterns, or an uncommon process to any of the other suppressors.

Suppressor Candidates	Description
Known Suppressors Identified	
bub2Δ	Mitotic exit network regulator, forms GTPase-activating Bfa1p-Bub2p complex that binds Tem1p and spindle pole bodies, blocks cell cycle progression before anaphase in response to spindle and kinetochore damage
bfa1Δ	Component of the GTPase-activating Bfa1p-Bub2p complex involved in multiple cell cycle checkpoint pathways that control exit from mitosis
kin4Δ	Kinase that acts by inhibiting the mitotic exit network (MEN) when the spindle position checkpoint is activated; localized asymmetrically to mother cell cortex, spindle pole body and bud neck
Protein Dephosphorylation (PP2A components)	
rts1Δ	B-type regulatory subunit of protein phosphatase 2A (PP2A); homolog of the mammalian B' subunit of PP2A
rts3Δ	Putative component of the protein phosphatase type 2A complex
Rho activity	
rga2Δ	GTPase-activating protein for the polarity-establishment protein Cdc42p; implicated in control of septin organization, pheromone response, and haploid invasive growth
bem2Δ	Rho GTPase activating protein (RhoGAP) involved in the control of cytoskeleton organization and cellular morphogenesis; required for bud emergence

Axial Budding Proteins

axl1Δ	Haploid specific endoprotease that performs one of two N-terminal cleavages during maturation of a-factor mating pheromone; required for axial budding pattern of haploid cells
axl2Δ	Integral plasma membrane protein required for axial budding in haploid cells, localizes to the incipient bud site and bud neck; glycosylated by Pmt4p; potential Cdc28p substrate
bud4Δ	Protein involved in bud-site selection and required for axial budding pattern; localizes with septins to bud neck in mitosis and may constitute an axial landmark for next round of budding; potential Cdc28p substrate

Misc. Suppressors

rbg1Δ	Member of the DRG family of GTP-binding proteins; interacts with translating ribosomes and with Tma46p
vps8Δ	Membrane-associated hydrophilic protein that interacts with the small GTPase, Vps21p, to facilitate soluble vacuolar protein localization; required for localization and trafficking of the CPY sorting receptor; contains a RING finger motif
bmh1Δ	14-3-3 protein, major isoform; controls proteome at post-transcriptional level, binds proteins and DNA, involved in regulation of many processes including exocytosis, vesicle transport, Ras/MAPK signaling, and rapamycin-sensitive signaling
ats1Δ	Protein required, with Elongator complex, Kti11p, and Kti12p, for modification of wobble nucleosides in tRN a potential role in regulatory interactions between microtubules and the cell cycle
amn1Δ	Protein required for daughter cell separation, multiple mitotic checkpoints, and chromosome stability; contains 12 degenerate leucine-rich repeat motifs; expression is induced by the Mitotic Exit Network (MEN)

3.2.1.3 Confirmation of synthetic genetic interactions

Although the screen was completed in triplicate, some of the crosses were unsuccessful. As a result, some of the candidates were only tested twice or even once. Furthermore, some of the candidates were only found to have a synthetic interaction with *lte1*Δ once or twice out of the three trials. Thus, to confirm the genetic interactions we performed tetrad analysis or random spore analysis [5].

Tetrad Analysis (TA) was performed on the candidates we hoped to pursue in further experiments. The *bem1Δ, bem4Δ, ldb18Δ, sac3Δ, and shs1Δ* strains were pursued due to their interesting prior characterization or lack of characterization. I will address this potential in the discussion/conclusions section. These strains were re-crossed to the *lte1*Δ query strain and analyzed by tetrad dissection to observe their genetic interactions. Our criteria for confirming a synthetic genetic interaction was the analysis of at least 6 full tetrads but often 12 or more tetrads were analyzed to ensure authenticity of interaction. The tetrad analysis confirmed that all these chosen candidates show synthetic interactions with the *lte1*Δ. Spores from full tetrads of the *bem1*Δ, *bem4*Δ, *ldb18*Δ, and *sac3*Δ crosses were PCR confirmed along with their *lte1*Δ counterpart to ensure identity of the strain. Further, a positive control of *slk19*Δ was used to ensure that tetrad analysis was performed properly (Table 3.4).

Random Spore Analysis (RSA) was used to confirm some of the remaining synthetic interactions. Here we set a standard of at least 200 spores observed on each of the single selection media to confirm synthetic lethality. If a double knockout strain was synthetically lethal, 200 spores would grow on both the single selection media (SD-ura or YPAD+G418) but not the double selection media (SD-ura+G418). If the interaction was a synthetic slow growth phenotype, the strain will grow noticeably slower on the double selection media. Overall, out of 19 strains subjected to RSA, 6 were confirmed as synthetic interactors with *lte1*Δ (Table 3.5).

As this is just preliminary data, several candidates were not analyzed due to limitations of time and cost and will have to be addressed in the future to complete the study. We also intend to confirm our RSA candidates by PCR to ensure the identity of the strain. To date only some of our strains tested by RSA have been PCR confirmed and will need to be completed in the future. Although, the RSA did confirm 6 candidates, several of which are consistent with the dSLAM study, there were some inconsistencies within the RSA analysis. These inconsistencies come in the form of false positives that make up the majority of the RSA confirmed candidates.

One reason I identified a large proportion of false positives was the approach I used for RSA. Typically false positives are avoided by the triplication of the screen and are eliminated by the TA or RSA confirmation step. However, here I am analyzing candidates that may have shown a genetic interaction with the query strain in only one trial. Although including these candidates ensures that I do not miss many potential interactors, it does produce a larger proportion of false positives, which have to be eliminated by confirmation. As we can see in Table 3.3, several synthetic lethal false positives only interacted with the query strain once. These false positives could have resulted from loss of cells or high mortality in ether during the SGA process.

Some of the false positives, however, are suspect. The *bik1Δ*, *dyn2Δ*, *dyn3Δ* and *pac1Δ* were synthetic growth hits in all three trials of the screen but were shown to be false positives by RSA. It is possible that these candidates genetically interact with *lte1Δ* as they are all components of the nuclear migration process, which is known to interact genetically with *lte1Δ* [8, 198]. However, none of these strains were hits with the dSLAM analysis [198]. Therefore, these strains will have to be reconstructed, PCR tested, and tetrad analysis should be performed to confirm the false-positive status of the double mutants.

Overall, the RSA results are incomplete and some need to be repeated. However, 4 of 6 interactions were confirmed and are consistent with the literature [8, 198]. Therefore, we believe that these mutants are really synthetically lethal with *lte1Δ*.

We chose to confirm the suppression candidates by PCR confirmation, re-crossing, and subsequent characterization of growth at 10° C. Although we have confirmed all of the identities of the suppressor candidates by PCR, we chose to abandon the re-crossing and suppression characterization test until a later date. Unfortunately, yeast strains grow too slowly at 10°C to facilitate an efficient and thorough study under time constraints. Wildtype yeast strains when grown at 10°C do not produce readily observable colonies until approximately 1 month of growth. Furthermore, as this is the rate for the wildtype strain, the rate of growth for a suppressed *lte1*Δ strain has the possibility of growing even slower. Thus, to conserve time we chose to pursue the synthetic interacting candidates.

Table 3.4. Confirmation of synthetic genetic interactions with *lte1*Δ by tetrad analysis. A haploid deletion of *lte1*Δ*::URA3* was crossed to 5 gene deletions (*bem1*Δ*::KanR, bem4*Δ*::KanR, ldb18*Δ*::KanR, sac3*Δ*::KanR, shs1*Δ*::KanR*) that displayed synthetic interactions with *lte1*Δ within the SGA. Candidates were chosen if their role within the MEN had not been established and/or if they had been poorly characterized to date. These diploids were then selected and sporulated. Spore coats were then digested using β-Glucuronidase and the four asci of each tetrad were dissected apart using a micromanipulator. Spores were then grown, tested for mating type, and tested for the presence of knockout cassettes. The progeny were then analyzed for synthetic growth defects or lethality in the double knockouts. Full tetrads were analyzed for spores not growing when double knockout was predicted and observed for growing double knockouts. Total spore count was also obtained and the expected number of double knockouts (1/4 of total) was compared to total double knockouts growing. From these data a conclusion was made as of the presence or absence of genetic interaction with query strain. The gene deletion *slk19*Δ*::KanR* was used as a positive control for synthetic lethality.

lte1Δ crossed to:	# full tetrads	# predicted *lte1Δ* *xxxΔ* spores not growing	# *lte1Δ* *xxxΔ* spores growing in full tetrads	total # spores assayed	expected # of lte1*Δ* *xxxΔ* spores	# *lte1Δ* *xxxΔ* spores growing	Synthetic Growth or Lethality
bem1Δ	*15*	18	0	78	19	0	SL
bem4Δ	*16*	15	0	81	20	1	SL
ldb18Δ	*13*	1	10(9SG)	82	20	16(15SG)	SG
sac3Δ	*12*	8	~~0~~ 2	59	15	0	SL
shs1	6	0	4 (4SG)	76	19	11(11SG)	SG
slk19	7	5	0	48	12	1	SL

Table 3.5. Confirmation of Synthetic Genetic interactions with *lte1*Δ by Random Spore Analysis. A haploid deletion of *lte1*Δ*::URA3* (*MAT**a***) was crossed to 19 gene deletion strains (*MATα xxx*Δ*::KanR*) that displayed synthetic interactions with *lte1*Δ within the Directed Synthetic Genetic Array. These candidates either have been previously characterized or don't have obvious direct potential roles in the regulation of Mitotic Exit. The resulting diploids were then selected and sporulated. The cultures were then treated with ether to kill diploids and 3 of 4 spores and plated on single and double knockout selection media. If candidates could grow on both single knockout selection media but was slow growing or not able to grow the double media, this indicates a synthetic defect (synthetic growth defect [SG], or synthetic lethal [SL]). However, if the strain could grow on the double selection media then it was identified as a false positive (FP) from the original screen. Results from original screen are also stated for comparison.

Candidates	Screen Results	PCR Confirmed	-ura	+G418	-ura+G418	SG,SL, or FP
*cin4*Δ	1SL	N	>300	>300	>300	FP
*rhb1*Δ	1SL	N	>300	>300	>300	FP
*mgm1*Δ	3SG	N	208	>300	2	SL
*ira2*Δ	1SL	N	>300	>300	>300	FP
*mog1*Δ	3SG	N	256	263	10	SL
*pxl1*Δ	1SG	N	>300	>300	>300	FP
*mdv1*Δ	1SG	N	>300	>300	>300	FP
*ugo1*Δ	2SG	N	228	>300	5	SL
*far1*Δ	1SL	N	>300	>300	>300	FP
*rts1*Δ	1SG+2Sup	Y	>300	>300	>300	FP
*tpd3*Δ	1SL	Y	>300	>300	>300	FP
*nip100*Δ	3SG	Y	>300	>300	>300	SG
*arp1*Δ	2SG	Y	>300	>300	>300	SG
*bik1*Δ	3SG	Y	>300	>300	>300	FP
*dyn2*Δ	3SG	Y	>300	>300	>300	FP
*dyn3*Δ	2SG	Y	>300	>300	>300	FP
*tub3*Δ	1SG	N	>300	>300	>300	FP
*pac1*Δ	3SG	Y	>300	>300	>300	FP
*pac11*Δ	2SG+1SL	Y	>300	>300	>300	SG

3.2.2 Phenotypes of several candidates

Some specific roles of a gene within *Saccharomyces cerevisiae* can be inferred by subjecting the deletion mutant to a simple test of growth sensitivity to temperature. As a result this technique can be used to test for a phenotype that can be used later for epistatic analysis. Normally, temperature sensitivity (TS) is determined at 37° C and cold sensitivity (CS) is tested at 15° C. For example, some deletions involved in the process of actin polarity and assembly are TS [210-212]. Also, strains lacking genes involved in nuclear migration are CS due to the accumulation of multinucleate cells over time [2, 98]. Thus, we took the *bem1*Δ, *bem4*Δ candidates (both shown to be involved in actin polarity) and *lbd18*Δ (a gene predicted to be involved in nuclear migration) and tested them for a growth phenotype at 37° C and 15° C. We also included the *sac3*Δ candidate, as its phenotype at various temperatures is unknown. The strains of the *bem1*Δ, *bem4*Δ, *ldb18*Δ, and *sac3*Δ deletions were replica-pinned and placed at 15°C, 30°C, and 37°C. The *bem1*Δ strain was sensitive to low as well as high temperatures. The *bem4*Δ strain displayed a slight TS phenotype, and a lethal CS phenotype. The *ldb18*Δ strain was found only to be CS. The *sac3*Δ strain, displayed a slow growth phenotype even at the optimal growth conditions of 30°C, but this growth defect does not seem to be affected by temperature (Figure 3.1).

3.2.3 Overexpression of candidate ORFs

Given that these candidates are possible activators of mitotic exit, overexpression could suppress the *lte1*Δ low temperature lethality. This is a common feature of other mitotic exit activators such as the PAK kinase Ste20p [188]. Hence we transformed the *lte1*Δ strain with vectors using the *GAL1* promoter (p*GAL1*) to drive overexpression of *BEM1, BEM4, LDB18,* and *SAC3*. *TEM1* overexpression is known to suppress *lte1*Δ and was used as a control [189]. The transformants were then subjected to overexpression at optimal (30°C) and semi-lethal (15°C) temperatures.

At optimal temperatures, the overexpression of all of the tested candidates (*BEM1, BEM4, LDB18, and SAC3*) caused growth defects. The *SAC3* overexpression was lethal in the *lte1*Δ cells. *BEM1* and, to a lesser extent, *BEM4* overexpression caused a severe growth defect in the *lte1*Δ strain. *LDB18* overexpression, however, produced a moderate/low growth defect. From the literature [189], *TEM1* overexpression had no adverse effects on the growth of the *lte1*Δ strain and suppressed the lte1Δ growth defect at 15° C (Figure 3.2a).

Although this system did cause lethality when induced, we decided to test suppression in case lethality is due to over-activation of mitotic exit, which may be detrimental at normal or high temperatures, but beneficial at low temperatures when cells are arresting in anaphase. To ensure that the lack of growth is due to lack of suppression and not lethality we tested this suppression of *lte1*Δ in semi-lethal conditions of 15° C. Thus, the *lte1*Δ will grow at a low level, which will indicate a lack of suppression. Conversely, a lack of growth at this temperature would indicate lethality due to overexpression.

None of the candidate strains were able to rescue the *lte1*Δ cold temperature sensitivity. Furthermore, no candidate grew to the same extent as the *lte1*Δ p*GAL* empty strain. Thus, it looks as though this overexpression system is lethal to *lte1*Δ cells. This result can be explained by a combination of two reasons. First, this could be due to the constitutive nature of the *GAL1* overexpression system. As we have expressed these proteins at such a high level this might have produced a protein level that is toxic to the cell. This would explain why all candidates displayed some degree of growth defects. Furthermore, *BEM1* overexpression has previously been shown to suppress the *lte1*Δ arrest [188]. This suppression however was produced by a multicopy plasmid containing the ORF's wildtype promoter. This system milder overexpression as regulation of gene expression is, to some extent, normal. Thus, to fully confirm that all of these candidates are lethal to the cell when overexpressed this assay needs to be repeated using *BEM1, BEM4, LDB18,* and *SAC3* overexpressed under their own promoters in a multicopy plasmid. Second, these *GAL1* inducible plasmids express their ORFs with protein A, 6xHis, and HA C-terminal tags which are together 19kDa in size. These tags may produce a dominant negative effect when expressed, as their phenotype under induction is worse than that of the corresponding knockout strains. Again this situation can be rectified by the use a multicopy overexpression system using the normal gene and regulatory untranslated regions. However, taking into account both of these reasons it should be noted that the positive control *TEM1* did not show lethality when overexpressed and suppressed the *lte1*Δ cold sensitive phenotype as previously shown [156, 162, 188]. Thus this protein either is not dominant negative when C-terminally tagged or is not toxic to the cell when overexpressed.

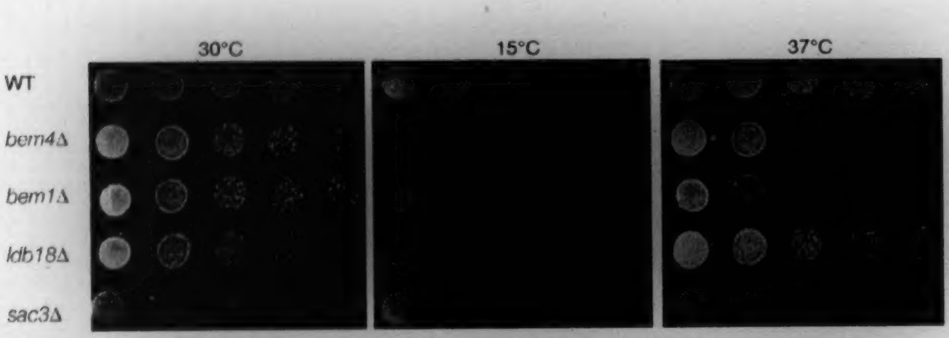

Figure 3.1. Phenotypic analysis of candidates. Haploid deletions of candidates were PCR tested and grown overnight in liquid YPAD media. Overnights cultures were diluted to an OD_{600} of 0.1. The strains were then grown to an OD_{600} of 1.0 and diluted serially to 10^{-4}. The original culture and its subsequent dilutions were then spotted onto YPAD solid media. Spotted plates were then placed at 30°C, 15°C, and 37°C. Growth rates were then observed after: 2 days at 30°C, 5 days at 15°C, and 1 day at 37°C.

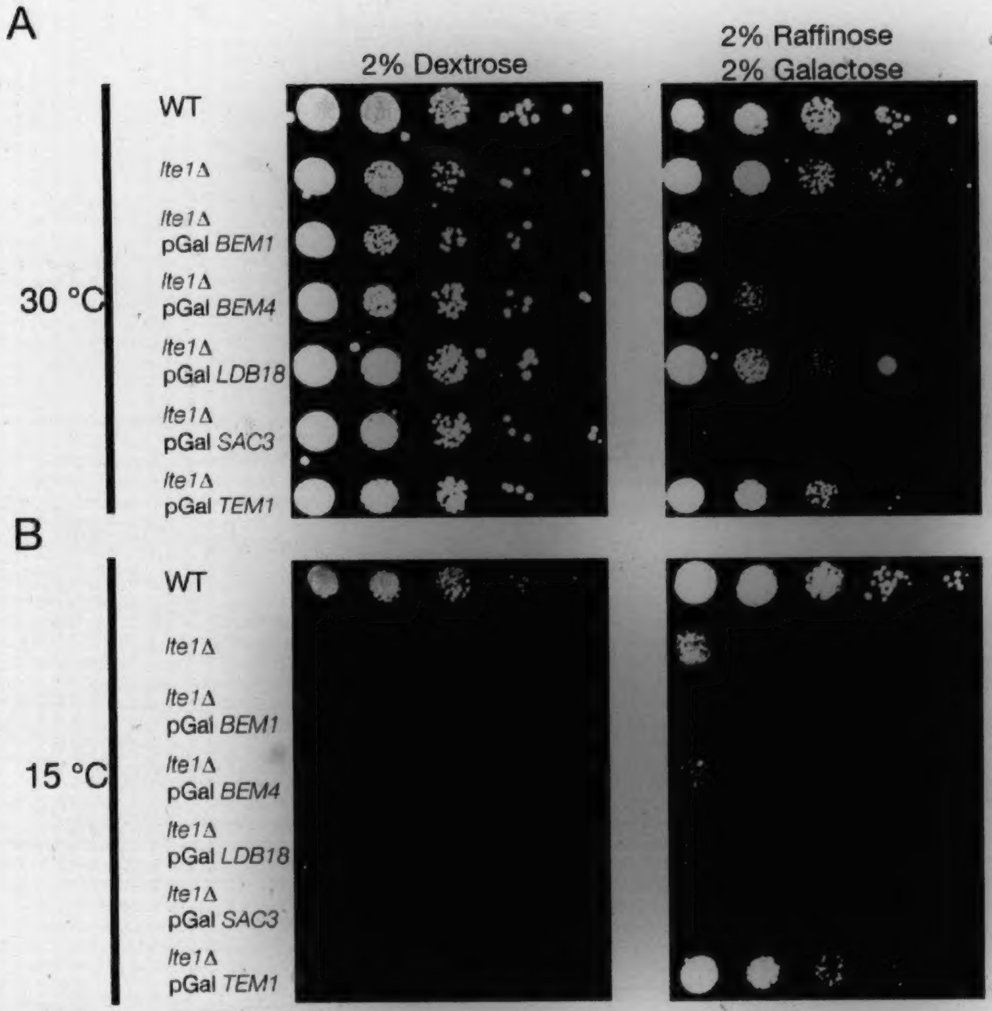
A
2% Dextrose
2% Raffinose
2% Galactose
30 °C
WT
lte1Δ
lte1Δ pGal BEM1
lte1Δ pGal BEM4
lte1Δ pGal LDB18
lte1Δ pGal SAC3
lte1Δ pGal TEM1
B
15 °C
WT
lte1Δ
lte1Δ pGal BEM1
lte1Δ pGal BEM4
lte1Δ pGal LDB18
lte1Δ pGal SAC3
lte1Δ pGal TEM1

Figure 3.2. *lte1*Δ dosage suppression assay. Galactose inducible plasmids containing ORFs identified in the SGA were transformed into an *lte1*Δ strain. Transformants were PCR tested to for the *LTE1* allele to ensure its absence. The confirmed strains were grown overnight in SD-ura liquid media and diluted to an OD_{600} of 0.05. The diluted strains were then grown until an OD_{600} of 0.5 was reached and then diluted serially to a final dilution of 10^{-4}. The strains were then spotted onto 2% dextrose media and 2% raffinose/galactose media which were incubated at 30°C for 5 hours. This incubation ensured that overexpression was induced prior to incubation at the semi-permissive temperature of 15°C. One set of dextrose plates along with one set of raffinose/galactose plates were placed at 15°C while one set of each was left at 30°C. Growth rates were then observed after 2 days at 30°C, and 5 days at 15°C.

3.2.4 Analysis of *BEM4*

3.2.4.1 Homology of *Bem4p*

Many of the components of the cell cycle are conserved from yeast to humans. Therefore, we decided to look for homologues of Bem4p in other eukaryotes [203]. After using BLAST we found several Bem4p homologues that have high similarity and identity to the protein. Homologues in *Ashbya gossypii*, *Kluyveromyces lactis*, and *Candida glabrata* all had greater than 27% identity and 52% similarity. However, we found no homologues in eukaryotes other than species found in the phylum *Ascomycota*. Furthermore, none of these homologues have been characterized so they provide no insight to Bem4p function (Figure 3.3).

3.2.4.2 Synthetic interactions with *bem4Δ*

Researchers reported previously that the *BEM4* protein interacts with the yeast Cdc42p polarity G-protein [212]. Furthermore, several other regulators of mitotic exit are involved in the Cdc42p signaling pathway (Figures 1.7) [188, 189]. These regulators are involved in Cdc42p localization and guanine nucleotide turnover as well as downstream effectors such as Ste20p, Gic1p, Gic2p, and Cla4p. Hence, we decided to look for synthetic interactions between the *bem4Δ* strain and deletions of several of the non-essential components of the Cdc42p signaling cascade. The following strains were tested: the Cdc42p signal effectors (*ste20Δ*, *gic1Δ*, *gic2Δ*, and *cla4Δ*) and Rho GAPs (*rga1Δ*, *rga2Δ*, *bem2Δ*, and *bem3Δ*) (Table 3.6). Unfortunately, the *CDC42* gene and its GEF *CDC24* were not used for this analysis as they are essential genes and conditional alleles could not be obtained in time. The Cdc42p scaffold protein gene *BEM1* was included as it is hypothesized to activate Cdc42p signaling by facilitating interactions between Cdc24p and Cdc42p [213]. Also we included the Rho GDI gene *RDI1* to examine the role of GDP/GTP turnover in the presence of *bem4Δ*.

Out of the signal transducers, *bem4Δ* was only synthetically lethal with *cla4Δ*. This confirms an earlier study that found *bem4Δ* as a hit in a SGA using a *cla4Δ* strain [61]. Further, this interaction also serves as a positive control. No synthetic interaction was seen with *bem4Δ* and any of the GAPs tested. However, the tetrad analysis with the other components demonstrated that *bem4*Δ is synthetic lethal with *bem1*Δ and also has a synthetic growth defect with *rdi1*Δ (Table 3.6).

However, it should be noted that the *ste20*Δ strain could be carrying a genetic modifier as it did not produce a synthetic interaction with *lte1*Δ (Table 3.1). Thus, to be conclusive this procedure needs to be repeated with a new deletion strain. The lack of synthetic lethality between *bem4*Δ and *gic1*Δ or *gic2*Δ also needs to be examined further. Although the *gic1*Δ *gic2*Δ double mutant is very sick, the two genes are thought to be partially redundant [65]. Therefore, a *bem4*Δ *gic1*Δ *gic2*Δ strain needs to be tested for synthetic lethality to determine if Bem4p and the Gics function in separate pathways.

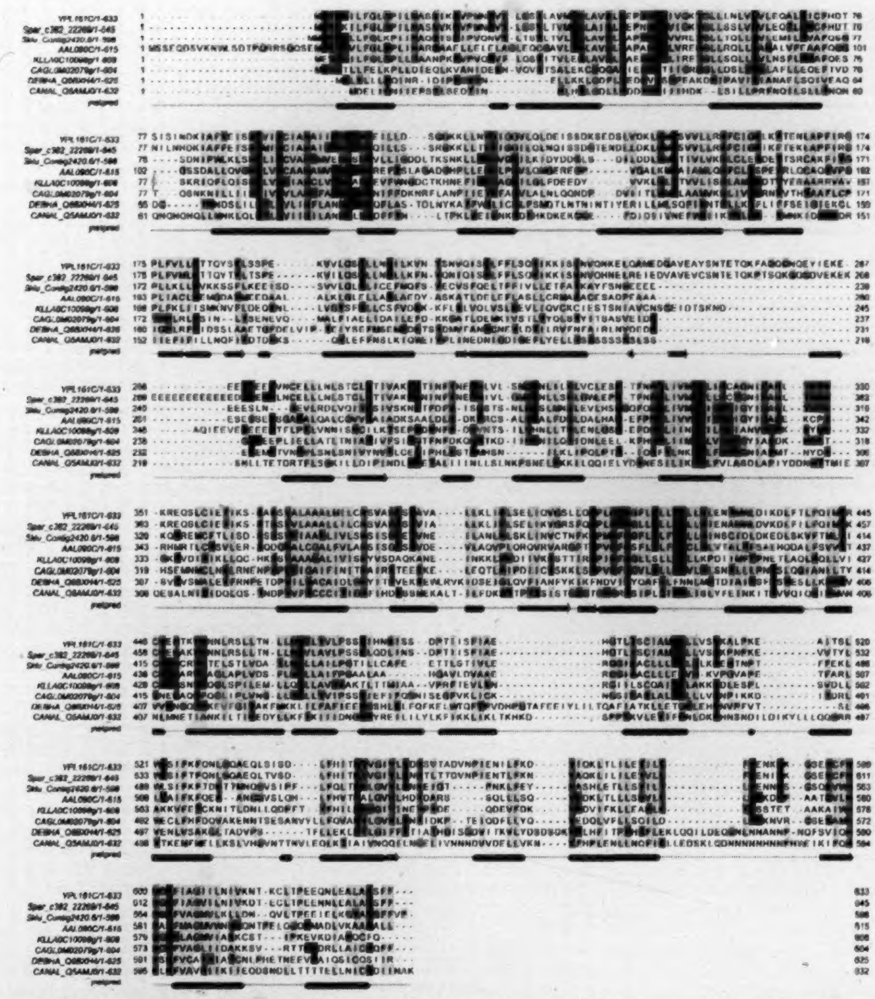

Figure 3.3. Homology of Bem4p protein sequences. The sequence of *Bem4* was retrieved from the Saccharomyces genome database (http://www.yeastgenome.org/). All other sequences were obtained from the NCBI PSI-BLAST and aligned using Jalview (version 2.2.1) [204]. The secondary structure predicted by Jalview is shown below the corresponding position on the alignment. Green arrows represent alpha helices, red cylinders represent beta strands.

YPL161c (Bem4p), *Saccharomyces cerevisiae* (budding yeast), Accession: NP_015164
Spar_c382_22269, *Saccharomyces paradoxus* (budding yeast) Contig: c382_22269
Sklu_Contig2420.6, *Saccharomyces kluyveri* (budding yeast) Contig: 2420.6
AAL090Cp, *Ashbya gossypii* (cotton mold) Accession: NP_982452
KLLAOC10098g, *Kluyveromyces lactis* (budding yeast) Accession: XP_452649
CAFLOM02079g, *Candida glabrata* (yeast) Accession: XP_449436
DEBHA_Q6BXH4, *Debaryomyces hansenii* (yeast) Accession: XP_457095
CANAL_Q5AMJ0, *Candida albicans* (yeast) Accession: SP_722873

Table 3.6. Synthetic genetic interactions between *bem4*Δ and the *CDC42* signaling pathway. Tetrad Analysis was performed by crossing the haploid deletion query strain *bem4*Δ*::NatR* to haploid deletion strains of various non-essential components of the *CDC42* signaling cascade (*xxx*Δ*::KanR*). Growth, dissection, and analysis were performed as in Table IV. However, the presence of the bem4Δ::NatR mutants was selected on YPAD+Nat. Progeny was then analyzed for synthetic growth defects or lethality within the double knockouts. Full tetrads were analyzed for spores not growing when double knockout was predicted and observed for growing double knockouts. Total spore count was also obtained and the expected number of double knockouts (1/4 of total) was compared to total double knockouts growing. From these data a conclusion was made as of the presence or absence of genetic interaction with query strain.

*bem4*Δ crossed to:	# full tetrads	# predicted bem4Δ *xxx*Δ spores not growing	# *lte1*Δ *xxx*Δ spores growing in full tetrads	total # spores assayed	expected # of *bem4*Δ *xxx*Δ spores	# *bem4*Δ *xxx*Δ spores growing	Synthetic Growth or Lethality
*bem1*Δ	*12*	16	0	103	26	4	SL
*bem2*Δ	*6*	2	3	59	15	17	None
*bem3*Δ	*4*	0	1	37	9	5	None
*cla4*Δ	*8*	6	0	54	14	2	SL
*gic1*Δ	*1*	0	1	34	9	9	None
*gic2*Δ	*7*	2	3	41	10	7	None
*rdi1*Δ	*13*	1	10(10SG)	91	23	19(14SG)	SG
*rga1*Δ	*11*	0	11	44	11	11	None
*rga2*Δ	*6*	0	7	63	16	18	None
*ste20*Δ	*3*	0	1	43	11	9	None

3.2.4.3 The effect of *bem4Δ* on septin structure

Loss of Cla4p was demonstrated previously to produce mislocalization of Lte1p and to impair mitotic exit [190]. Prior research demonstrated that Cla4p is a regulator of septin structure and Bem4p interacts with several of the septins [214]. Hence we hypothesized that a *bem4Δ* strain will have septin defects, which may cause mislocalization of MEN components or regulators of the MEN.

To analyze the function of Bem4p in septin structure, we used a plasmid containing a septin protein fused to a GFP tag (*CDC3*-GFP) [173]. The *bem4Δ* strain displayed a range of septin defects. Some of the cells had a near normal phenotype with a thin single or double ring. Others, however, had a thickened septin collar, or a disorganized structure with large gaps in the rings (Figure 3.4). Thus, Bem4p is necessary for proper septin structure.

3.2.4.4 *bem4Δ* suppressed by Cdc42p GAP *bem3Δ* deletion

The Cdc42p signaling cascade has a defined role in actin assembly. Its constitutive activation has also been shown to suppress *lte1Δ* [188]. This observation is also consistent with the finding that many of the Cdc42p signal transducers show synthetic interactions with the MEN components. Together, these data show that activation of the Cdc42p signaling cascade triggers mitotic exit. Together with our finding that *bem4Δ* is synthetic lethal with *lte1Δ*, these observations lead us to propose the following hypothesis: Bem4p has an activating role on mitotic exit via the Cdc42p signaling cascade. Consequently, we wanted to see if *bem4Δ* could be suppressed by activation of the Cdc42p signaling cascade.

To achieve Cdc42p over activation, we crossed a deletion of one of its GAPs, *bem3Δ*, to a *bem4Δ* strain. We then tested the double knockout for suppression of any of the temperature sensitive defects seen in the single *bem4Δ*. Although the lethality caused by the cold temperatures was not suppressed the temperature sensitivity of the *bem4Δ* was partially suppressed by deleting *BEM3*. This finding suggests that Bem4p has a role in activation of the Cdc42p G-protein signaling (Figure 3.5).

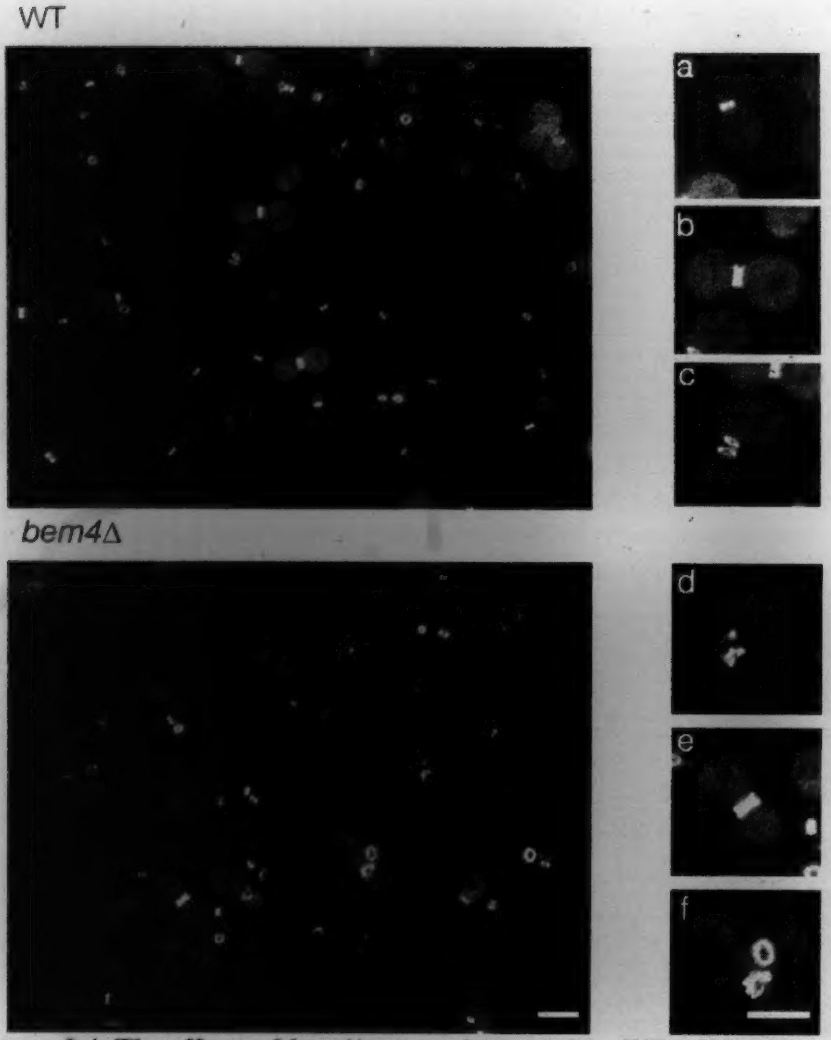

Figure 3.4. The effects of *bem4*Δ on septin assembly. WT and bem4Δ cells were transformed with p1316 (*PRS315 Cdc3*-GFP), grown overnight in YPAD, and transferred to fresh SD-leu and grown to mid log phase. Cells were then observed microscopically with a spinning disk confocal microscope. *bem4*Δ cells displayed fragmented septins (d), thickened septin collars (e), and incomplete fission of the septin double ring upon cytokinesis (f). Normal septin morphology at these three stages is shown in a-c. Scale bars are equal to 10μm.

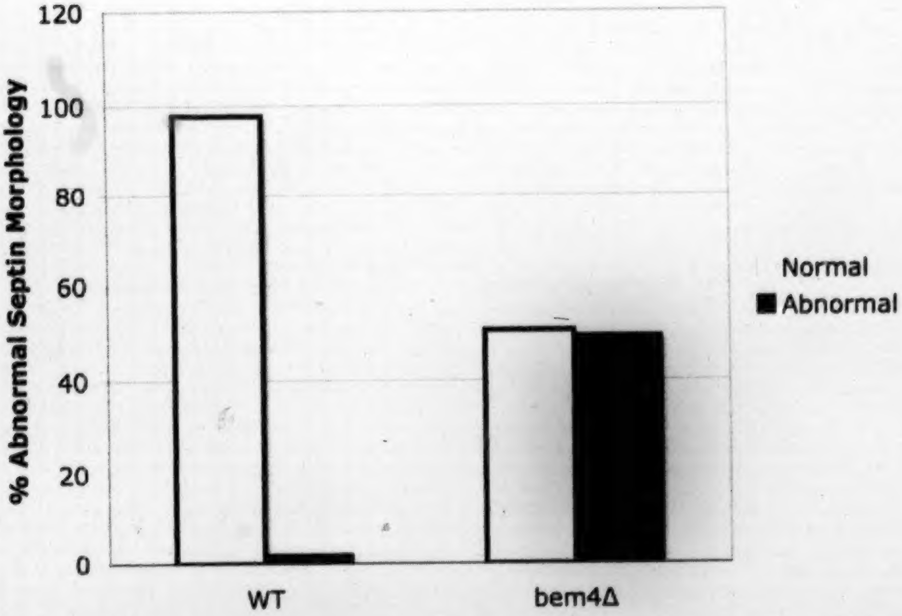

Figure 3.5. Quantification of septin morphology defects. Three 2D projections from each wildtype and *bem4Δ* strains were used to determine the proportion of abnormal septin collars versus the proportion of normal septin collars.

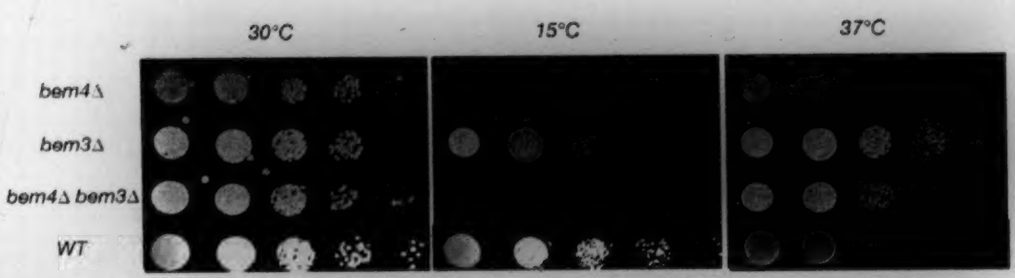
30°C
15°C
37°C
bem4Δ
bem3Δ
bem4Δ bem3Δ
WT

Figure 3.6. Effect of *bem3Δ* on *bem4Δ* strain. Haploid strains *bem4Δ*, *bem3Δ* (the *CDC42* GAP), *bem4Δbem3Δ*, and WT grown overnight in YPAD. Subsequently, these strains were diluted and pinned as presented in Figure 3.1. Pinned plates were then placed at 30°C, 15°C, and 37°C. Growth rates were then observed after 2 days at 30°C, 5 days at 15°C, and 1 day at 37°C.

3.3 Discussion and conclusions

3.3.1 Genetic screen to identify enhancers/inhibitors of mitotic exit

Activators/inhibitors of mitotic exit were identified via a SGA. Here we took advantage of the *lte1*Δ phenotypes (relatively normal mitotic exit at 30°C, and arrest in late mitosis at 10°C) [31] to find mutants that are synthetic lethal/sick with, or suppressors of *lte1*Δ, respectively. Mutants that are synthetic lethal/sick with *lte1*Δ have the potential to be positive regulators of mitotic exit or make up pathways that are parallel with Lte1p. Conversely, suppressors of *lte1*Δ cold temperature arrest have the potential to be negative regulators of mitotic exit such as components of the spindle position checkpoint (Figure 1.7). Therefore, we performed this two-pronged genetic screen to identify both activating and inhibitory components of mitotic exit.

Out of the 163 candidates screened, I identified 20 deletions that appeared to suppress the *lte1*Δ cold temperature arrest (Table 3.1). Of these 20 suppressing deletions, 4 served as positive controls as they were identified in previous studies. The remaining 16 suppressors have the potential to play a major role in the spindle position checkpoint. I will address these candidates in the future directions section.

I also identified 43 haploid deletion strains that gave a synthetic genetic interaction with *lte1*Δ (Table 3.1). Of these 43 genetic interactors, we confirmed 5 interactions (*BEM1, BEM4, LDB18, SAC3,* and *SHS1*) by the process of tetrad analysis (Table 3.4). 19 of the remaining candidates were checked by random spore analysis. The preliminary results from this procedure confirmed 6 synthetic genetic interactions with *lte1*Δ (*MGM1, MOG1, UGO1, NIP100, ARP1,* and *PAC11*) (Table 3.5). Of the confirmed 11 interactions, 9 were identified in the dSLAM study by Ye *et al.* [198]. The two unique identified genes were *UGO1* and *PAC11*. Although my study is not complete, genes were identified in several processes: nuclear migration, nuclear export, septin structure, and cell/actin polarity. The gene *LDB18* is involved in nuclear positioning (Ranran Zhang/Neil Adames, personal communication) [198]. The identification of lethality between mutants in several nuclear migration proteins and a mutant defective in mitotic exit stresses the necessity of proper positioning of the nucleus within neck during mitosis. I have also identified a nuclear export gene *SAC3* [215, 216]. This finding, although interesting, is not unexpected, as the nucleus does not break down in *S. cerevisiae* during mitosis. Several components involved in mitotic exit are known to be transported across the nuclear membrane during mitosis. Cdc14p is one example, whose localization is crucial to proper mitotic exit.

Another set of proteins known to influence mitotic exit and the cell cycle as a whole are the septins [138, 173]. Here I have identified a genetic interaction between *lte1*Δ and the non-essential septin gene *shs1*Δ. Interestingly, this protein is known to be involved in localizing Lte1p [173]. As I will address later in the discussion, this interaction is both interesting and unexpected. Finally, the most promising set of activator candidates are the genes involved in cell/actin polarity. The *BEM1* gene has a known role in cell/actin polarity [213, 217, 218]. This process has recently been linked to activation of mitotic exit. Thus, our results confirm prior studies. *BEM4* is also implicated in the polarity pathway, however the exact mechanism is unknown [211, 212]. Thus, this gene provides a good candidate for further investigation.

3.3.2 New evidence for the activation of mitotic exit by the Cdc42p signaling pathway

3.3.2.1 Bem4p as an activator of mitotic exit

We identified *BEM4* as a gene necessary when mitotic exit is hampered by the loss of Lte1p. Bem4p was previously shown in a two-hybrid screen to interact with Cdc42p and Rho1p, yet Bem4p shows no GEF, GAP, or GDI activity toward Rho1p [211]. Our phenotypic results, as well as prior studies indicate that Bem4p plays a role in actin polarity within budding yeast (Figure 3.1) [211, 212]. As I have described earlier, Cdc42p and its effectors control the process of actin polarity, and activate mitotic exit [188, 189]. Two of these mitotic exit enhancing effectors are Ste20p and Gic1p, both of which have been shown to interact with Bem4p via two hybrid analysis [219]. Hence, Bem4p has the potential to be involved in Cdc42p signaling, through which it aids activation of actin polarity and mitotic exit.

3.3.2.2 Bem4p shows homology with several budding yeast homologues

The components involved in actin polarity and Cdc42p signaling are conserved throughout several organisms and cell types [220]. Consequently, I examined the homology of Bem4p in detail by PSI-BLAST analysis [203]. Upon alignment of the protein sequence to several homologues we found that Bem4p was highly conserved (greater than 52% identity). Despite this, all identified homologues were only in the Phylum *Ascomycota*. Interestingly, the majority of the conserved homologues identified are within the genomes of budding yeasts within this Phylum. Although this protein is not conserved among other eukaryotes it could be hypothesized that Bem4p enables proper Cdc42p signaling in budding yeasts.

3.3.2.3 Synthetic interactions of *bem4Δ* support role in Cdc42p signaling.

Synthetic lethality between *bem4Δ* and *lte1Δ* suggests that Bem4p activates mitotic exit via a parallel pathway. This activation could be by enabling Cdc42p signaling directly, or by activating Cdc42p's effector pathways - Ste20p, and/or Gic1p/Gic2p [188, 189]. Also Bem4p may be a Cdc42p effector itself. Consequently, I looked for synthetic lethality between the components of this signaling pathway and *bem4Δ* (Table 3.6). I used *CLA4* as a positive control since these two genes (*bem4Δ cla4Δ*) have been shown to be synthetically lethal in a previous SGA [61].

Results of the tetrad analysis found that *bem4Δ* is not synthetically lethal with the other Cdc42p effectors *STE20*, *GIC1*, or *GIC2* (Table 3.6). This could place Bem4p in either or both of these pathways (Figure 3.6). Moreover, this discovery provides evidence against Bem4p as an independent effector of Cdc42p as we would expect *bem4Δ* to be lethal with *ste20Δ*, *gic1Δ*, *and gic2Δ*, as well as *cla4Δ*. However, these findings do need to be confirmed in other strain backgrounds (to ensure a lack of second site mutations), and a *bem4Δ gic1Δ gic2Δ* strain needs to be tested.

Another interesting finding is that *bem4Δ* is synthetically lethal with *bem1Δ* (Table 3.6). Bem1p is the scaffold protein for the Cdc42p signaling complex and as such is thought to activate Cdc42p by linking it to Cdc24p [221]. This result tells us that the proper assembly and functioning of the Cdc42 complex is essential when Bem4p's function is removed. This result implies that Bem4p has an activating role on signaling. Another synthetic lethal interaction we identified was one between *rdi1Δ* and *bem4Δ*. This interaction is curious as Rdi1p is a GDI whose function is to prevent the turnover of GDP to GTP on Rho type GTPases [222]. This is interesting because it seems that Bem4p has an activating role in Cdc42p signaling. Thus, deleting a GDI should suppress any *bem4Δ* defects. However, since Rdi1p also removes Cdc42p from the plasma membrane [52] this genetic interaction with *bem4Δ* might be related to Cdc42p location. For example, there may be a Rdi1p-dependent pool of Cdc42p that functions within the cytoplasm – perhaps at the SPB- to effect mitotic exit.

Finally, we have confirmed that *bem4Δ* is in fact synthetically lethal with *cla4Δ* implying that Bem4p acts to promote cell division in a separate pathway from Cla4p signaling.

3.3.2.4 A deletion of *BEM4* negatively affects septin structure

Septin structure plays a role in Mitotic Exit [173] and Bem4p interacts physically with several septin proteins [214, 219]. The Cdc42p signaling cascade is partially responsible for proper septin assembly through Cla4p. Thus, we hypothesized that Bem4p may be involved in septin assembly.

We used a Cdc3-GFP plasmid and fluorescence microscopy to observe septin dynamics in a *bem4Δ* strain. Within the *bem4Δ* mutant we observed diverse septin defects (Figure 3.4). A small proportion of cells have fragmented septin rings, while many show thickened collars, which look like they have cytokinetic defects. The diverse defects are apparent throughout the cell cycle. Furthermore, these defects were present at all stages of the cell cycle. Normal septin structures were also observed within many of the *bem4Δ* cells. The observed heterogeneity in septin defects is typical of many septin assembly mutants and may arise as the cells age and undergo more cell cycles. Regardless of the cause of the phenotypic heterogeneity, it is clear that Bem4p has a role in septin assembly or maintenance.

One explanation for the septin defects in *bem4Δ* cells is that Cla4p could be activated by Bem4p in some fashion such as assisting Cdc42p activation. However, this hypothesis would not explain why a *cla4Δ bem4Δ* strain is lethal which indicates that they are functioning separately. Thus, it is more probable that Bem4p is directly involved in septin assembly as it interacts with several of the septin subunits. However, this role will have to be further investigated and will be addressed in the future directions section.

3.3.2.5 Bem4p as a possible activator of Cdc42p signaling

I decided to test whether an overactive Cdc42p could suppress some of the *bem4Δ* defects. I crossed the *bem4Δ* mutant to a GAP deficient strain (*bem3Δ*) in which Cdc42p is overactive. These tests have led to two distinct conclusions. First, as shown by Figure 3.5, we can see that a deletion of *BEM3* partially suppresses the temperature sensitive phenotype of *bem4Δ*. Thereby, Bem4p may be an activator of the Cdc42p signaling pathway. Secondly, *bem3Δ* does not suppress the cold temperature defects seen in a *bem4Δ* strain. Cold-sensitivity is often an indication of microtubule defects, while sensitivity to high temperatures is a hallmark of actin defects. Therefore, it could be that Bem4p has an actin function that is suppressed by increased Cdc42p activity. On the bother hand the microtubule-related function of Bem4p could be independent of Cdc42p activity and, therefore not suppressed by loss of Bem3p.

Although these results are promising they are preliminary. These data need to be complemented with similar results using the remaining Cdc42p GAPs to see if this suppression is *bem3Δ* is specific or a general characteristic of all Cdc42p GAPs.

3.3.2.6 Hypothesized role of Bem4p in activating mitotic exit

While several hypotheses can be derived from these data, we have come up with a single explanation that best fits our data. Our hypothesis predicts that *BEM4* is both involved in septin assembly and Ste20p and Gic1p/Gic2p signaling (Figure 3.6). Although speculative, an attractive model is that Bem4p may aid in, and monitor, septin assembly. Upon proper completion of this task it then activates Ste20p and Gic1p/Gic2p signaling to aid in mitotic exit. This hypothesis is not unfounded, as Bem4p has been predicted prior to be a signal between the septins and Cdc42p as it interacts physically with both sets of proteins [219]. I have based this hypothesis is derived from the findings that a *bem4Δ* strain has septin structural defects, *bem4Δ* is not synthetic lethal with *ste20Δ*, *gic1Δ*, or *gic2Δ*, and that Bem4p plays an activating role in Cdc42p signaling. Furthermore, the prediction that Bem4p is part of the Ste20p and Gic1p/Gic2p pathways is supported by the discovery that Bem4p interacts with Ste20p, Gic1p, the septins and not Cla4p in a two-hybrid screen [219]. Thus, Bem4p may modulate the interaction between Cdc42p and Ste20p/Gic1p as it interacts with all of these proteins [211, 212].

This explanation addresses one of my main goals - to learn more about the mechanism of mitotic exit activation via Ste20p. However, here I have shown that Bem4p could be within the Ste20p and Gic1p/Gic2p signaling pathways. This is a very interesting result as it implies that Bem4p plays a role in mitotic exit activation thus explaining the *lte1Δ bem4Δ* synthetic lethality. Therefore, I believe the final characterization of this protein and its role in mitotic exit is important to the field.

3.3.2.7 Bem1p as an activator of mitotic exit

As I have discussed earlier, the Cdc42p signaling pathway has recently been shown to activate mitotic exit [188, 189]. One of the components identified in this function is Bem1p. Bem1p has already been shown to activate mitotic exit when overexpressed in an *lte1Δ ste20Δ* background [189]. This mechanism of activation remains elusive, as Bem1p is known as a scaffold protein for Bud1p, Cdc42p, Cdc24p, and Ste20p [221]. However, it is hypothesized that Bem1p activates mitotic exit by somehow activating the Cdc42p signaling pathway [188, 189]. Within this study, I have supported this hypothesis, as I have found that *BEM1* is a necessary gene in the presence of hindered mitotic exit (*lte1Δ*).

Now that a direct link between mitotic exit and Bem1p has been established this protein holds a large potential for further investigation. The mechanism for Bem1p's effect on mitotic exit is currently unknown. Also, we have found that *bem1Δ* exacerbates the dynein phenotype of a *dyn1Δ* strain (Hao Wang/ Neil Adames, personal communication). This is a known phenotype of SPC mutants. Hence, it looks as if Bem1p is both activating and inhibiting mitotic exit, suggesting it may be involved in regulating the timing of mitotic exit rather than simply serving as a positive signal.

3.3.3 Proper nuclear migration is necessary in the presence of mitotic exit defects

Prior to this study, it was known that nuclear migration plays an important preparatory role in mitotic exit. The gene knockout of *lte1Δ* is synthetically lethal with *kar9Δ*, *dyn1Δ*, and *jnm1Δ* [8]. Furthermore, defects seen in nuclear migration mutants are exacerbated by impairing the SPC [30]. Thus, we included several nuclear migration proteins in the screen to identify new components in this pathway that interact genetically with *lte1*Δ.

One of the most interesting genes we identified was *LDB18*. *LDB18* is uncharacterized, except that is it predicted to be part of the dynein pathway based on genetic interactions with tubulin folding cofactors [198]. Subsequently, our lab has identified Ldb18p as a dynactin component homologous to the human dynactin component p24 (Ranran Zhang/Neil Adames, personal communication). Additionally, our lab has also shown that *ldb18*Δ cells have a dynein phenotype and fail to undergo microtubule sliding in GFP-Tub cells (Ranran Zhang/Neil Adames, personal communication). The nuclear migration defect of the *ldb18*Δ strain is as severe as that of a *dyn1*Δ strain (Ranran Zhang/Neil Adames, personal communication). This result is consistent with the synthetic lethal interaction with *LTE1* that we have observed as other identified dynactin components in yeast are also synthetically lethal with *LTE1* [8, 198]. These observations support the conclusion that Ldb18p is the *S. cerevisiae* homologue of the dynactin subunit p24/22.

3.3.5 Proper nuclear export is involved in mitotic exit

As the nuclear membrane does not breakdown during the process of mitosis in yeast, proper nuclear import and export are necessary for shuttling mitotic components across this barrier. We included a select few non-essential nuclear transport genes within our screen. Presumably, if these components are hits with *lte1*Δ then they may be involved in the transport of factors necessary for mitotic exit. In this group of proteins, we identified Sac3p (a protein involved in mRNA and protein export) to be necessary in the absence of *lte1*Δ (Table 3.1).

SAC3 is a multi-copy suppressor of actin mutations [223]. Further, observations of the gene knockout indicates a role in mitosis as these cells are commonly found as large budded cells that are arrested with a single nucleus in anaphase [224]. The known role of Sac3p is to facilitate protein and/or mRNA export, as *sac3*Δ cells accumulate mRNA and protein within the nucleus [215, 216]. Sac3p has also been found to interact and localize with nuclear pores [215, 216]. Moreover, the severity of the deletion of this protein attests to the fact of how important this protein is in the cell. As we have seen in our phenotypic assay, the *sac3Δ* strain has reduced viability (Figure 3.1). Further we also observed that these growth defects are independent of temperature, so they could be due to overall cell cycle defect such as impaired mitotic exit. The role of Sac3p in nuclear export has prompted the hypothesis prior that Sac3p may be necessary for export of mitosis specific factors such as cyclin B [215]. Given that we have seen an interaction between *sac3Δ* and *lte1Δ* we predict that this nuclear export may be necessary for export of MEN proteins such as Cdc14p. Hence; characterization of this candidate provides a great opportunity to understand the intricacies of mitosis in the presence of a nuclear membrane.

3.3.4 Septin structure and mitotic exit

Earlier I addressed the necessity of septins as a diffusion barrier as well as a signaling platform in mitosis. Within our screen we included septin related proteins, as well as the non-essential septin protein Shs1p, which we identified as a synthetic growth hit in our screen. *SHS1* has proved to be an interesting candidate because it has a role localizing Lte1p [173]. Therefore, this raised two red flags for us: why is a strain with a deletion of a gene involved in localizing Lte1p sick when *LTE1* is absent, and why wasn't the synthetic interaction identified before [173]? As these flags raised doubt in the validity of our finding our doubt was dispelled when we realized that our results were also confirmed by the dSLAM analysis performed by Ye *et al.* [198]. Thus, we believe Shs1p not only has a role in localizing Lte1p but activates mitotic exit by a separate method as well. This mechanism may be acting as a diffusion barrier for other proteins necessary for mitotic exit such as Cdc42p components. However, this hypothesis is just speculative.

3.3.6 dSLAM vs. SGA

Generally, the synthetic interaction results are consistent with the dSLAM study. Out of the 11 candidates that I positively confirmed, I have found 9 in common between the two studies (*bem4Δ*, *bem1Δ*, *shs1Δ*, *ldb18Δ*, *sac3Δ*, *mgm1Δ*, *mog1Δ*, *nip100Δ*, and *arp1Δ*). The dSLAM study missed *pac11Δ* and *ugo1Δ*. I believe that our results are accurate. This assumption is based upon previous characterization of both of these genes. Ugo1p is a protein found in a complex with Mgm1p (another gene identified by our screen and the dSLAM study) [198]. Interestingly, both of these genes cause loss of mtDNA when deleted and are necessary for mitochondrial membrane fusion [225]. Thus, it is fathomable that since the phenotypes of both proteins are so similar that *lte1Δ* may interact with both, and *ugo1Δ* was missed by the dSLAM study [198]. Furthermore, we think that *PAC11* is a likely real hit as it is the IC for the *S. cerevisiae* dynein complex and both the dSLAM study [198] and Tong *et al.* [8] has found that the *dyn1Δ* is lethal when combined with the *lte1Δ*. We base this assumption on the finding that the *pac11Δ* dynein phenotype is equivalent to the dyn1Δ strain, and this phenotype is not exacerbated in the double knockout strain [98]. Therefore, it is likely that the *pac11Δ* is lethal with the *lte1Δ* strain, however both of these interactions were confirmed by RSA and as such are just preliminary.

However, within the 163 strains that I tested I failed to identify 6 interactions found within the dSLAM study: *ste20Δ*, *fus3Δ*, *she10Δ*, *she1Δ*, *kar9Δ*, and *ctf18Δ* (Table 3.1). Three of these interactions (*ste20Δ*, *kar9Δ*, and *cft18Δ*) are well documented to interact genetically with *lte1Δ*. These errors could be due to second site mutations within the strains, strain contamination over time due to handling of the 96 well plates, or disomy.

3.3.7 Future directions

3.3.7.1 Follow up of Bem4p analysis

The preliminary characterization of the candidate *BEM4* has been promising. Further characterization to test the function of Bem4p in Cdc42p and mitotic exit signaling has the potential to identity a new direct regulator of mitotic exit. The first step in testing my hypothesis is the careful observation of the septin defects seen in *bem4Δ* strain. Using the *bem4Δ* strain with the Cdc3p-GFP plasmid and subjecting it to a series of movies taken over several cell cycles can achieve this. These movies will show us specifically when the defects occur and how they accumulate. Is the *bem4Δ* septin defect in assembly of specific septin structures during one of the cell cycle phases or is there a problem in maintaining septin structure? Furthermore, these movies should be complemented by a quantification of the septin defects. This quantification will produce a phenotype that may be used to screen for epistatic analysis with other septin assembly regulators.

Once the septin defects are known the localization of Bem4p will be investigated. My hypothesis predicts that the proper assembly of septins leads to activation of mitotic exit. It is possible that this activation may be due to a transfer of Bem4p localization from the septin neck to the bud cortex where it can activate Cdc42p signaling. Thus, live cell imaging of a Bem4p-GFP strain would be informative.

I also have to show that Bem4p is activating mitotic exit. I intend to approach this problem first by attempting to suppress the *lte1*Δ cold temperature arrest with a multicopy *BEM4* plasmid rather than the *GAL1*-driven multicopy *BEM4* C-terminal tag fusion. Furthermore, to ensure that the lethality between *lte1*Δ and *bem4*Δ is due to impaired mitotic exit, the double mutant will be created in a strain carrying a repressible *LTE1* expression plasmid. This strain can then be used to determine the terminal phenotype of the double mutant. Next it should be determined that this arrest can be overcome by overexpressing *CDC14* or inhibiting the SPC after repressing *LTE1*. These data will show that *BEM4* is an activator of mitotic exit and works parallel to Lte1p.

Finally, I have hypothesized that Bem4p activation of mitotic exit is through the Cdc42p effectors Ste20p and Gic1p as these proteins interact physically with Bem4p in a two-hybrid assay [219]. This interaction needs to be confirmed by another method such as co-immunoprecipitation. Once this interaction is confirmed then assays will be required to test whether activation of mitotic exit it through these pathways. However, this may prove challenging as Bem4p may be acting in both pathways. One way in which this may be achieved is using an *lte1*Δ *bem4*Δ strain that has the repressible *LTE1* plasmid. Within this strain *STE20* and *GIC1* could be overexpressed. If overexpression of either of these genes does not show suppression of the *lte1*Δ *bem4*Δ synthetic lethality this would indicate that Bem4p acts downstream or that it's in a separate parallel pathway. Conversely, if they do suppress, it could indicate that Bem4p acts upstream or that it is in a separate parallel pathway. However, these data would not be conclusive and thus would need to be followed up by subsequent analysis.

Overall these tests have the potential of showing that Bem4p is involved in septin assembly and signals mitotic exit through Cdc42p effectors. In turn, this result would answer questions of the mechanism of Ste20p and Cdc42p in activating mitotic exit. Furthermore, on a more global level we have shown that Bem4p is not a conserved protein among metazoans. This is unlike several other components involved in regulating mitosis/mitotic exit such as Cdc14p (CDC14A and CDC14B), Cdc5p (PLK1), and Cdc42p (CDC42) (reviewed in [172, 226]). Thus, the demonstrated importance of *BEM4* in the cell combined with its lack of conservation may allude to being a good target for anti-fungal treatments. Therefore, this gene has proven interesting and should be characterized further.

3.3.7.2 Confirmation and Analysis of *lte1*Δ suppressors

Many possible suppressors of *lte1*Δ lethality at 10°C were identified in my screen. Although the suppressors were not confirmed we believe that many of them are real due to the identification of all positive controls included in the screen: *bub2*Δ, *bfa1*Δ, and *kin4*Δ (Table 3.3). Further, *bub2*Δ and *bfa1*Δ strains were both included in the screen twice and were identified both times. The inhibitor of premature MEN signaling *amn1*Δ was also identified by this screen (Table 3.3). This result is also expected as *amn1*Δ strains are known to have increased Tem1p-Cdc15p interactions throughout the cell cycle that lead to MEN activation [208]. Within the remaining possible suppressor candidates lays the potential of identifying a new SPC component or MEN inhibitor. Several of these candidates have also proven to have interesting functions in the same cellular processes.

For example, I identified three of the four genes required for the haploid axial budding pattern - *AXL1*, *AXL2*, and *BUD4*. At present no direct link has been identified between mitotic exit and bud site selection. However, given that we identified three of the four genes involved in this process, we feel that these suppressor candidates are likely real.

Another set of candidates are the Rho GAPs *BEM2* and *RGA2*. Both of these genes encode proteins that are GAPs for Cdc42p (Figure 3.6). This result is not unexpected, as Cdc42p and many of its downstream effectors have been shown to be mitotic exit activators. However, it is curious that BEM3 and RGA1 (the remaining Cdc42 GAPs) were not hits within the screen. This result may suggest that the function of Cdc42p in mitotic exit is negatively regulated by only two of the four Cdc42p GAP proteins. Thus, these suppressor candidates, if confirmed, will give a clearer picture as to how mitotic exit is regulated by Cdc42p.

Arguably the most interesting suppressor candidate in the screen is the gene *BMH1*. Bmh1p is a 14-3-3 protein that binds a variety of enzymes and signaling proteins to modulate their activity, conformation, stability, localization, and function (reviewed in [227]). Bmh1p has particularly peaked our interest as *bmh1*Δ increases the occurrence of binucleate unbudded cells in a *dyn1*Δ mutant (Hao Wang/Neil Adames, unpublished data). This phenotype is characteristic of SPC mutants. Further, my identification of *bmh1*Δ as a suppressor of *lte1*Δ cold sensitivity is consistent with a role of Bmh1p in negative regulation of mitotic exit, possibly as a SPC component. Moreover, a recent proteomic analysis revealed that Bmh1p may physically interact with Bub2p, Bfa1p, and Kin4p [228]. This suggests that Bmh1p is a SPC component that may somehow modulate the activities of the other SPC components.

Overall, many of the unconfirmed suppressor candidates have the potential to be negative regulators of mitotic exit. Therefore, these candidates need to be confirmed. Unfortunately, this is a long process, as the confirmation needs to be undertaken at 10°C and yeast grow slowly at this temperature. After confirmation these candidates then need to be run through a series of tests typical of SPC characterization. These tests include: overexpression of candidates to observe cell cycle arrest, assay for exacerbated dynein phenotype when combined with the *dyn1*Δ mutation, and epistasis with the other SPC components. Together these results will indicate whether the confirmed suppressors are components of the SPC or inhibit mitotic exit by a separate mechanism.

CHAPTER 4- IDENTIFICATION AND CHARACTERIZATION OF *YER071c* AS A *Saccharomyces cerevisiae* TCTEX HOMOLOGUE (PROJECT #2)

4.2 Results

4.2.1 *YER071c* sequence alignment/phylogenetic tree

Several Dynein/Dynactin components found in metazoans have no known homologues in *S. cerevisiae*. However, upon performing a BLAST search of fungal and metazoan components of the dynein/dynactin complex, we found a homologue of the Tctex family of dynein light chains. This homologue was the uncharacterized ORF *YER071c*.

Alignment of Yer071cp with its fungal and metazoan Tctex proteins showed that the fungal homologues were divergent from metazoan Tctex proteins. Nonetheless, the predicted secondary structure is well conserved among all orthologues. Also, the predicted secondary structure matches the solved structure of the *Chlamidomonas* Tctex protein *[229]*. Finally, the best-conserved regions of *Yer071c* correspond to the regions thought to interact with the DIC [230]. These residues lie at the junctions between the α2 helix and the β2 sheet and the β3 and β4 sheets, which all lie on the same face of the Tctex homodimer (Figure 4.1).

We also produced a phylogenetic tree to further understand the relationship of *YER071c* to other eukaryotic Tctex dynein light chains. As with other dynein and dynactin components, the fungal Tctex homologues form their own family. However, *YER071c* is very similar to the *Saccharomyces pombe* homologue that has been shown to be a dynein light chain (Figure 4.2) [231]. Therefore, although there is low similarity and identity of Yer071cp to metazoan Tctex proteins Yer071cp shows good homology to other homologues in lower eukaryotes that are hypothesized to have the same role (Figure 4.2).

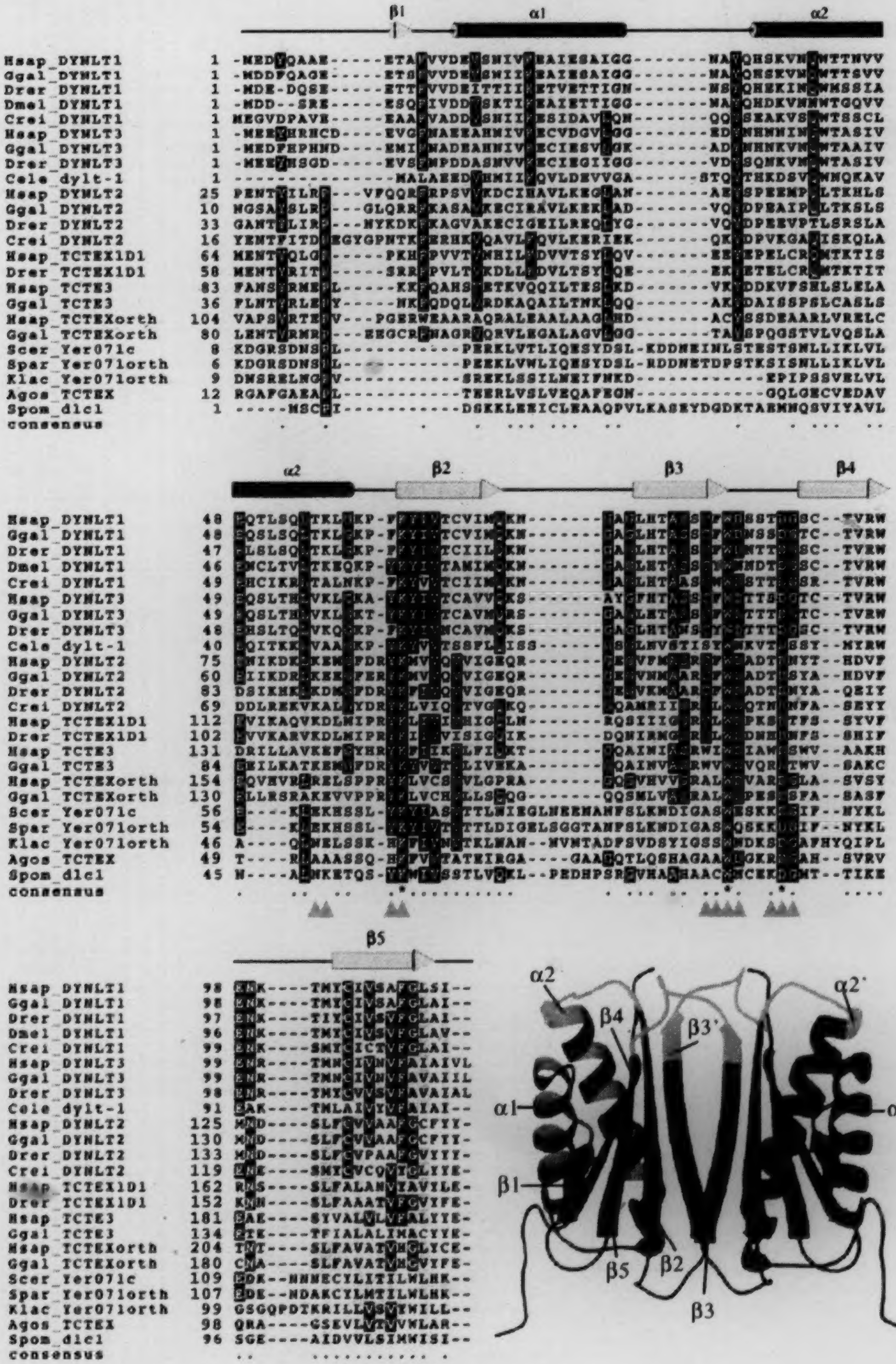
β1
α1
α2
Hsap_DYNLT1
Ggal_DYNLT1
Drer_DYNLT1
Dmel_DYNLT1
Crei_DYNLT1
Hsap_DYNLT3
Ggal_DYNLT3
Drer_DYNLT3
Cele_dylt-1
Hsap_DYNLT2
Ggal_DYNLT2
Drer_DYNLT2
Crei_DYNLT2
Hsap_TCTEX1D1
Drer_TCTEX1D1
Hsap_TCTE3
Ggal_TCTE3
Hsap_TCTEXorth
Ggal_TCTEXorth
Scer_Yer071c
Spar_Yer071orth
Klac_Yer071orth
Agos_TCTEX
Spom_dlc1
consensus
β2
β3
β4
β5
α2
β4
β3'
α2'
α1
α1'
β1
β5
β2
β3

Figure 4.1. Homology of *Yer071c* protein sequence to dynein light chain TCTEX family homologues. The sequences for *Yer071c* and its *Saccharomyces paradoxus* orthologue were retrieved from the *Saccharomyces* genome database (http://www.yeastgenome.org/). Sequences from other TCTEX DLC homologues were obtained using the sequences for various TCTEX homologues as queries for NCBI PSI-BLAST. These sequences were then aligned using Jalview (version 2.2.1) and conserved residues presented using Boxshade (version 3.2.1) [204] (http://www.ch.embnet.org/software/BOX_form.html). Residues conserved in at least half of the species are shown in black and similar residues are shown in grey. The average predicted secondary structure for all sequences was determined using Jalview and shown below the alignment. Positions of the Tctex residues that are thought to interact with the dynein intermediate chain are denoted by green arrows [230]. The solved solution structure of *Chlamydomonas* is shown at the bottom right [229]. Green portions of the solution structure represent areas that interact with the dynein intermediate chain and thus correspond to the residues indicated with green arrows.
Hsap_DYNLT1, *Homo sapiens* (human), Accession: NP_006510
Ggal_DYNLT1, *Gallus gallus* (chicken), Accession: XP_001232357
Drer_DYNLT1, *Danio rerio* (zebrafish), Accession: XP_686753
Dmel_DYNLT1, *Drosophila melanogaster* (fruit fly) Accession: NP_477356
Crei_DYNLT1, *Chlamydomonas reinhardtii* (green algae) Accession: AAB 58383
Hsap_DYNLT3, *Homo sapiens* (human), Accession: P51808
Ggal_DYNLT3, *Gallus gallus* (chicken), Accession: XP_416782
Drer_DYNLT3, *Danio rerio* (zebrafish), Accession: NP_991171
Cele_dylt-1, *Caenorhabditis elegans* (worm) Accession: NP_492063
Hsap_DYNLT2, *Homo sapiens* (human), Accession: AAN34631
Ggal_DYNLT2, *Gallus gallus* (chicken), Accession: XP_422724
Drer_DYNLT2, *Danio rerio* (zebrafish), Accession: AAH90516
Crei_DYNLT2, *Chlamydomonas reinhardtii* (green algae) Accession: AAB58383
Hsap_TCTEX1D1, *Homo sapiens* (human), Accession: EAX06518
Drer_TCTEX1D1, *Danio rerio* (zebrafish), Accession: AAH81403
Hsap_TCTE3, *Homo sapiens* (human), Accession: NP_777570
Ggal_TCTE3, *Gallus gallus* (chicken), Accession: XP_419596
Hsap_TCTEXorth, *Homo sapiens* (human), Accession: AAH92499
Ggal_TCTEXorth, *Gallus gallus* (chicken), Accession: XP_426650
Scer_Yer071c, *Saccharomyces cerevisiae* (budding yeast), Accession: NP_010994
Spar_Yer071corth, *Saccharomyces paradoxus* (budding yeast) Contig: c421_6328
Klac_Yer071corth, *Kluyveromyces lactis* (budding yeast) Accession: XP_452548
Agos_TCTEX, *Ashbya gossypii* (cotton mold) Accession: NP_983358
Spom_dlc1, *Schizosaccharomyces pombe* (fission yeast) Accession: T37893

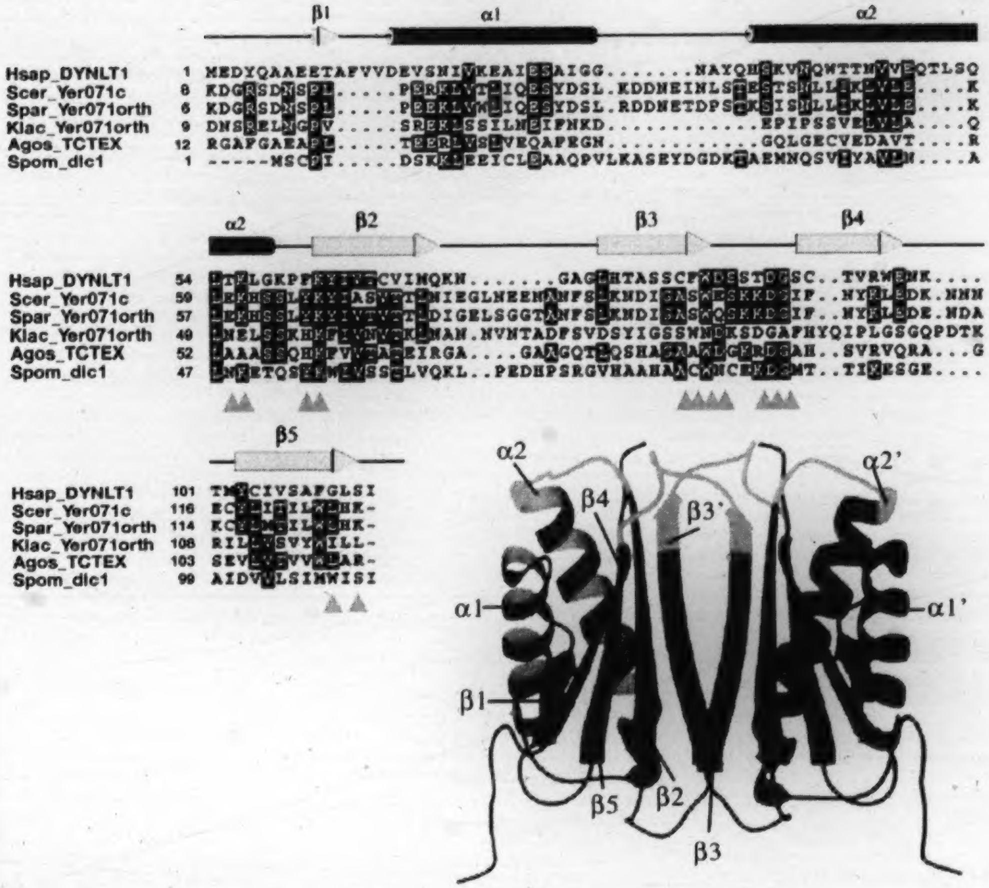
β1
α1
α2
β2
β3
β4
β5
Hsap_DYNLT1
Scer_Yer071c
Spar_Yer071orth
Klac_Yer071orth
Agos_TCTEX
Spom_dlc1
α2
α2'
β4
β3'
α1
α1'
β1
β5
β2
β3

Figure 4.2 Homology of *Yer071c* protein sequence to fungal TCTEX family homologues. Figure was created as in Figure 4.1.

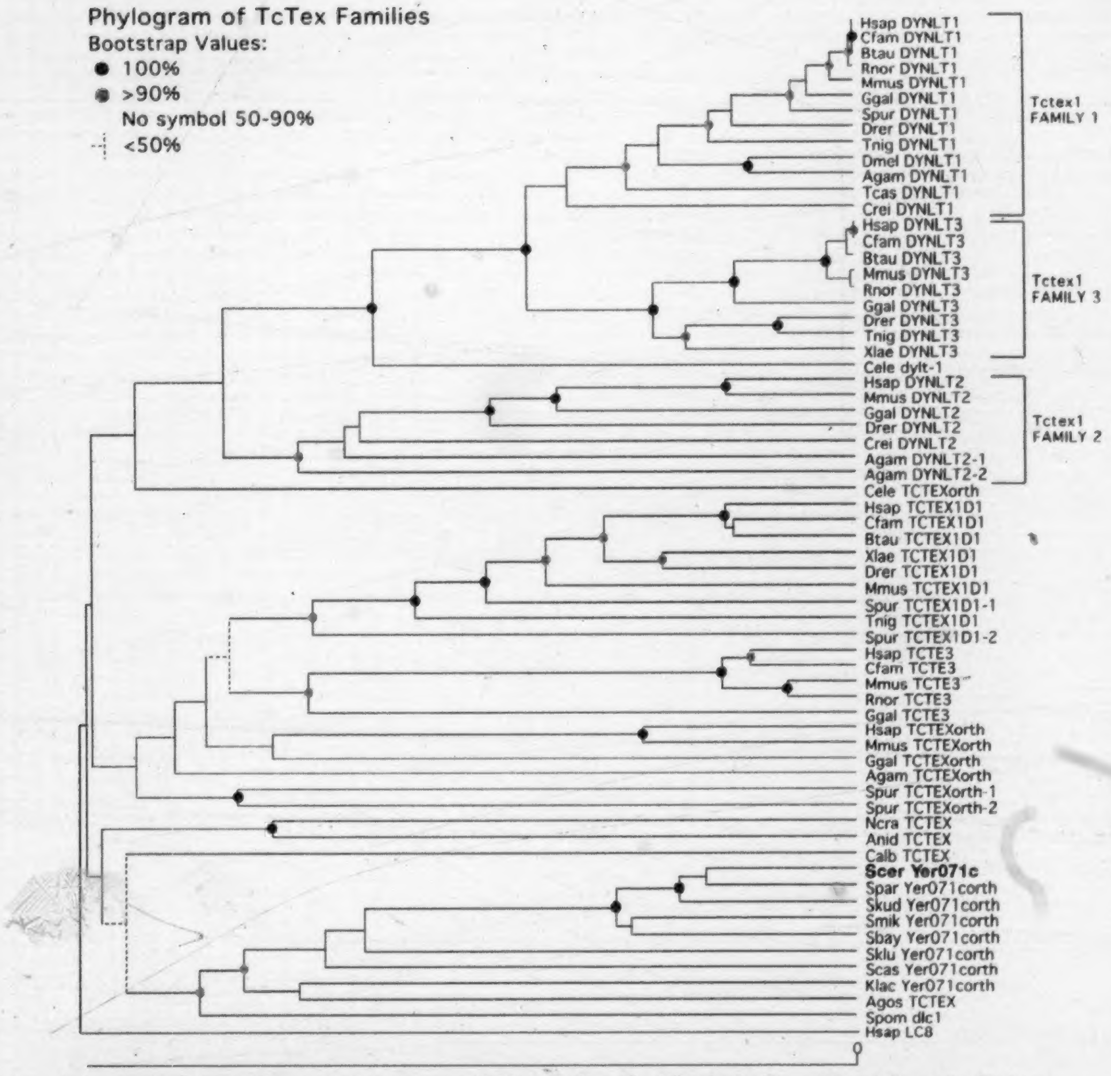
Phylogram of TcTex Families
Bootstrap Values:
● 100%
● >90%
No symbol 50-90%
<50%
Hsap DYNLT1
Cfam DYNLT1
Btau DYNLT1
Rnor DYNLT1
Mmus DYNLT1
Ggal DYNLT1
Spur DYNLT1
Drer DYNLT1
Tnig DYNLT1
Dmel DYNLT1
Agam DYNLT1
Tcas DYNLT1
Crei DYNLT1
Tctex1 FAMILY 1
Hsap DYNLT3
Cfam DYNLT3
Btau DYNLT3
Mmus DYNLT3
Rnor DYNLT3
Ggal DYNLT3
Drer DYNLT3
Tnig DYNLT3
Xlae DYNLT3
Tctex1 FAMILY 3
Cele dylt-1
Hsap DYNLT2
Mmus DYNLT2
Ggal DYNLT2
Drer DYNLT2
Crei DYNLT2
Agam DYNLT2-1
Agam DYNLT2-2
Tctex1 FAMILY 2
Cele TCTEXorth
Hsap TCTEX1D1
Cfam TCTEX1D1
Btau TCTEX1D1
Xlae TCTEX1D1
Drer TCTEX1D1
Mmus TCTEX1D1
Spur TCTEX1D1-1
Tnig TCTEX1D1
Spur TCTEX1D1-2
Hsap TCTE3
Cfam TCTE3
Mmus TCTE3
Rnor TCTE3
Ggal TCTE3
Hsap TCTEXorth
Mmus TCTEXorth
Ggal TCTEXorth
Agam TCTEXorth
Spur TCTEXorth-1
Spur TCTEXorth-2
Ncra TCTEX
Anid TCTEX
Calb TCTEX
Scer Yer071c
Spar Yer071corth
Skud Yer071corth
Smik Yer071corth
Sbay Yer071corth
Sklu Yer071corth
Scas Yer071corth
Klac Yer071corth
Agos TCTEX
Spom dlc1
Hsap LC8

Figure 4.3. Phylogenetic tree predictions for the TCTEX family of dynein light chains. Protein sequences were aligned using Jalview (version 2.2.1) [204]. The Jalview output was then imported into TreeTop Phylogenetic Tree Predictor to produce a phylogenetic distance matrix, which was used to produce a phylogenetic tree via TreeView (version 0.5.1). The distance between two homologues represents their topological deviation. Bootstrap values represent the proportion of branching in a particular pattern in all permutations. The most parsimonious tree is shown. Accession numbers not given in Figure 4.1 are provided below.

Cfam_DYNLT1, *Canis familiaris* (dog), Accession: XP_855051
Btau_DYNLT1, *Bos taurus* (cow), Accession: NP_777045
Rnor_DYNLT1, *Rattus noregicus* (rat), Accession: NP_112608
Mmus_DYNLT1, *Mus musculus* (mouse), Accession: NP_033368
Spur_DYNLT1, *Strongylocentrotus purpuratus* (sea urchin), Accession: XP_783725
Tnig_DYNLT1, *Tetraodon nigroviridis* (puffer fish), Accession: CAG03601
Agos_DYNLT1, *Ashbya gossypii* (fungi), Accession: XP_321929
Tcas_DYNLT1, *Tribolium castaneum* (flower beetle), Accession: XP_973473
Cfam_DYNLT3, *Canis familiaris* (dog), Accession: NP_001003001
Btau_DYNLT3, *Bos taurus* (cow), Accession: NP_001094690
Mmus_DYNLT3, *Mus musculus* (mouse), Accession: NP_080251
Rnor_DYNLT3, *Rattus noregicus* (rat),Accession: NP_001013246
Tnig_DYNLT3, *Tetraodon nigroviridis* (puffer fish), Accession: CAG05832
Xlae_DYNLT3, *Xenopus laevis* (frog), Accession: NP_001088001
Mmus_DYNLT2, *Mus musculus* (mouse), Accession: NP_778195
Agos_DYNLT2-1, *Ashbya gossypii* (fungi), Accession: XP_558570
Agos_DYNLT2-2, *Ashbya gossypii* (fungi), Accession: XP_001688519
Cele_TCTEXorth, *Caenorhabditis elegans* (worm), Accession: NP_495718.1
Cfam_TCTEX1D1, *Canis familiaris* (dog), Accession: XP_852192
Btau_TCTEX1D1, *Bos taurus* (cow), Accession: XP_600758
Xlae_TCTEX1D1, *Xenopus laevis* (frog), Accession: NP_001090117
Mmus_TCTEX1D1, *Mus musculus* (mouse), Accession: NP_080376
Spur_TCTEX1D1-1, *Strongylocentrotus purpuratus* (Sea urchin), Accession: XP_784517
Tnig_TCTEX1D1, *Tetraodon nigroviridis* (puffer fish), Accession: CAF96343
Spur_TCTEX1D1-2, *Strongylocentrotus purpuratus* (sea urchin), Accession: XP_785107
Cfam_TCTE3, *Canis familiaris* (dog), Accession: XP_532273
Mmus_TCTE3, *Mus musculus* (mouse), Accession: XP_001477736
Rnor_TCTE3, *Rattus noregicus* (rat), Accession: XP_344847
Mmus_TCTEXorth, *Mus musculus* (mouse), Accession: NP_079605
Agam_TCTEXorth, *Anopheles gambia* (mosquito), Accession: XP_321929
Spur_TCTEXorth-1, *Strongylocentrotus purpuratus* (sea urchin), Accession: XP_782355
Spur_TCTEXorth-2, *Strongylocentrotus purpuratus* (sea urchin), Accession: XP_795964
Ncra_TCTEX, *Neurospora crassa* (fungi), Accession: XP_956555
Anid_TCTEX, *Aspergillus nidulans* (fungi), Accession: XP_658937
Calb_TCTEX, *Candida albicans* (fungi), Accession: XP_715380
Skud_Yer071corth, *Saccharomyces kudriavzevii* (yeast), Contig: 1843.4
Smik_Yer071corth, *Saccharomyces mikata* (yeast), Contig: c616_6616
Sbay_Yer071corth, *Saccharomyces bayanus* (yeast), Contig: c371_6993
Sklu_Yer071corth, *Saccharomyces kluyveri* (yeast), Contig: 2369.3
Scas_Yer071corth, *Saccharomyces castellii* (yeast), Contig: 701.12

4.2.2 *yer071c*Δ nuclear migration assay

Loss of most yeast dynein/dynactin components results in nuclear migration errors [98, 99, 129]. Nuclear migration defects are due to the inability of the nuclei to penetrate into the bud cell. As a result, aberrant mitosis occurs and the mother cell is left with two nuclei (multinucleate) while the bud is left with none. This process has been well characterized within *Saccharomyces cerevisiae* and thus can be used to predict whether the dynein pathway is affected by a given mutation.

A *yer071c*Δ strain was subjected to a nuclear migration assay and compared to a *dyn1*Δ (the dynein heavy chain) mutant, which completely destroys the dynein pathway. The deletion of the ORF *YER071c* had no detectable nuclear migration defect beyond the basal levels seen in the wildtype strain.

The lack of a nuclear migration defect in the *yer071c*Δ cells could be due to redundancy with the Dyn2p dynein light chain (the LC8 homologue). We then decided to look at the *dyn2*Δ and *dyn2*Δ *yer071c*Δ double mutant for the severity of the nuclear migration defects. The defect in the *dyn2*Δ mutant was not nearly as severe as the *dyn1*Δ mutant. However, the nuclear migration defect in the *dyn2*Δ *yer071c*Δ double mutant was more severe than the *dyn2*Δ single mutant and nearly as severe as the *dyn1*Δ mutant. Therefore, the deletion of *YER071c* exacerbates the nuclear positioning defect in a *dyn2*Δ (Figure 4.3).

4.2.3 Synthetic interactions with *yer071c*Δ

Another characteristic of the dynein components is that they are synthetically lethal with the *Kar9* components [8, 193]. The *Kar9* components make up the parallel pathway in nuclear positioning, which is essential if the dynein pathway is knocked out. Using this characteristic we tested whether *yer071c*Δ produced any synthetic interactions with the *Kar9* components. Conversely, we also tested for synthetic interactions with the dynein pathway. This was included because if the deletion produces synthetic interaction with the dynein pathway then it is not a direct component of the dynein pathway.

Tetrad analysis demonstrated that there were no genetic interactions of the *yer071*Δ with either the dynein or *Kar9* pathways. Since the *yer071c*Δ mutant has no nuclear positioning defect on it's own, there is probably no exacerbation of nuclear migration defects seen in Kar9 pathway mutants, and therefore no synthetic lethality (Table 4.1).

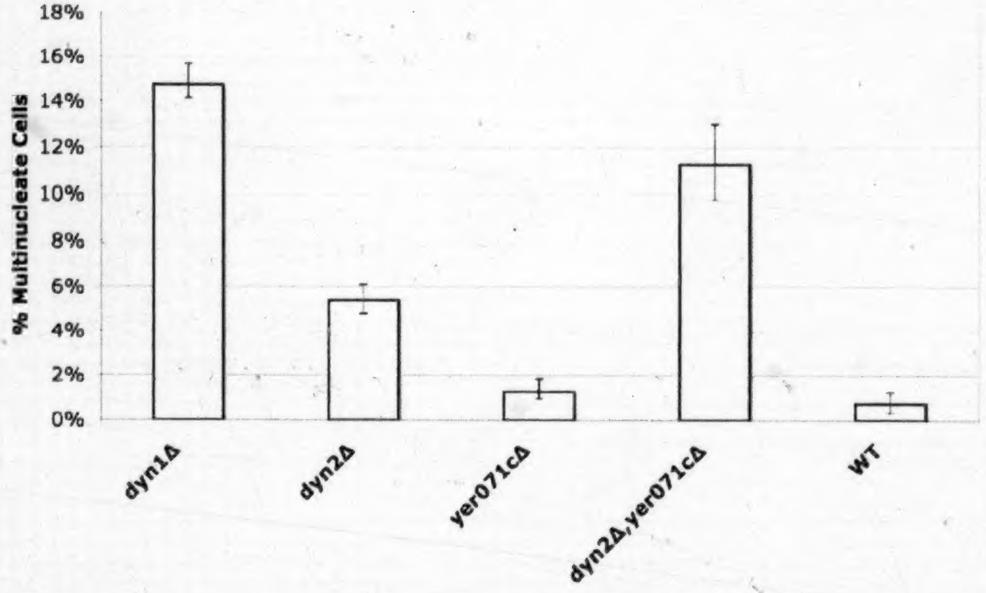

Figure 4.4. Nuclear positioning defects in *dyn2Δ, yer071cΔ, and dyn2Δ yer071cΔ* strains. Single colonies of each of the knockouts were used to inoculate 5 ml YPAD liquid media and grown overnight at 30°C. The overnight cultures were then used to inoculate a new 5 ml culture to an OD_{600} of 0.05. The new inoculation was then grown at 15°C until an OD_{600} of 0.7 was reached. The culture was then stained with DAPI. At lease 300 cells were counted for each of the strains. This procedure was repeated in triplicate. The mean proportion of nuclear positioning defects for each strain was then calculated, averaged for all three trials, and standard deviation was calculated.

Table 4.1. Synthetic Genetic interactions between *yer071c* and the dynein and *Kar9* pathways. A haploid deletion of *yer071c*Δ*::URA3* was crossed to haploid deletions of various components of the dynein and *Kar9* (*xxx*Δ*::KanR*) pathways. These diploids were then selected and sporulated for 5 days. Spore coats were digested using β-Glucuronidase and the four asci of each tetrad were dissected apart using a micromanipulator. Spores were then grown for 2 days and used to test for mating type, and for the presence of knockout cassettes (using either SD-ura or YPAD+G418 media). The progeny were then analyzed for synthetic growth defects or lethality within the double knockouts. Full tetrads were analyzed for spores not growing when double knockout was predicted and observed for growing double knockouts. Total spore count was also obtained and the expected number of double knockouts (1/4 of total) was compared to total double knockouts growing. From these data a conclusion was made as of the presence or absence of genetic interaction with query strain.

yer071c Δ *crossed to:*	# full tetrads	# predicted *yer071c*Δ *xxx*Δ spores not growing	# *yer071c* Δ *xxx*Δ spores growing in full tetrads	total # spores assayed	expected # of *yer071c* Δ *xxx*Δ spores	# *yer071c* Δ *xxx*Δ spores growing	Synthetic Growth or Lethality
*dyn1*Δ	1	0	1	30	8	11	None
*dyn3*Δ	12	1	9	87	21	17	None
*pac11*Δ	11	0	11	89	23	20	None
*pac1*Δ	15	2	13	93	24	28	None
*nip100*Δ	12	3	10	71	18	19	None
*jnm1*Δ	16	2	17	90	23	30	None
*arp1*Δ	13	0	14	85	19	23	None
*bik1*Δ	15	2	11	81	20	14	None
*bim1*Δ	15	1	10	98	25	20	None
*kar9*Δ	9	0	8	77	20	22	None
*bni1*Δ	7	1	5	58	15	13	None

4.3 Discussion and conclusions

4.3.1 Identification of a new *S. cerevisiae* dynein light chain

Upon analysis of homologues of various dynein components we identified a *S. cerevisiae* homologue of the TCTEX dynein light chain family. This homologue was the uncharacterized ORF *YER071c*, which displays conservation within the protein residues that are thought to interact with the dynein intermediate chain. Further, this homologue exists within a phylogenic family of Tctex homologues with several yeast species.

Several dynein mutants produce a characteristic proportion of binucleate cells. We assayed the *yer071c*Δ strain for this phenotype. Although this assay showed that *YER071c* did not display this phenotype we have shown that this deletion exacerbates the binucleate phenotype of a *dyn2*Δ (the only other identified *S. cerevisiae* dynein light chain) strain. We hypothesize that these observations are due to a semi redundancy between the two dynein light chains.

Another characteristic of dynein mutants is that they show synthetic lethal interactions when combined with mutants in the Kar9 pathway of nuclear migration. Thus, we assayed the *yer071c*Δ for lethality when combined with Kar9 pathway deletions. Here we observed that this deletion produced no synthetic interaction with the Kar9 pathway. This we hypothesize is due to the redundancy between Yer071cp and Dyn2p.

4.3.2 *YER071c* is the *S. cerevisiae* homologue of the Tctex family of dynein light chains

Yer071cp is an uncharacterized ORF in *S. cerevisiae*. *YER071c* encodes a protein that is only 129 aa in length and 14.5 KDa in weight. Here we have shown that Yer071cp shows homology to the previously identified Tctex family of dynein light chains in other species (Figure 4.1). This homology is not rigorously conserved throughout the protein. However, it seems as though the regions within the protein that are predicted to have secondary structure important for the functioning of the dynein light chain are more conserved. The second alpha helix and beta sheets 2-5 are examples of this (Figure 4.1). Moreover, the areas predicted to interact with the dynein light chain's binding partner, the dynein intermediate chain, are conserved within Yer071cp and throughout the species examined. This conservation suggests that *YER071c* encodes a functional dynein light chain.

Yer071cp's phylogeny seems to be characteristic of a *S. cerevisiae* homologue of a dynein/dynactin component. Although this component is not highly related to the human orthologue we can see that Yer071cp branched off with close relatives such as *S. pombe, S. paradoxus* and several other *Saccharomyces* orthologues (Figure4.2). Thus, the phylogeny also points to *YER071c* being the *S. cerevisiae* homologue of the Tctex dynein light chain.

4.3.3 Yer071cp may be redundant with Dyn2p

Deletion strains of dynein components have a nuclear positioning defects in cold temperatures [78, 98]. Here we have shown by DAPI straining *yer071c*Δ strains that this strain is absent of a typical dynein phenotype. We have also shown that a *dyn2*Δ strain has a less severe dynein phenotype than a *dyn1*Δ strain. This implies that the dynein pathway is impaired but not completely debilitated. Furthermore, the double mutant (*yer071c*Δ *dyn2*Δ) exacerbates the dynein phenotype of a single *dyn2*Δ strain (Figure 4.3). Although this new proportion of defected cells is comparable to *dyn1*Δ it is still lower overall. Interestingly, this may point the presence of another dynein light chain.

These data suggest that the light chain Dyn2p can compensate for the deletion of Yer071cp however the converse is not true. Consequently, the Yer071cp seems to compensate for the deletion of Dyn2p phenotype of the double knockout is worse than that of either single. In turn, it looks as though the two proteins share some functional overlap.

Confirmation of this redundancy hypothesis comes from the genetic interactions seen with *YER071C*. The majority gene in the dynein pathway are synthetic lethal with genes in the Kar9 pathway [8]. Here we have seen that when combined with any deletions of the Kar9 components no synthetic interactions are observed. The same was seen for dynein deletions. Thus, the finding that the function of Yer071cp is not needed upon debilitation of the Kar9 pathway supports our functional redundancy hypothesis.

Additionally, the genetic analysis of the double deletion strain would fruitless as a *dyn2Δ* strain is lethal with all the Kar9 components [8].

4.3.4 Conclusions

The overall conservation of several important secondary structures within the Yer071cp protein and the small but observable phenotype of *yer071cΔ dyn2Δ* strain suggest that *YER071c* may in fact be the *S. cerevisiae* homologue of the Tctex family members. Interesting as this finding is, it seems as though the importance of this protein is limited as it seems to be completely redundant with Dyn2p and Dyn2p seems to be partially redundant to it. Overall, this study partially satisfies the question of why the other dynein light chains are not found in *S. cerevisiae*. Further, the combined deletions of the two dynein light chains not being as severe as the deletion of the heavy chain predicts that there could be remaining light chains not discovered thus far.

4.3.5 Future directions

Several tests need to be completed before *YER071c* can be conclusively determined to be a dynein light chain. Primarily, Yer071cp should co-immunoprecipitate with the dynein complex. Given that several of the points which the Tctex light chains interact with the dynein intermediate chain are conserved this protein should be able to interact with the *S. cerevisiae* intermediate chain Pac11p. This test will be the definitive answer of whether Yer071cp is part of the complex. This test should be followed up by several biochemical assays to elucidate all Yer071cp's binding partners to further understand the function behind this protein as well as dynein in general.

Second, fluorescence microscopy of Yer071cp needs to be completed to ascertain whether it co-localizes with other dynein components as well as the microtubule plus ends. This evidence will not only support our finding but will indicate its assembly within the complex thus aiding in our understanding of how dynein is regulated in yeast.

Finally, overexpression assays to determine the relationship of this redundancy is necessary. If the phenotype of *dyn2Δ* is suppressed by overexpression of Yer071cp this would suggest that in fact they are doing a similar if not identical function within the cell.

This finding would strengthen the case that in fact Yer071cp is a functioning dynein light chain.

CHAPTER 5- REFERENCES

1. Jaspersen, S.L., et al., *A late mitotic regulatory network controlling cyclin destruction in Saccharomyces cerevisiae.* Mol Biol Cell, 1998. **9**(10): p. 2803-17.
2. Li, Y.Y., et al., *Disruption of mitotic spindle orientation in a yeast dynein mutant.* Proc Natl Acad Sci U S A, 1993. **90**(21): p. 10096-100.
3. Hartwell, L.H., *Twenty-five years of cell cycle genetics.* Genetics, 1991. **129**(4): p. 975-80.
4. Hartwell, L.H., *Nobel Lecture. Yeast and cancer.* Biosci Rep, 2002. **22**(3-4): p. 373-94.
5. Burke, D.J., Dawson, D., Sterns, T. , *Methods in Yeast Genetics: A Cold Srping Harbor Laboratory Course Manual.* 2000.
6. Winzeler, E.A., et al., *Functional characterization of the S. cerevisiae genome by gene deletion and parallel analysis.* Science, 1999. **285**(5429): p. 901-6.
7. Giaever, G., et al., *Functional profiling of the Saccharomyces cerevisiae genome.* Nature, 2002. **418**(6896): p. 387-91.
8. Tong, A.H., et al., *Global mapping of the yeast genetic interaction network.* Science, 2004. **303**(5659): p. 808-13.
9. King, S.M., *The dynein microtubule motor.* Biochim Biophys Acta, 2000. **1496**(1): p. 60-75.
10. Neil A. Campbell, J.B.R., *Biology.* 7th ed. 2004: Benjamin Cummings.
11. Nasmyth, K., *At the heart of the budding yeast cell cycle.* Trends Genet, 1996. **12**(10): p. 405-12.
12. Bloom, J. and F.R. Cross, *Multiple levels of cyclin specificity in cell-cycle control.* Nat Rev Mol Cell Biol, 2007. **8**(2): p. 149-60.
13. Cross, F.R., *Starting the cell cycle: what's the point?* Curr Opin Cell Biol, 1995. **7**(6): p. 790-7.
14. Nash, R., et al., *The WHI1+ gene of Saccharomyces cerevisiae tethers cell division to cell size and is a cyclin homolog.* Embo J, 1988. **7**(13): p. 4335-46.
15. Hadwiger, J.A., et al., *A family of cyclin homologs that control the G1 phase in yeast.* Proc Natl Acad Sci U S A, 1989. **86**(16): p. 6255-9.
16. Dirick, L., T. Bohm, and K. Nasmyth, *Roles and regulation of Cln-Cdc28 kinases at the start of the cell cycle of Saccharomyces cerevisiae.* Embo J, 1995. **14**(19): p. 4803-13.
17. Costanzo, M., et al., *CDK activity antagonizes Whi5, an inhibitor of G1/S transcription in yeast.* Cell, 2004. **117**(7): p. 899-913.
18. de Bruin, R.A., et al., *Cln3 activates G1-specific transcription via phosphorylation of the SBF bound repressor Whi5.* Cell, 2004. **117**(7): p. 887-98.
19. Winey, M., et al., *Genetic determinants of spindle pole body duplication in budding yeast.* Cold Spring Harb Symp Quant Biol, 1991. **56**: p. 705-8.
20. Lew, D.J. and S.I. Reed, *Morphogenesis in the yeast cell cycle: regulation by Cdc28 and cyclins.* J Cell Biol, 1993. **120**(6): p. 1305-20.

21. Oehlen, L.J. and F.R. Cross, *G1 cyclins CLN1 and CLN2 repress the mating factor response pathway at Start in the yeast cell cycle.* Genes Dev, 1994. **8**(9): p. 1058-70.
22. Schwob, E., et al., *The B-type cyclin kinase inhibitor p40SIC1 controls the G1 to S transition in S. cerevisiae.* Cell, 1994. **79**(2): p. 233-44.
23. Schwob, E. and K. Nasmyth, *CLB5 and CLB6, a new pair of B cyclins involved in DNA replication in Saccharomyces cerevisiae.* Genes Dev, 1993. **7**(7A): p. 1160-75.
24. Surana, U., et al., *The role of CDC28 and cyclins during mitosis in the budding yeast S. cerevisiae.* Cell, 1991. **65**(1): p. 145-61.
25. Richardson, H., et al., *Cyclin-B homologs in Saccharomyces cerevisiae function in S phase and in G2.* Genes Dev, 1992. **6**(11): p. 2021-34.
26. Fitch, I., et al., *Characterization of four B-type cyclin genes of the budding yeast Saccharomyces cerevisiae.* Mol Biol Cell, 1992. **3**(7): p. 805-18.
27. Jaspersen, S.L. and D.O. Morgan, *Cdc14 activates cdc15 to promote mitotic exit in budding yeast.* Curr Biol, 2000. **10**(10): p. 615-8.
28. Hu, F., et al., *Regulation of the Bub2/Bfa1 GAP complex by Cdc5 and cell cycle checkpoints.* Cell, 2001. **107**(5): p. 655-65.
29. Hu, F. and S.J. Elledge, *Bub2 is a cell cycle regulated phospho-protein controlled by multiple checkpoints.* Cell Cycle, 2002. **1**(5): p. 351-5.
30. Bloecher, A., G.M. Venturi, and K. Tatchell, *Anaphase spindle position is monitored by the BUB2 checkpoint.* Nat Cell Biol, 2000. **2**(8): p. 556-8.
31. Adames, N.R., J.R. Oberle, and J.A. Cooper, *The surveillance mechanism of the spindle position checkpoint in yeast.* J Cell Biol, 2001. **153**(1): p. 159-68.
32. Adams, I.R. and J.V. Kilmartin, *Localization of core spindle pole body (SPB) components during SPB duplication in Saccharomyces cerevisiae.* J Cell Biol, 1999. **145**(4): p. 809-23.
33. Knop, M., et al., *The spindle pole body component Spc97p interacts with the gamma-tubulin of Saccharomyces cerevisiae and functions in microtubule organization and spindle pole body duplication.* Embo J, 1997. **16**(7): p. 1550-64.
34. Knop, M. and E. Schiebel, *Spc98p and Spc97p of the yeast gamma-tubulin complex mediate binding to the spindle pole body via their interaction with Spc110p.* Embo J, 1997. **16**(23): p. 6985-95.
35. Knop, M. and E. Schiebel, *Receptors determine the cellular localization of a gamma-tubulin complex and thereby the site of microtubule formation.* Embo J, 1998. **17**(14): p. 3952-67.
36. Neff, N.F., et al., *Isolation of the beta-tubulin gene from yeast and demonstration of its essential function in vivo.* Cell, 1983. **33**(1): p. 211-9.
37. Schatz, P.J., et al., *Two functional alpha-tubulin genes of the yeast Saccharomyces cerevisiae encode divergent proteins.* Mol Cell Biol, 1986. **6**(11): p. 3711-21.
38. Fan, J., et al., *Microtubule minus ends can be labelled with a phage display antibody specific to alpha-tubulin.* J Mol Biol, 1996. **259**(3): p. 325-30.
39. Nogales, E., *A structural view of microtubule dynamics.* Cell Mol Life Sci, 1999. **56**(1-2): p. 133-42.

40. Roof, D.M., P.B. Meluh, and M.D. Rose, *Kinesin-related proteins required for assembly of the mitotic spindle.* J Cell Biol, 1992. **118**(1): p. 95-108.
41. Winey, M., et al., *Three-dimensional ultrastructural analysis of the Saccharomyces cerevisiae mitotic spindle.* J Cell Biol, 1995. **129**(6): p. 1601-15.
42. Pereira, G. and E. Schiebel, *Centrosome-microtubule nucleation.* J Cell Sci, 1997. **110 (Pt 3)**: p. 295-300.
43. Amberg, D.C., *Three-dimensional imaging of the yeast actin cytoskeleton through the budding cell cycle.* Mol Biol Cell, 1998. **9**(12): p. 3259-62.
44. dMoseley, J.B. and B.L. Goode, *The yeast actin cytoskeleton: from cellular function to biochemical mechanism.* Microbiol Mol Biol Rev, 2006. **70**(3): p. 605-45.
45. Kilmartin, J.V. and A.E. Adams, *Structural rearrangements of tubulin and actin during the cell cycle of the yeast Saccharomyces.* J Cell Biol, 1984. **98**(3): p. 922-33.
46. Adams, A.E. and J.R. Pringle, *Relationship of actin and tubulin distribution to bud growth in wild-type and morphogenetic-mutant Saccharomyces cerevisiae.* J Cell Biol, 1984. **98**(3): p. 934-45.
47. Bi, E., et al., *Involvement of an actomyosin contractile ring in Saccharomyces cerevisiae cytokinesis.* J Cell Biol, 1998. **142**(5): p. 1301-12.
48. Henchoz, S., et al., *Phosphorylation- and ubiquitin-dependent degradation of the cyclin-dependent kinase inhibitor Far1p in budding yeast.* Genes Dev, 1997. **11**(22): p. 3046-60.
49. Shimada, Y., M.P. Gulli, and M. Peter, *Nuclear sequestration of the exchange factor Cdc24 by Far1 regulates cell polarity during yeast mating.* Nat Cell Biol, 2000. **2**(2): p. 117-24.
50. Nern, A. and R.A. Arkowitz, *Nucleocytoplasmic shuttling of the Cdc42p exchange factor Cdc24p.* J Cell Biol, 2000. **148**(6): p. 1115-22.
51. Caviston, J.P., S.E. Tcheperegine, and E. Bi, *Singularity in budding: a role for the evolutionarily conserved small GTPase Cdc42p.* Proc Natl Acad Sci U S A, 2002. **99**(19): p. 12185-90.
52. Richman, T.J., et al., *Analysis of cell-cycle specific localization of the Rdi1p RhoGDI and the structural determinants required for Cdc42p membrane localization and clustering at sites of polarized growth.* Curr Genet, 2004. **45**(6): p. 339-49.
53. Imamura, H., et al., *Bni1p and Bnr1p: downstream targets of the Rho family small G-proteins which interact with profilin and regulate actin cytoskeleton in Saccharomyces cerevisiae.* Embo J, 1997. **16**(10): p. 2745-55.
54. Evangelista, M., et al., *Bni1p, a yeast formin linking cdc42p and the actin cytoskeleton during polarized morphogenesis.* Science, 1997. **276**(5309): p. 118-22.
55. Evangelista, M., S. Zigmond, and C. Boone, *Formins: signaling effectors for assembly and polarization of actin filaments.* J Cell Sci, 2003. **116**(Pt 13): p. 2603-11.
56. Ash, J., et al., *Genetic analysis of the interface between Cdc42p and the CRIB domain of Ste20p in Saccharomyces cerevisiae.* Genetics, 2003. **163**(1): p. 9-20.

57. Lamson, R.E., M.J. Winters, and P.M. Pryciak, *Cdc42 regulation of kinase activity and signaling by the yeast p21-activated kinase Ste20.* Mol Cell Biol, 2002. **22**(9): p. 2939-51.

58. Drogen, F., et al., *Phosphorylation of the MEKK Ste11p by the PAK-like kinase Ste20p is required for MAP kinase signaling in vivo.* Curr Biol, 2000. **10**(11): p. 630-9.

59. Holly, S.P. and K.J. Blumer, *PAK-family kinases regulate cell and actin polarization throughout the cell cycle of Saccharomyces cerevisiae.* J Cell Biol, 1999. **147**(4): p. 845-56.

60. Wu, C., et al., *Activation of myosin-I by members of the Ste20p protein kinase family.* J Biol Chem, 1996. **271**(50): p. 31787-90.

61. Goehring, A.S., et al., *Synthetic lethal analysis implicates Ste20p, a p21-activated potein kinase, in polarisome activation.* Mol Biol Cell, 2003. **14**(4): p. 1501-16.

62. Qi, M. and E.A. Elion, *Formin-induced actin cables are required for polarized recruitment of the Ste5 scaffold and high level activation of MAPK Fus3.* J Cell Sci, 2005. **118**(Pt 13): p. 2837-48.

63. Eby, J.J., et al., *Actin cytoskeleton organization regulated by the PAK family of protein kinases.* Curr Biol, 1998. **8**(17): p. 967-70.

64. Kadota, J., et al., *Septin ring assembly requires concerted action of polarisome components, a PAK kinase Cla4p, and the actin cytoskeleton in Saccharomyces cerevisiae.* Mol Biol Cell, 2004. **15**(12): p. 5329-45.

65. Brown, J.L., et al., *Novel Cdc42-binding proteins Gic1 and Gic2 control cell polarity in yeast.* Genes Dev, 1997. **11**(22): p. 2972-82.

66. Kawasaki, R., et al., *The upstream regulator, Rsr1p, and downstream effectors, Gic1p and Gic2p, of the Cdc42p small GTPase coordinately regulate initiation of budding in Saccharomyces cerevisiae.* Genes Cells, 2003. **8**(3): p. 235-50.

67. Stearns, T., *Motoring to the finish: kinesin and dynein work together to orient the yeast mitotic spindle.* J Cell Biol, 1997. **138**(5): p. 957-60.

68. Adames, N.R. and J.A. Cooper, *Microtubule interactions with the cell cortex causing nuclear movements in Saccharomyces cerevisiae.* J Cell Biol, 2000. **149**(4): p. 863-74.

69. Shaw, S.L., et al., *Astral microtubule dynamics in yeast: a microtubule-based searching mechanism for spindle orientation and nuclear migration into the bud.* J Cell Biol, 1997. **139**(4): p. 985-94.

70. Carminati, J.L. and T. Stearns, *Microtubules orient the mitotic spindle in yeast through dynein-dependent interactions with the cell cortex.* J Cell Biol, 1997. **138**(3): p. 629-41.

71. Cottingham, F.R. and M.A. Hoyt, *Mitotic spindle positioning in Saccharomyces cerevisiae is accomplished by antagonistically acting microtubule motor proteins.* J Cell Biol, 1997. **138**(5): p. 1041-53.

72. Miller, R.K. and M.D. Rose, *Kar9p is a novel cortical protein required for cytoplasmic microtubule orientation in yeast.* J Cell Biol, 1998. **140**(2): p. 377-90.

73. Lee, L., et al., *Control of mitotic spindle position by the Saccharomyces cerevisiae formin Bni1p.* J Cell Biol, 1999. **144**(5): p. 947-61.

74. Beach, D.L., et al., *The role of the proteins Kar9 and Myo2 in orienting the mitotic spindle of budding yeast.* Curr Biol, 2000. **10**(23): p. 1497-506.

75. Schwartz, K., K. Richards, and D. Botstein, *BIM1 encodes a microtubule-binding protein in yeast.* Mol Biol Cell, 1997. **8**(12): p. 2677-91.

76. Amberg, D.C., et al., *Aip3p/Bud6p, a yeast actin-interacting protein that is involved in morphogenesis and the selection of bipolar budding sites.* Mol Biol Cell, 1997. **8**(4): p. 729-53.

77. Muhua, L., T.S. Karpova, and J.A. Cooper, *A yeast actin-related protein homologous to that in vertebrate dynactin complex is important for spindle orientation and nuclear migration.* Cell, 1994. **78**(4): p. 669-79.

78. Eshel, D., et al., *Cytoplasmic dynein is required for normal nuclear segregation in yeast.* Proc Natl Acad Sci U S A, 1993. **90**(23): p. 11172-6.

79. Miller, R.K., D. Matheos, and M.D. Rose, *The cortical localization of the microtubule orientation protein, Kar9p, is dependent upon actin and proteins required for polarization.* J Cell Biol, 1999. **144**(5): p. 963-75.

80. Yeh, E., et al., *Dynamic positioning of mitotic spindles in yeast: role of microtubule motors and cortical determinants.* Mol Biol Cell, 2000. **11**(11): p. 3949-61.

81. Kurihara, L.J., et al., *Nuclear congression and membrane fusion: two distinct events in the yeast karyogamy pathway.* J Cell Biol, 1994. **126**(4): p. 911-23.

82. Liakopoulos, D., et al., *Asymmetric loading of Kar9 onto spindle poles and microtubules ensures proper spindle alignment.* Cell, 2003. **112**(4): p. 561-74.

83. Maekawa, H., et al., *Yeast Cdk1 translocates to the plus end of cytoplasmic microtubules to regulate bud cortex interactions.* Embo J, 2003. **22**(3): p. 438-49.

84. Miller, R.K., S.C. Cheng, and M.D. Rose, *Bim1p/Yeb1p mediates the Kar9p-dependent cortical attachment of cytoplasmic microtubules.* Mol Biol Cell, 2000. **11**(9): p. 2949-59.

85. Lee, L., et al., *Positioning of the mitotic spindle by a cortical-microtubule capture mechanism.* Science, 2000. **287**(5461): p. 2260-2.

86. Korinek, W.S., et al., *Molecular linkage underlying microtubule orientation toward cortical sites in yeast.* Science, 2000. **287**(5461): p. 2257-9.

87. Tirnauer, J.S. and B.E. Bierer, *EB1 proteins regulate microtubule dynamics, cell polarity, and chromosome stability.* J Cell Biol, 2000. **149**(4): p. 761-6.

88. Wu, X., X. Xiang, and J.A. Hammer, 3rd, *Motor proteins at the microtubule plus-end.* Trends Cell Biol, 2006. **16**(3): p. 135-43.

89. Schroer, T.A., *Microtubules don and doff their caps: dynamic attachments at plus and minus ends.* Curr Opin Cell Biol, 2001. **13**(1): p. 92-6.

90. Tirnauer, J.S., et al., *Yeast Bim1p promotes the G1-specific dynamics of microtubules.* J Cell Biol, 1999. **145**(5): p. 993-1007.

91. Bloom, K., *It's a kar9ochore to capture microtubules.* Nat Cell Biol, 2000. **2**(6): p. E96-8.

92. Huisman, S.M. and M. Segal, *Cortical capture of microtubules and spindle polarity in budding yeast - where's the catch?* J Cell Sci, 2005. **118**(Pt 3): p. 463-71.

93. Huisman, S.M., et al., *Differential contribution of Bud6p and Kar9p to microtubule capture and spindle orientation in S. cerevisiae.* J Cell Biol, 2004. **167**(2): p. 231-44.

94. Miller, R.K., et al., *The kinesin-related proteins, Kip2p and Kip3p, function differently in nuclear migration in yeast.* Mol Biol Cell, 1998. **9**(8): p. 2051-68.
95. Gupta, M.L., Jr., et al., *Plus end-specific depolymerase activity of Kip3, a kinesin-8 protein, explains its role in positioning the yeast mitotic spindle.* Nat Cell Biol, 2006. **8**(9): p. 913-23.
96. Yin, H., et al., *Myosin V orientates the mitotic spindle in yeast.* Nature, 2000. **406**(6799): p. 1013-5.
97. Hwang, E., et al., *Spindle orientation in Saccharomyces cerevisiae depends on the transport of microtubule ends along polarized actin cables.* J Cell Biol, 2003. **161**(3): p. 483-8.
98. Lee, W.L., M.A. Kaiser, and J.A. Cooper, *The offloading model for dynein function: differential function of motor subunits.* J Cell Biol, 2005. **168**(2): p. 201-7.
99. Lee, W.L., J.R. Oberle, and J.A. Cooper, *The role of the lissencephaly protein Pac1 during nuclear migration in budding yeast.* J Cell Biol, 2003. **160**(3): p. 355-64.
100. Paschal, B.M. and R.B. Vallee, *Retrograde transport by the microtubule-associated protein MAP 1C.* Nature, 1987. **330**(6144): p. 181-3.
101. King, S.J., et al., *Subunit organization in cytoplasmic dynein subcomplexes.* Protein Sci, 2002. **11**(5): p. 1239-50.
102. Koonce, M.P., *Identification of a microtubule-binding domain in a cytoplasmic dynein heavy chain.* J Biol Chem, 1997. **272**(32): p. 19714-8.
103. Koonce, M.P. and I. Tikhonenko, *Functional elements within the dynein microtubule-binding domain.* Mol Biol Cell, 2000. **11**(2): p. 523-9.
104. Karki, S. and E.L. Holzbaur, *Affinity chromatography demonstrates a direct binding between cytoplasmic dynein and the dynactin complex.* J Biol Chem, 1995. **270**(48): p. 28806-11.
105. Vaughan, K.T., E.L. Holzbaur, and R.B. Vallee, *Subcellular targeting of the retrograde motor cytoplasmic dynein.* Biochem Soc Trans, 1995. **23**(1): p. 50-4.
106. Paschal, B.M., et al., *Homology of the 74-kD cytoplasmic dynein subunit with a flagellar dynein polypeptide suggests an intracellular targeting function.* J Cell Biol, 1992. **118**(5): p. 1133-43.
107. Kahana, J.A., et al., *The yeast dynactin complex is involved in partitioning the mitotic spindle between mother and daughter cells during anaphase B.* Mol Biol Cell, 1998. **9**(7): p. 1741-56.
108. Bowman, A.B., et al., *Drosophila roadblock and Chlamydomonas LC7: a conserved family of dynein-associated proteins involved in axonal transport, flagellar motility, and mitosis.* J Cell Biol, 1999. **146**(1): p. 165-80.
109. King, S.M., et al., *The mouse t-complex-encoded protein Tctex-1 is a light chain of brain cytoplasmic dynein.* J Biol Chem, 1996. **271**(50): p. 32281-7.
110. King, S.M. and R.S. Patel-King, *The M(r) = 8,000 and 11,000 outer arm dynein light chains from Chlamydomonas flagella have cytoplasmic homologues.* J Biol Chem, 1995. **270**(19): p. 11445-52.
111. King, S.M., et al., *Cytoplasmic dynein contains a family of differentially expressed light chains.* Biochemistry, 1998. **37**(43): p. 15033-41.

112. Susalka, S.J., et al., *The roadblock light chain binds a novel region of the cytoplasmic Dynein intermediate chain.* J Biol Chem, 2002. **277**(36): p. 32939-46.

113. Nyarko, A., et al., *Interactions of LC8 with N-terminal segments of the intermediate chain of cytoplasmic dynein.* ScientificWorldJournal, 2003. **3**: p. 647-54.

114. Makokha, M., et al., *Interactions of cytoplasmic dynein light chains Tctex-1 and LC8 with the intermediate chain IC74.* Biochemistry, 2002. **41**(13): p. 4302-11.

115. Benison, G., A. Nyarko, and E. Barbar, *Heteronuclear NMR identifies a nascent helix in intrinsically disordered dynein intermediate chain: implications for folding and dimerization.* J Mol Biol, 2006. **362**(5): p. 1082-93.

116. DiBella, L.M., et al., *The Tctex1/Tctex2 class of dynein light chains. Dimerization, differential expression, and interaction with the LC8 protein family.* J Biol Chem, 2001. **276**(17): p. 14366-73.

117. DiBella, L.M., et al., *A novel Tctex2-related light chain is required for stability of inner dynein arm I1 and motor function in the Chlamydomonas flagellum.* J Biol Chem, 2004. **279**(20): p. 21666-76.

118. Tai, A.W., et al., *Rhodopsin's carboxy-terminal cytoplasmic tail acts as a membrane receptor for cytoplasmic dynein by binding to the dynein light chain Tctex-1.* Cell, 1999. **97**(7): p. 877-87.

119. Dick, T., U. Surana, and W. Chia, *Molecular and genetic characterization of SLC1, a putative Saccharomyces cerevisiae homolog of the metazoan cytoplasmic dynein light chain 1.* Mol Gen Genet, 1996. **251**(1): p. 38-43.

120. Rosenbaum, J.L. and G.B. Witman, *Intraflagellar transport.* Nat Rev Mol Cell Biol, 2002. **3**(11): p. 813-25.

121. Schroer, T.A., *Dynactin.* Annu Rev Cell Dev Biol, 2004. **20**: p. 759-79.

122. Schafer, D.A., et al., *Ultrastructural analysis of the dynactin complex: an actin-related protein is a component of a filament that resembles F-actin.* J Cell Biol, 1994. **126**(2): p. 403-12.

123. Bingham, J.B. and T.A. Schroer, *Self-regulated polymerization of the actin-related protein Arp1.* Curr Biol, 1999. **9**(4): p. 223-6.

124. Eckley, D.M., et al., *Analysis of dynactin subcomplexes reveals a novel actin-related protein associated with the arp1 minifilament pointed end.* J Cell Biol, 1999. **147**(2): p. 307-20.

125. Vaughan, K.T. and R.B. Vallee, *Cytoplasmic dynein binds dynactin through a direct interaction between the intermediate chains and p150Glued.* J Cell Biol, 1995. **131**(6 Pt 1): p. 1507-16.

126. King, S.J. and T.A. Schroer, *Dynactin increases the processivity of the cytoplasmic dynein motor.* Nat Cell Biol, 2000. **2**(1): p. 20-4.

127. Waterman-Storer, C.M., S. Karki, and E.L. Holzbaur, *The p150Glued component of the dynactin complex binds to both microtubules and the actin-related protein centractin (Arp-1).* Proc Natl Acad Sci U S A, 1995. **92**(5): p. 1634-8.

128. Clark, S.W. and M.D. Rose, *Alanine scanning of Arp1 delineates a putative binding site for Jnm1/dynamitin and Nip100/p150Glued.* Mol Biol Cell, 2005. **16**(9): p. 3999-4012.

129. McMillan, J.N. and K. Tatchell, *The JNM1 gene in the yeast Saccharomyces cerevisiae is required for nuclear migration and spindle orientation during the mitotic cell cycle.* J Cell Biol, 1994. **125**(1): p. 143-58.

130. Olson, E.C. and C.A. Walsh, *Smooth, rough and upside-down neocortical development.* Curr Opin Genet Dev, 2002. **12**(3): p. 320-7.

131. Carvalho, P., J.S. Tirnauer, and D. Pellman, *Surfing on microtubule ends.* Trends Cell Biol, 2003. **13**(5): p. 229-37.

132. Carvalho, P., et al., *Cell cycle control of kinesin-mediated transport of Bik1 (CLIP-170) regulates microtubule stability and dynein activation.* Dev Cell, 2004. **6**(6): p. 815-29.

133. Li, J., W.L. Lee, and J.A. Cooper, *NudEL targets dynein to microtubule ends through LIS1.* Nat Cell Biol, 2005. **7**(7): p. 686-90.

134. Heil-Chapdelaine, R.A., J.R. Oberle, and J.A. Cooper, *The cortical protein Num1p is essential for dynein-dependent interactions of microtubules with the cortex.* J Cell Biol, 2000. **151**(6): p. 1337-44.

135. Farkasovsky, M. and H. Kuntzel, *Cortical Num1p interacts with the dynein intermediate chain Pac11p and cytoplasmic microtubules in budding yeast.* J Cell Biol, 2001. **152**(2): p. 251-62.

136. Pearson, C.G. and K. Bloom, *Dynamic microtubules lead the way for spindle positioning.* Nat Rev Mol Cell Biol, 2004. **5**(6): p. 481-92.

137. Versele, M. and J. Thorner, *Some assembly required: yeast septins provide the instruction manual.* Trends Cell Biol, 2005. **15**(8): p. 414-24.

138. Longtine, M.S. and E. Bi, *Regulation of septin organization and function in yeast.* Trends Cell Biol, 2003. **13**(8): p. 403-9.

139. Hartwell, L.H., *Genetic control of the cell division cycle in yeast. IV. Genes controlling bud emergence and cytokinesis.* Exp Cell Res, 1971. **69**(2): p. 265-76.

140. Smith, G.R., et al., *GTPase-activating proteins for Cdc42.* Eukaryot Cell, 2002. **1**(3): p. 469-80.

141. Gladfelter, A.S., et al., *Septin ring assembly involves cycles of GTP loading and hydrolysis by Cdc42p.* J Cell Biol, 2002. **156**(2): p. 315-26.

142. Longtine, M.S., H. Fares, and J.R. Pringle, *Role of the yeast Gin4p protein kinase in septin assembly and the relationship between septin assembly and septin function.* J Cell Biol, 1998. **143**(3): p. 719-36.

143. Schmidt, M., et al., *Septins, under Cla4p regulation, and the chitin ring are required for neck integrity in budding yeast.* Mol Biol Cell, 2003. **14**(5): p. 2128-41.

144. Weiss, E.L., et al., *Chemical genetic analysis of the budding-yeast p21-activated kinase Cla4p.* Nat Cell Biol, 2000. **2**(10): p. 677-85.

145. Dobbelaere, J., et al., *Phosphorylation-dependent regulation of septin dynamics during the cell cycle.* Dev Cell, 2003. **4**(3): p. 345-57.

146. Wan, J., H. Xu, and M. Grunstein, *CDC14 of Saccharomyces cerevisiae. Cloning, sequence analysis, and transcription during the cell cycle.* J Biol Chem, 1992. **267**(16): p. 11274-80.

147. Visintin, R., et al., *The phosphatase Cdc14 triggers mitotic exit by reversal of Cdk-dependent phosphorylation.* Mol Cell, 1998. **2**(6): p. 709-18.

148. Sheaff, R.J. and J.M. Roberts, *End of the line: proteolytic degradation of cyclin-dependent kinase inhibitors.* Chem Biol, 1996. **3**(11): p. 869-73.

149. Toyn, J.H., et al., *The Swi5 transcription factor of Saccharomyces cerevisiae has a role in exit from mitosis through induction of the cdk-inhibitor Sic1 in telophase.* Genetics, 1997. **145**(1): p. 85-96.

150. Schwab, M., A.S. Lutum, and W. Seufert, *Yeast Hct1 is a regulator of Clb2 cyclin proteolysis.* Cell, 1997. **90**(4): p. 683-93.

151. Visintin, R., E.S. Hwang, and A. Amon, *Cfi1 prevents premature exit from mitosis by anchoring Cdc14 phosphatase in the nucleolus.* Nature, 1999. **398**(6730): p. 818-23.

152. Straight, A.F., et al., *Net1, a Sir2-associated nucleolar protein required for rDNA silencing and nucleolar integrity.* Cell, 1999. **97**(2): p. 245-56.

153. Shou, W., et al., *Exit from mitosis is triggered by Tem1-dependent release of the protein phosphatase Cdc14 from nucleolar RENT complex.* Cell, 1999. **97**(2): p. 233-44.

154. Traverso, E.E., et al., *Characterization of the Net1 cell cycle-dependent regulator of the Cdc14 phosphatase from budding yeast.* J Biol Chem, 2001. **276**(24): p. 21924-31.

155. Lee, S.E., et al., *Order of function of the budding-yeast mitotic exit-network proteins Tem1, Cdc15, Mob1, Dbf2, and Cdc5.* Curr Biol, 2001. **11**(10): p. 784-8.

156. Grandin, N., A. de Almeida, and M. Charbonneau, *The Cdc14 phosphatase is functionally associated with the Dbf2 protein kinase in Saccharomyces cerevisiae.* Mol Gen Genet, 1998. **258**(1-2): p. 104-16.

157. Toyn, J.H. and L.H. Johnston, *The Dbf2 and Dbf20 protein kinases of budding yeast are activated after the metaphase to anaphase cell cycle transition.* Embo J, 1994. **13**(5): p. 1103-13.

158. Shou, W., et al., *Cdc5 influences phosphorylation of Net1 and disassembly of the RENT complex.* BMC Mol Biol, 2002. **3**: p. 3.

159. Visintin, R., F. Stegmeier, and A. Amon, *The role of the polo kinase Cdc5 in controlling Cdc14 localization.* Mol Biol Cell, 2003. **14**(11): p. 4486-98.

160. Mah, A.S., J. Jang, and R.J. Deshaies, *Protein kinase Cdc15 activates the Dbf2-Mob1 kinase complex.* Proc Natl Acad Sci U S A, 2001. **98**(13): p. 7325-30.

161. Bardin, A.J., R. Visintin, and A. Amon, *A mechanism for coupling exit from mitosis to partitioning of the nucleus.* Cell, 2000. **102**(1): p. 21-31.

162. Shirayama, M., Y. Matsui, and E.A. Toh, *The yeast TEM1 gene, which encodes a GTP-binding protein, is involved in termination of M phase.* Mol Cell Biol, 1994. **14**(11): p. 7476-82.

163. Pereira, G., et al., *The Bub2p spindle checkpoint links nuclear migration with mitotic exit.* Mol Cell, 2000. **6**(1): p. 1-10.

164. Visintin, R. and A. Amon, *Regulation of the mitotic exit protein kinases Cdc15 and Dbf2.* Mol Biol Cell, 2001. **12**(10): p. 2961-74.

165. Luca, F.C., et al., *Saccharomyces cerevisiae Mob1p is required for cytokinesis and mitotic exit.* Mol Cell Biol, 2001. **21**(20): p. 6972-83.

166. Stoepel, J., et al., *The mitotic exit network Mob1p-Dbf2p kinase complex localizes to the nucleus and regulates passenger protein localization.* Mol Biol Cell, 2005. **16**(12): p. 5465-79.

167. Mah, A.S., et al., *Substrate specificity analysis of protein kinase complex Dbf2-Mob1 by peptide library and proteome array screening.* BMC Biochem, 2005. **6**: p. 22.

168. Yeh, E., et al., *Spindle dynamics and cell cycle regulation of dynein in the budding yeast, Saccharomyces cerevisiae.* J Cell Biol, 1995. **130**(3): p. 687-700.

169. Wang, Y., F. Hu, and S.J. Elledge, *The Bfa1/Bub2 GAP complex comprises a universal checkpoint required to prevent mitotic exit.* Curr Biol, 2000. **10**(21): p. 1379-82.

170. Fraschini, R., et al., *Budding yeast Bub2 is localized at spindle pole bodies and activates the mitotic checkpoint via a different pathway from Mad2.* J Cell Biol, 1999. **145**(5): p. 979-91.

171. Li, R., *Bifurcation of the mitotic checkpoint pathway in budding yeast.* Proc Natl Acad Sci U S A, 1999. **96**(9): p. 4989-94.

172. D'Amours, D. and A. Amon, *At the interface between signaling and executing anaphase--Cdc14 and the FEAR network.* Genes Dev, 2004. **18**(21): p. 2581-95.

173. Castillon, G.A., et al., *Septins have a dual role in controlling mitotic exit in budding yeast.* Curr Biol, 2003. **13**(8): p. 654-8.

174. D'Aquino, K.E., et al., *The protein kinase Kin4 inhibits exit from mitosis in response to spindle position defects.* Mol Cell, 2005. **19**(2): p. 223-34.

175. Pereira, G. and E. Schiebel, *Kin4 kinase delays mitotic exit in response to spindle alignment defects.* Mol Cell, 2005. **19**(2): p. 209-21.

176. Wang, Y. and T.Y. Ng, *Phosphatase 2A negatively regulates mitotic exit in Saccharomyces cerevisiae.* Mol Biol Cell, 2006. **17**(1): p. 80-9.

177. Wang, Y. and D.J. Burke, *Cdc55p, the B-type regulatory subunit of protein phosphatase 2A, has multiple functions in mitosis and is required for the kinetochore/spindle checkpoint in Saccharomyces cerevisiae.* Mol Cell Biol, 1997. **17**(2): p. 620-6.

178. Yellman, C.M. and D.J. Burke, *The role of Cdc55 in the spindle checkpoint is through regulation of mitotic exit in Saccharomyces cerevisiae.* Mol Biol Cell, 2006. **17**(2): p. 658-66.

179. Queralt, E., et al., *Downregulation of PP2A(Cdc55) phosphatase by separase initiates mitotic exit in budding yeast.* Cell, 2006. **125**(4): p. 719-32.

180. Stark, M.J., *Yeast protein serine/threonine phosphatases: multiple roles and diverse regulation.* Yeast, 1996. **12**(16): p. 1647-75.

181. Zabrocki, P., et al., *The Saccharomyces cerevisiae type 2A protein phosphatase Pph22p is biochemically different from mammalian PP2A.* Eur J Biochem, 2002. **269**(14): p. 3372-82.

182. Stegmeier, F., R. Visintin, and A. Amon, *Separase, polo kinase, the kinetochore protein Slk19, and Spo12 function in a network that controls Cdc14 localization during early anaphase.* Cell, 2002. **108**(2): p. 207-20.

183. Yoshida, S. and A. Toh-e, *Budding yeast Cdc5 phosphorylates Net1 and assists Cdc14 release from the nucleolus.* Biochem Biophys Res Commun, 2002. **294**(3): p. 687-91.

184. Stegmeier, F., et al., *The replication fork block protein Fob1 functions as a negative regulator of the FEAR network.* Curr Biol, 2004. **14**(6): p. 467-80.

185. Zachariae, W. and K. Nasmyth, *Whose end is destruction: cell division and the anaphase-promoting complex.* Genes Dev, 1999. **13**(16): p. 2039-58.
186. Sullivan, M., C. Lehane, and F. Uhlmann, *Orchestrating anaphase and mitotic exit: separase cleavage and localization of Slk19.* Nat Cell Biol, 2001. **3**(9): p. 771-7.
187. Sullivan, M. and F. Uhlmann, *A non-proteolytic function of separase links the onset of anaphase to mitotic exit.* Nat Cell Biol, 2003. **5**(3): p. 249-54.
188. Hofken, T. and E. Schiebel, *A role for cell polarity proteins in mitotic exit.* Embo J, 2002. **21**(18): p. 4851-62.
189. Hofken, T. and E. Schiebel, *Novel regulation of mitotic exit by the Cdc42 effectors Gic1 and Gic2.* J Cell Biol, 2004. **164**(2): p. 219-31.
190. Seshan, A., A.J. Bardin, and A. Amon, *Control of Lte1 localization by cell polarity determinants and Cdc14.* Curr Biol, 2002. **12**(24): p. 2098-110.
191. Chiroli, E., et al., *Budding yeast PAK kinases regulate mitotic exit by two different mechanisms.* J Cell Biol, 2003. **160**(6): p. 857-74.
192. Seshan, A. and A. Amon, *Ras and the Rho effector Cla4 collaborate to target and anchor Lte1 at the bud cortex.* Cell Cycle, 2005. **4**(7): p. 940-6.
193. Tong, A.H., et al., *Systematic genetic analysis with ordered arrays of yeast deletion mutants.* Science, 2001. **294**(5550): p. 2364-8.
194. Pan, X., et al., *dSLAM analysis of genome-wide genetic interactions in Saccharomyces cerevisiae.* Methods, 2007. **41**(2): p. 206-21.
195. Pan, X., et al., *A robust toolkit for functional profiling of the yeast genome.* Mol Cell, 2004. **16**(3): p. 487-96.
196. Keng, T., et al., *LTE1 of Saccharomyces cerevisiae is a 1435 codon open reading frame that has sequence similarities to guanine nucleotide releasing factors.* Yeast, 1994. **10**(7): p. 953-8.
197. Wickner, R.B., et al., *Molecular cloning of chromosome I DNA from Saccharomyces cerevisiae: isolation of the MAK16 gene and analysis of an adjacent gene essential for growth at low temperatures.* Yeast, 1987. **3**(1): p. 51-7.
198. Ye, P., et al., *Gene function prediction from congruent synthetic lethal interactions in yeast.* Mol Syst Biol, 2005. **1**: p. 2005 0026.
199. Kato, M. and W.B. Dobyns, *Lissencephaly and the molecular basis of neuronal migration.* Hum Mol Genet, 2003. **12 Spec No 1**: p. R89-96.
200. den Hollander, P. and R. Kumar, *Dynein light chain 1 contributes to cell cycle progression by increasing cyclin-dependent kinase 2 activity in estrogen-stimulated cells.* Cancer Res, 2006. **66**(11): p. 5941-9.
201. Knop, M., et al., *Epitope tagging of yeast genes using a PCR-based strategy: more tags and improved practical routines.* Yeast, 1999. **15**(10B): p. 963-72.
202. Gelperin, D.M., et al., *Biochemical and genetic analysis of the yeast proteome with a movable ORF collection.* Genes Dev, 2005. **19**(23): p. 2816-26.
203. Altschul, S.F., et al., *Gapped BLAST and PSI-BLAST: a new generation of protein database search programs.* Nucleic Acids Res, 1997. **25**(17): p. 3389-402.
204. Clamp, M., et al., *The Jalview Java alignment editor.* Bioinformatics, 2004. **20**(3): p. 426-7.

205. Jensen, S., et al., *Temporal coupling of spindle disassembly and cytokinesis is disrupted by deletion of LTE1 in budding yeast.* Cell Cycle, 2004. **3**(6): p. 817-22.
206. D'Amours, D., F. Stegmeier, and A. Amon, *Cdc14 and condensin control the dissolution of cohesin-independent chromosome linkages at repeated DNA.* Cell, 2004. **117**(4): p. 455-69.
207. Pan, X., et al., *A DNA integrity network in the yeast Saccharomyces cerevisiae.* Cell, 2006. **124**(5): p. 1069-81.
208. Wang, Y., et al., *Exit from exit: resetting the cell cycle through Amn1 inhibition of G protein signaling.* Cell, 2003. **112**(5): p. 697-709.
209. Shields, C.M., et al., *Saccharomyces cerevisiae Ats1p interacts with Nap1p, a cytoplasmic protein that controls bud morphogenesis.* Curr Genet, 2003. **44**(4): p. 184-94.
210. Bender, A. and J.R. Pringle, *Use of a screen for synthetic lethal and multicopy suppressee mutants to identify two new genes involved in morphogenesis in Saccharomyces cerevisiae.* Mol Cell Biol, 1991. **11**(3): p. 1295-305.
211. Hirano, H., et al., *ROM7/BEM4 encodes a novel protein that interacts with the Rho1p small GTP-binding protein in Saccharomyces cerevisiae.* Mol Cell Biol, 1996. **16**(8): p. 4396-403.
212. Mack, D., et al., *Identification of the bud emergence gene BEM4 and its interactions with rho-type GTPases in Saccharomyces cerevisiae.* Mol Cell Biol, 1996. **16**(8): p. 4387-95.
213. Bose, I., et al., *Assembly of scaffold-mediated complexes containing Cdc42p, the exchange factor Cdc24p, and the effector Cla4p required for cell cycle-regulated phosphorylation of Cdc24p.* J Biol Chem, 2001. **276**(10): p. 7176-86.
214. Casamayor, A. and M. Snyder, *Molecular dissection of a yeast septin: distinct domains are required for septin interaction, localization, and function.* Mol Cell Biol, 2003. **23**(8): p. 2762-77.
215. Jones, A.L., et al., *SAC3 may link nuclear protein export to cell cycle progression.* Proc Natl Acad Sci U S A, 2000. **97**(7): p. 3224-9.
216. Lei, E.P., et al., *Sac3 is an mRNA export factor that localizes to cytoplasmic fibrils of nuclear pore complex.* Mol Biol Cell, 2003. **14**(3): p. 836-47.
217. Chenevert, J., et al., *A yeast gene (BEM1) necessary for cell polarization whose product contains two SH3 domains.* Nature, 1992. **356**(6364): p. 77-9.
218. Chenevert, J., N. Valtz, and I. Herskowitz, *Identification of genes required for normal pheromone-induced cell polarization in Saccharomyces cerevisiae.* Genetics, 1994. **136**(4): p. 1287-96.
219. Drees, B.L., et al., *A protein interaction map for cell polarity development.* J Cell Biol, 2001. **154**(3): p. 549-71.
220. Etienne-Manneville, S., *Cdc42--the centre of polarity.* J Cell Sci, 2004. **117**(Pt 8): p. 1291-300.
221. Madden, K. and M. Snyder, *Cell polarity and morphogenesis in budding yeast.* Annu Rev Microbiol, 1998. **52**: p. 687-744.
222. Masuda, T., et al., *Molecular cloning and characterization of yeast rho GDP dissociation inhibitor.* J Biol Chem, 1994. **269**(31): p. 19713-8.
223. Bauer, A. and R. Kolling, *Characterization of the SAC3 gene of Saccharomyces cerevisiae.* Yeast, 1996. **12**(10): p. 965-75.

224. Bauer, A. and R. Kolling, *The SAC3 gene encodes a nuclear protein required for normal progression of mitosis.* J Cell Sci, 1996. **109 (Pt 6)**: p. 1575-83.

225. Sesaki, H., et al., *Mgm1p, a dynamin-related GTPase, is essential for fusion of the mitochondrial outer membrane.* Mol Biol Cell, 2003. **14**(6): p. 2342-56.

226. Irazoqui, J.E., A.S. Gladfelter, and D.J. Lew, *Cdc42p, GTP hydrolysis, and the cell's sense of direction.* Cell Cycle, 2004. **3**(7): p. 861-4.

227. van Heusden, G.P. and H.Y. Steensma, *Yeast 14-3-3 proteins.* Yeast, 2006. **23**(3): p. 159-71.

228. Kakiuchi, K., et al., *Proteomic analysis of in vivo 14-3-3 interactions in the yeast Saccharomyces cerevisiae.* Biochemistry, 2007. **46**(26): p. 7781-92.

229. Wu, H., et al., *Solution structure of the Tctex1 dimer reveals a mechanism for dynein-cargo interactions.* Structure, 2005. **13**(2): p. 213-23.

230. Mok, Y.K., K.W. Lo, and M. Zhang, *Structure of Tctex-1 and its interaction with cytoplasmic dynein intermediate chain.* J Biol Chem, 2001. **276**(17): p. 14067-74.

231. Miki, F., et al., *The 14-kDa dynein light chain-family protein Dlc1 is required for regular oscillatory nuclear movement and efficient recombination during meiotic prophase in fission yeast.* Mol Biol Cell, 2002. **13**(3): p. 930-46.

Fun Sun
VACATIONS

Offer Extended to Feb 2/08!

FIRST Night in Anaheim

Only $20.08

Book one of these 6 properties with a minimum air & 4 nights and your first night is only $20.08 plus tax... not per person... **per room!**

- **Cortona Inn & Suites**
- **Clarion Anaheim Resort Hotel**
- **Super 8 Motel Anaheim**
- **Ramada Maingate at the Park**
- **Holiday Inn Anaheim Resort**
- **Knott's Berry Farm Resort & Hotel**

Offer restricted to Fun Sun's lead in category. New bookings only. Bookings made: January 10 – February 2/08. Travel: January 10 – December 15/08. Restrictions apply. Subject to availability.

*Visit **www.funsunvacations.com** for more details.*

CONTACT YOUR TRAVEL AGENT TO BOOK!

A5045B | Jan 28/08 | Fun Sun Vacations

BC Registration: 3522-1 | ON Registration: 50014991

For Fax Number Removal Please Call 1888 662 2677 & Quote Document Number 2001 3107
For Fax Broadcasting Information Please Contact: SERVICE@ALLPOINTSSOLUTIONS.COM